Sinhgad Technical Education Society's®
NBN SINHGAD TECHNICAL INSTITUTES CAMPUS
Approved by AICTE, New Delhi, Recognized by Government of Maharashtra &
Affiliated to University of Pune (ID No. - PU/PN/Engg/432/2012)
S. No. 10/1, Ambegaon (Budruk), Off Sinhgad Road, Pune 411041
Sinhgad Institutes
•Tel. : +91-20-24355042 / 46, +91-20-24610880/881 • Tele Fax : +91-20-24355042 • Website : www.sinhgad.edu
• Email : nbnssoe@sinhgad.edu / nbnssoms@sinhgad.edu / nbnssocs@sinhgad.edu

INDEX

Number of papers published per teacher in the Journals notified on UGC website and in other journals during the year 2021

Research Article

Machine Learning based Autonomous Fire Combat Turret

Makrand M Jadhav[a], Gajanan H. Chavan[b], and Altaf O. Mulani[c]
[a]
Associate Professor, Electronics & Telecommunication Dept., NBN Sinhgad School of Engineering, Pune, India
[b]Assistant Professor, Electronics & Telecommunication Dept., V.I.I.T., Pune, India
[c]Associate Professor, Electronics & Telecommunication Dept., SKNSCOE, India

Article History: Received: 11 January 2021; Accepted: 27 February 2021; Published online: 5 April 2021

Abstract: The time lag between the identification and the initiation of the actuation protocol is more in conventional fire combat system. This in turn increases the response time resulting in financial loss as well as injuries to human beings. In this paper an efficient method of fire combat is proposed to eliminate resource loss. This system extinguishes fire before it reaches its destructive level. It eliminates all the flaws of the conventional fire extinguishers and improves the damage limitation by raising an alarm. Further by applying HAAR cascade classifier machine learning algorithm, accuracy of 70-75 % is achieved to detect fire. It also provides minimum latency and optimal response in detecting fires and differentiating them from false triggers. It is observed that the response time of proposed fire combat system is 2-4 seconds. The automatic mode is reliable in the presence of multiple units that are deployed in the same area of interest. The system is able to cover the entire hemispheric 3D volume of the room as per the industrial and domestic safety standards.

Keywords: CATIA, CNC, GPIO, IDE, TFT.

1. Introduction

Fire breakouts cause a lot of damage to life and property. The conventional methods for fire detection and extinguishing make use of gas sensors and temperature sensors. Here, smoke detection and temperature variation sensing form the basis of these techniques. These systems offer more latency in detecting fire and hence more damage. Further, water sprinklers are used for combating fire breakouts. But the drawback of using sprinklers is that they deploy water-jets throughout the given room and hence fail to combat fires that are localized to a certain area of the room. Deploying waterjets over electrical equipment leads to short circuits and could thereby worsen the situation. On the other hand, resolving such methods leads to off target deployment of water. Therefore, this demands that the response time of conventional fire combat system needs to be reduced as it does not provide immediate assistance in critical situations [1-2].

The time lag between the identification and the initiation of the actuation protocol is a major concern. The arrival time of fire brigade further compromises the damage limitation. It is important that an efficient method for combating fire must be developed, tested and implemented to overhaul the flaws offered by the pre-existing systems [3]. This work eliminates all the flaws of the conventional fire extinguishers. It reduces damage limitation by raising an alarm as well as initiating the actuation protocol as quick as possible. The Computer Aided Three-dimensional Interactive Application (CATIA) is used as 3D software to generate model dimensions and create reference dimensions of the system [4].

This work aims at developing a more efficient and responsive fire combat system with added functionalities such as early fire detection, self-learning algorithm lessens the response time, remote sensing and control over the actuation protocol. The actuation module for systems works in response to an external control signal provided by the image processing module. The major components of this module are positioning system comprising of two servo motors, a submersible water pump, a hose pipe assembly, a mode control switch and a camera mounted on the mechanical assembly for imaging as well as surveillance purposes. After reception of the control signal, the submersible water pump via hose pipe assembly deploys a water-jet and resumes the surveillance. Alternately in an impending case of a malignant fire the security personnel can take over the control from the auto-surveillance mode. It can remotely control the positioning of the hose pipe and effectively deploy a water-jet extinguishing agent.

In this paper a system is proposed that extinguishes fire before it reaches its destructive level. The object detection algorithm is used in implementing the fire recognition phase of the turret's functionality based on machine learning. Further, system provides minimum latency and optimal response in detecting fires and differentiating them from false triggers. This paper consists of seven sections. Section I gives the introduction and motivation of this work in present scenario. Section II presents an brief view of the literature survey. Section III presents design and implementation aspect. Section IV elaborates object detection algorithm with machine learning techniques. Development of mechanical model of the system is presented in section V. Section VI ıders the results in detail. Whereas Section VII gives the conclusion followed with future scope.

2. Literature Review

In this section the contemporary technologies and the existing state of art techniques are discussed briefly. The conventional methods for fire detection and extinguishing make use of IR sensors and temperature sensors. On the other hand, fire alarm scheme consists of devices that are connected together to detect presence of smoke or fire or carbon monoxide or other emergencies in [5]. It also warns persons with the help of visual and audio appliances. In such systems alarms are activated automatically with the help of smoke or heat detectors. Whereas a manual fire alarm activation devices is used in some systems. Alarms considered are either motorized bells. Further, it can also be a wall mountable sounders or horns. Water sprinklers used for combating fire breakouts is explained in [6]. But the main drawback of using sprinklers is that they deploy water-jets throughout the given room and hence fail to efficiently combat fires that are limited to a certain area of the room. The identification protocol involved in identification of the flames or any such fire outbreak is usually carried out by considering the physical parameters and the chemical properties of the residues after combustion [7]. Smoke density over a region of interest or a random increase in the temperature of an area of interest is being monitored in the state of art systems. These smoke sensors and heat monitors are configured an arrays of integrated sensing elements connected in feedback discussed in [8].

In addition to water sprinklers immobile hose pipes targeting water jet deployment over one particular area of interest are installed [9]. Their targets are to be manually adjusted and there is no control over the amount of water deployed. Thus there is a compromise over the amount of the water being used. These water jet deploying hose pipes are solenoid valve operated. GSM Modules are also interfaced in addition to the locally raised alarm. The GSM module enables sending text messages to the nearest proximally present emergency services or the fire combat brigade itself. Such fire-sprinkler system are considered as fire- protection method described in [10]. Here, water supply arrangement is proposed to provide adequate pressure as well as flow-rate in controlling the fire. Further fire sprinklers are attached to a water supply piping system. Such system is preferred for large commercial buildings as well as factories. Presently, these are cost effective systems available for homes as well as small buildings worldwide. Here 40 million sprinkler heads are fitted every year. It is concluded that buildings supported with such systems ae able to control 96% of fires. Widely used systems for automatic fire detection and extinguishing are gas sensor based presented in [11]. These systems have fixed mounted water sprays for the extinguishing purpose. This type of system detects the presence of any gas in atmosphere. It deploys the water sprays if the gas is detected. Another system similar to this is where it uses temperature sensor instead of gas sensor. The working principle remains same just that the extinguishing condition changes depending upon the temperature threshold is crossed. A 3D scanning system is proposed [12]. It translates into a virtual object by scanning a real time stationary object. A 3D digital model is built with such associated data. This unit operates at 650 nm. A tilting angle of 60 degrees is considered and the unit is spaced at 15 cm distance from web cam. Today in era of mobile, an efficient polar code based OFDM system is proposed in [13 -14] to accommodate more people to use such system to save the life of human beings in the society.

Based on collective information assimilated by Department of Fire Control Mumbai Municipal Corporation, Table 1 highlights various causes of fire breakouts recorded in Maharashtra, India.

Table 1. List of incidents caused due to fire

Particulars	Causes
A Fire breaks out injured firemen were injured near Fort area, Mint Road, Mumbai. Further, few more got injured in a massive fire erupts. This happened in in an industrial area near Andheri, Mumbai.	Electrical failure
The Income Tax office caught major fire that was positioned in the Scindia House, New Fort, New Delhi. It has killed firemen's and labours.	Domestic Negligence
A Cine Vista: Film studio located on Kanjur Marg(West) got damaged in a massive fire. Few technicians met with an accident. Nearly 100 labourers in Goregaon were rescued by the fire brigade.	Short circuit
A fire broke out in a commercial complex located in Mumbai. It has killed fourteen firemen.	Negligence smoking
A fire broke out in Army building of Colaba area, South Mumbai.	Mishandling of Explosives
A massive fire broke out in a chemical factory. The site was located in Asalfa Village, Ghatkopar. The occurred due to negligent storage of highly corrosive substances..	Negligent storage of corrosive substances
A fire broke out injured residents in a building due to leakage in Malad.	LPG leakage
A fire broke out that damaged a cloth mill located in Italian Industrial Estate, Goregaon, Mumbai.	Electrical Sparking

Four people died and five people were injured after A fire broke out in Maimoon building injured many peoples. This was a residential territory placed in the suburban part of Marol, Mumbai.	Inefficient Fire combat system
A massive fire broke out at a Snack shop has killed many peoples. This shop is placed in Saki Naka area, Khairani Road.	Negligent microwave usage

The available present systems are not preferred in manufacturing industries where there is possibility of fire in a remote part of room that is not under the mounted sprays. In first case where gas sensor is used, it is possible by a person to false trigger the fire alarm caused due to smoking under the sensor or mischief. In the second case that uses the temperature sensor, the sensors may bet triggered due to industrial components getting too hotter crossing the threshold limit and thus causing alarm. Thus flaws of the conventional systems need to be solved for protection of life and property. Therefore, system is proposed that can detect fire by machine learning technique. Further, it can access any remote area in the room.

3. Design and Implementation of Autonomous Fire Combat System

A block diagram of Autonomous Fire Combat System is shown in Figure 1. Software used is Processing 3 IDE. Two servo motors and a mode switch are conneted to the microcontroller. The camera module constantly checks of any fire to be detected. If a fire is detected, the motors rotates accordingly. Thus the fire extinguishing outlet controlled by the solenoid valve can face the specific coordinates. A xcluma Thin Film Transistor (TFT) is connected as a display device to the microcontroller. The manual mode of operation is controlled by an optical mouse.

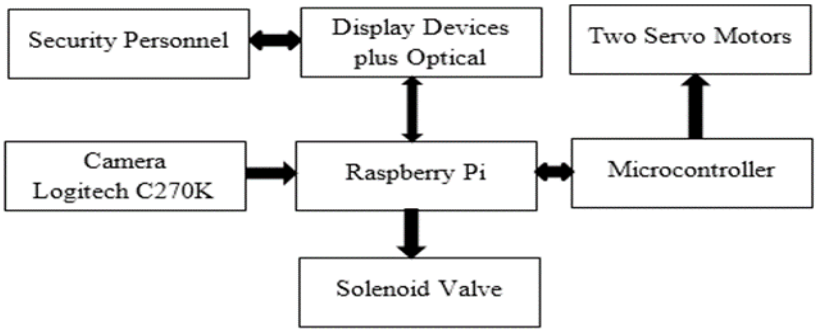

Figure 1. Block diagram of Autonomous Fire Combat System

The detailed system functionality is described with flow chart in Figure 2 and Algorithm 1.

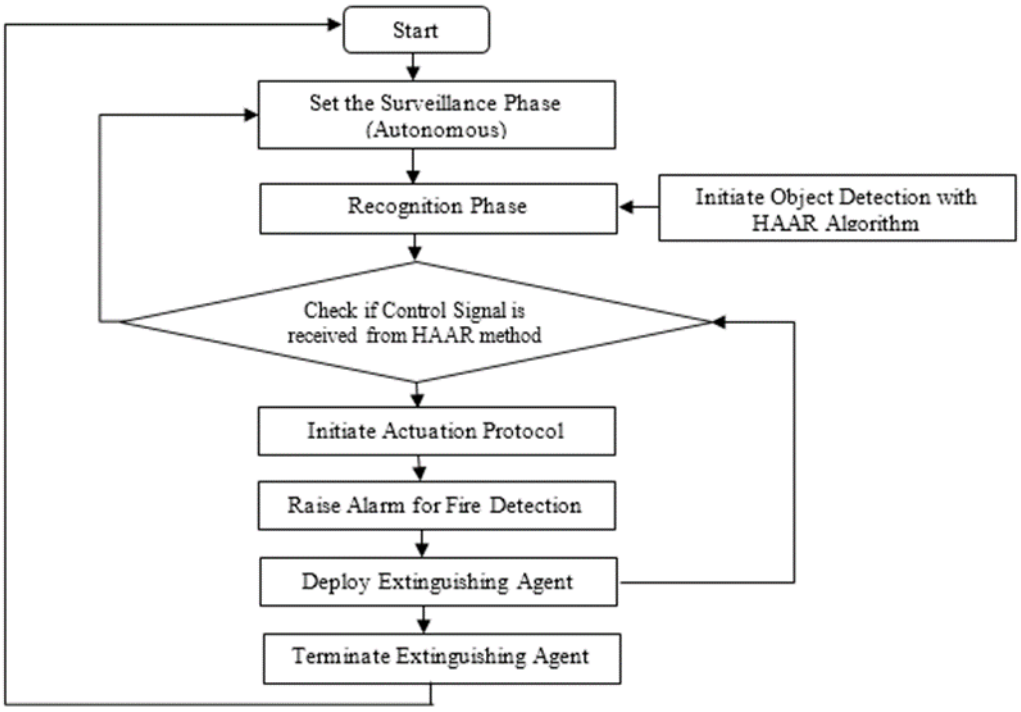

Figure 2. Flow Chart of System functionality

The system operating in manual mode takes feed from optical mouse, Further the python library pyautogui, urns the coordinates of cursor on screen as well as dimension of screen. Let as well as represents the

dimension of screen, as well as denotes location of cursor and as well as gives angle for movement. The angle calculated for motor rotation is serially fed to Arduino given by

$$x-axis\ rotation \qquad x_d = \frac{x_p * 180}{x_c} \tag{1}$$

$$y-axis\ rotation \qquad y_d = \frac{y_p * 180}{y_c} \tag{2}$$

Figure 3. Flow Chart of System functionality

Learning Algorithm 1:

- Initialize all the power connections.
- Open the .py application to launch the control console.
- Use 'S' key to toggle the mode (Manual/Automatic). Here the default mode is programmed to be automatic mode.
- In Manual mode use 'F' key to deploy the extinguishing agent.
- In Automatic mode the system will run autonomously to detect, process and terminate the fire.

Figure 3. represents Arduino and Raspberry pi control with flow chart. Here, Arduino works on instructions received from Raspberry Pi. It is coded to perform particular function for certain type of input. On the other hand, Raspberry Pi performs various tasks such as image detection, sending command to Arduino etc. It computes necessary data needed and delivers it to Arduino. The high torque servo motors can handle high load that occurs during the firing of water jet.

4. Object Detection with Machine Learning

Object detection algorithm used in implementing the fire recognition phase of the turret's functionality is the ar Cascade Method. It uses the principle of machine learning. It uses the concept of image or video features

to recognize objects. This approach makes use of a cascade function. This function is trained by positive as well as negative images. This cascade function can distinguish fire from each individual frame captured by the turret's surveillance phase. A huge Haar features are needed to detect an object by enough accuracy. Therefore, are structured into cascade in generation of strong classifier as shown in Figure 4.

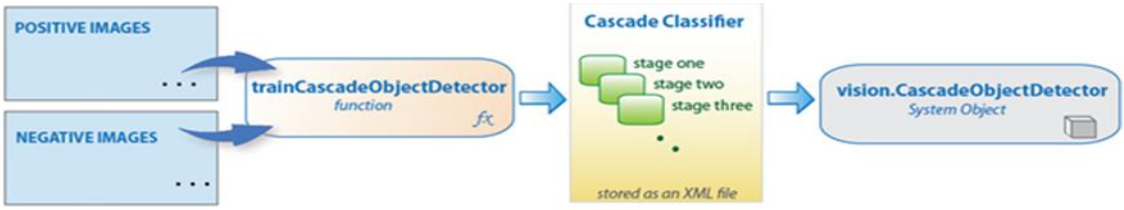

Figure 4. Object Detection with Cascade Classifier [4]

There are four stages to implement this function. First is Haar Feature based selection. Second is creation of Integral Images followed with Adaboost training as well as cascading classifiers. An Haar feature based on cascade classifiers detect objects. This is also identified as machine learning centered approach for face detection. Further, is also detect objects in other images. This algorithm initially requires lots of positive as well as negative face images to train the classifier. It extracts Haar features of face images and looks like convolutional kernel. Thus each feature represents as single value. It is obtained by deducting pixel sum belonging to white rectangle as well as to black rectangle. It is observed that creating Haar Cascade looks intimidating at the beginning but it's not as difficult a task. It finds the best threshold for each feature. This classifies faces as positive or negative images. But evidently it may also result in generation of errors or misclassifications. Thus features that has error rate minimum is chosen to best classify face and non-face images. This process task must be completed with minimum delay and more accuracy. To start, each image is assigned equal weight. The weights of images that are misclassified are increased after every iteration of classification. The process repeats again to calculate fresh error rates as well as weights. It is continued till desirable accuracy as well as error rate with good number of features are extracted.

OpenCV is used to train designed classifier for any objects. It emanates with a trainer and detector. Initially thousands of negative images are gathered. Such negative image does not comprise the object for which the Haar cascade is designed. Thereafter one positive face image as object is needed that can be detected by the Haar cascaded function. This detection is as per training by vector file obtained from machine learning techniques. This file contains features for further matching. These bunch of negative as well as positive face images is used to train Haar cascade. After training is done a vector file is created. This vector file is used in the program which detects the required image from the video feed. The speed to evaluate features does not sufficiently compensate for their numbers. However, it is observed that a standard sub-window having pixel size of 24x24 provides 162,336 likely features. Thus it is extortionately costly to evaluate complete features of them when testing an image.

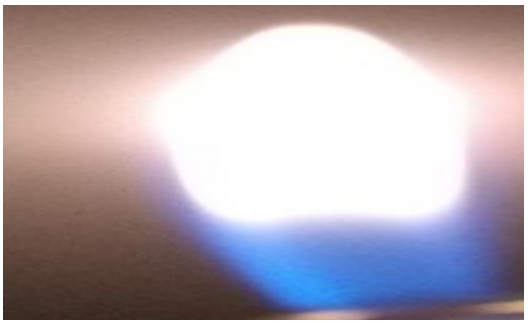

Figure 5 (a). Sample Negative Image

Figure 5(b). Sample Positive Image

A variant of learning algorithm named AdaBoost is employed for developing the framework for object detection. It extracts best image features as well as train the classifiers. It constructs a robust classifier obtained from linear combination of weights. Thus simple weak classifier mentioned can be expressed by

$$h(x) = \text{sgn}(\sum_{j=1}^{M} \alpha_j h_j(x) \qquad (3)$$

Thereafter, every weak classifier is treated as threshold function that is feature based f . as given by

$$h_j = \begin{matrix} -s_j & \textit{if } f_j < \theta_j \\ s_j & \textit{otherwise} \end{matrix} \qquad (4)$$

Let θ_j be the optimal threshold value with polarity $s_j \in \pm 1$ obtained in the training along with the coefficients α_j.

Learning Algorithm 2

Input: A Set of *N* positive as well as negative training images with label represent by variable i (x^i , y^i) .

If image I is a face then y^i = 1 else y^i = -1.

1. Initialization: A weight $w_1^i = \frac{1}{N}$ is assigned to each image i .
2. For each feature f_j *where* $j = 1 \ldots M$, total sum of assigned weights is equal to one.
3. Apply this feature to all image in the training set. Then find optimal threshold value as well as polarity that minimizes the weighted classification error i.e. where

$$\theta_j, s_j = \arg\min \sum_{i=1}^{N} w_j^i \varepsilon_j^i \qquad \textit{where} \quad \varepsilon_j^i = \begin{matrix} 0 & \textit{if } y^i = h_j(x^i, \theta_j, s_j) \\ 1 & \textit{otherwise} \end{matrix}$$

4. Assign a weight α_j *to* h_j that is inversely proportional to the error rate.
5. The weights w_{j+1}^i for the next iteration are reduced for those images that was correctly classified.
6. Set the final classifier to $h(x) = \text{sgn}(\sum_{j=1}^{M} \alpha_j h_j(x)$

Cascade architecture provides positive face images that equals to 0.01 percentage size of all sub-windows. An equal computation time is spent on extracting features of all sub-windows. A 2-feature classifier attains 100 percentage detection rate as well as 50 percentages false positive rate. Further, cascade of progressively complex classifiers accomplishes even enhanced detection rates.

5. Development of Mechanical Model of the Proposed System

The machining steps involved to develop mechanical model mechanical aspects in the manufacturing process is described in this section. It holds the camera, the hose pipe and the servo motors.

- **Selection of Material:** The chassis of the camera hose pipe assembly is based on mild steel. The factors favoring the choice of this material are strength, ease of machining operations, cost and designing.
- **3D modelling using CATIA:** CATIA modelling relies on spline modelling. It generates coherent solids that can be easily transformed into a physical object. Bending tolerances were considered during the design. Various points that were considered during 3D modelling are: different bodies in the model don't intersect, elements in model has a thickness, object has a clear interior as well as exterior face. Further files with optimal size of less than 50Mb after the export is enough not to lose any detail or information. Thereafter, MG99R motors are placed orthogonal to each other such that the aperture of the camera is placed at the intersection of the two axes of rotation as Shown in Figure (a). Each servo motor provides a rotation of 180 degrees. The figure (b) illustrate the 3D extruded representation of the Housing assembly for the camera and the servo motor. Dimensions of the housing are 5cm x 10 cm x 12cm. The U shaped bracket as illustrated above provides two points of attachment for the horn of the servo motor. Dimensions of the U shaped bracket are 15cm x 5cm x 1.5 cm.

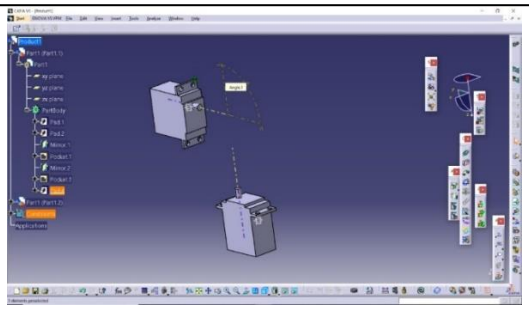

(a) Orthogonal Orientation of Motors

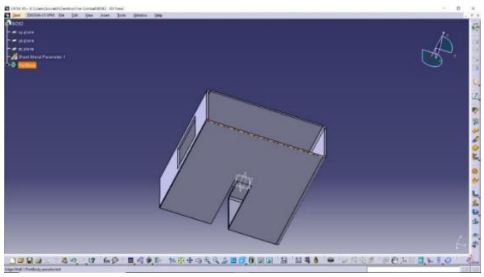

(b) Housing for servo motor and camera

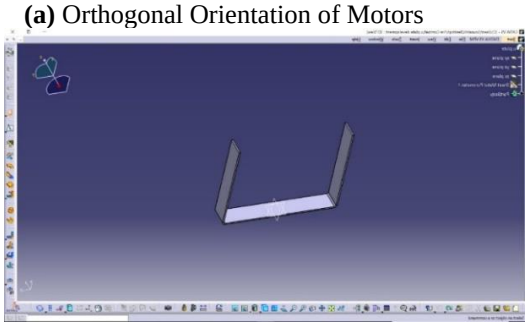

(c) U shaped bracket for holding the camera housing

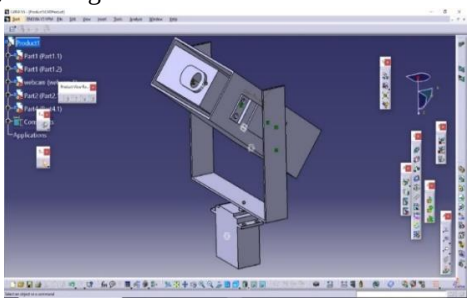

(d) 3D modelling

Figure 6 (a-d). Steps in developing mechanical model with CATIA

- **Laser Cutting:** This technology is used to cut materials. It is helpful in industrial manufacturing applications. It works on principle of guiding laser power output most commonly through optics.

(a) Laser Cutting of the Job in progress

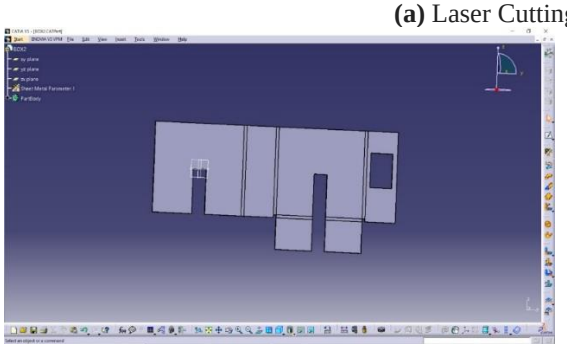

b) Camera motor housing

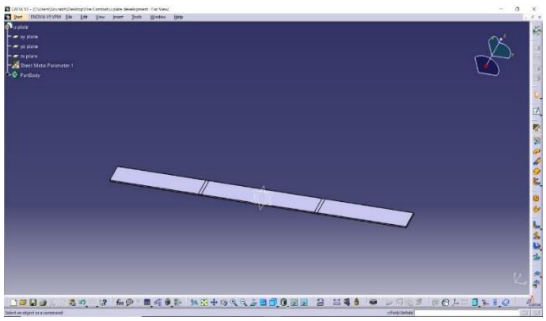

c) U shaped bracket

Figure 7. Flat-out representation

A 2D orthogonal view is extracted from the previously rendered 3D model. This 2D sketch is used to derive the G-code. The laser optics as well as Computer Numerical Control (CNC) directs the generated light beam. In general, commercial laser is preferred to cut materials. It comprises a motion control based system. This helps to track a G-code pattern on the material under the cut area as shown in Figure 7. The concentrated laser beam focused keeps portion of edge and is able to provide high quality material surface finish. It either melts or burns to get vaporized. Further it is blown away with the help jet of gas.

- **CNC Bending and Grinding**

CNC bending operation is a manufacturing process. It is carried with the help of CNC press brakes. The sheet metal work can be bended just a tiny mm across to the sections. In down forming machine, brakes have fixed bottom bed available with V- block clamp in place. It may either have a top beam traveling under the force along-with V- blade tools. Whereas in up-forming machine it is seen that bottom bend is moving whereas top beam is fixed. Both process method produces the similar components of sheet metal. However, there remain no restraints ıe component design that can suit to either machines. Arc welding is a welding process that joins metal to ıl. An electricity is used to produce sufficient heat to melt metal. Whereas results in a binding of the metals

after cooling. Grinding is a rough machining process in which grinding wheel is used as a cutting tool. In general, grinding was used to improve aesthetic finish of the chassis and also to even out the wielding points.

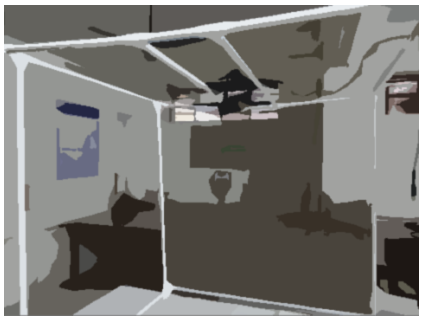

Figure 8 (a)Job after machining operations **Figure 8 (b) Final Hardware Assembly**

To enhance the aesthetics and to improve resistance to corrosion, the surface of the work piece is sprayed with a rust proof primer aerosol. This is followed by application of a matte finished aerosol paint.

6. Result and Discussions

This work eliminates all the flaws of the conventional fire extinguishers. A prototype is design as per the industrial and domestic safety standards. A machine learning algorithm provides minimum latency and optimal response in detecting fires and differentiating them from false triggers. Simulation of this project is done in Proteus8.1.

Figure 9. Fire Detected in Script

Figure 9. shows the implementation of python code. When the code is running, it will detect a fire in live video. When it detects fire, a square box will be used to enlighten the detected fire. Rapid fire detection detects the object to be detected and returns its coordinate pixels. It helps to locate the required object from the entire image. Along with the visual detection, python code also returns the x-y coordinates of the detections. The detection is in pixels. This pixel is later converted to degrees the motors need to rotate to make the detected fire center of the detection.

Arduino and Python Script

Output: Pin 3 – Condition to Arduino for fire detected and initiate extinguisher.
Pin 5 – Condition pin to Arduino to work on autonomous or manual mode
Serial – Motor coordinates sent to Arduino to rotate motor as per.
Display: Detected fire highlighted in Blue Square.

```
#include <Servo.h>
int i=0, j=0, f1=0, f2=0;
static int v = 0;
Servo Servo1;  //X-Axis
Servo Servo2;  //Y-Axis
void spiral(int x, int y)
  // spiral motor movement
{int x1=x-27;int y1=y-27;
int x2=x+27;int y2=y+27;
int temp=y1,k;
for(int  i=0;i<35;i++)
//out to in
{ for(k=x1;k<x2;k++)
{Servo1.write(k);
Servo2.write(temp);
    lay(10); } temp=k;
   (k=y1;k<y2;k++)
Servo1.write(temp);
Servo2.write(k);
delay(10);
}temp=k;
x1++;  x2--;  y1++;
y2--;  }
for(int  i=0;i<35;i++)
//in to out
{for(k=x1;k<x2;k++
)
{ Servo1.write(k);
Servo2.write(temp);
delay(10);
 } temp=k;
for(k=y1;k<y2;k++)
{
Servo1.write(temp);
x1--;  x2++;  y1--;  y2++;
}}
void setup()
{Serial.begin(9600);
pinMode(5, INPUT);  //fire
pinMode(4, OUTPUT);
//solenoid
Servo1.attach(8);
Servo2.attach(10);
Servo1.write(0);
Servo2.write(0);
pinMode(2,INPUT);
delay(100); }
void loop()
{if(digitalRead(2)==HIGH
)     //for mouse control
 { if ( Serial.available())

if(digitalRead(5)==HIGH)
//if  fire  extinguish
command received
{digitalWrite(4,HIGH);
spiral(i,j);
digitalWrite(4,LOW);}}els
e
 //for  automatic  motor
movement
{ if (f1==0){ j++; }
else if(f1==1){ j--; }
if(j==180 || j==0){
if (f2==0){ i++;
if(f1==0){ f1=1;}
else{ f1=0;  }   }
 if(i==180 || i==0)
```

{ Servo1.write(temp); Servo2.write(k);delay(10); } temp=k; for(k=x2;k>x1;k--) {Servo1.write(k); Servo2.write(temp); delay(10); } temp=k; for(k=y2;k>y1;k--){	Servo2.write(k); delay(10); } temp=k; for(k=x2;k>x1;k--) { Servo1.write(k); Servo2.write(temp); delay(10); } temp=k; for(k=y2;k>y1;k--) {Servo1.write(temp); Servo2.write(k); delay(10); } temp=k;	{char ch = Serial.read(); switch(ch) { case '0'...'9': v = v * 10 + ch - '0'; break; case 'x': // if it's x Servo1.write(v); v = 0; break; case 'y': Servo2.write(v); v = 0; break; } }	{ if(f2==0){ f2=1; } else{ f2=0; } } } Servo1.write(i) Servo2.write(j); if(digitalRead(5)==HIGH) //if fire extinguish command received {digitalWrite(4,HIGH); spiral(i,j); digitalWrite(4,LOW); } delay(200); } }

```
import cv2
from time import sleep
import RPi.GPIO as GPIO
import pyautogui, sys
import serial
port = "/dev/ttyUSB0"    #Microcontroller Port Name
rate = 9600              #Transmission Rate
xs,ys = pyautogui.size()  #Dimentions of Display Screen
xc = xs/2     yc = ys/2
s1 = serial.Serial(port,rate)  #initiate serial communication
s1.flushInput()#Ignore any existiong error communication
state = True     #Initiate module to automatic mode
GPIO.setwarnings(False)
GPIO.setmode(GPIO.BOARD)
GPIO.setup(3,GPIO.OUT,initial=GPIO.LOW)
#Condition pin for spray
GPIO.setup(5,GPIO.OUT,initial=GPIO.LOW)
#Condition pin for motor control
fire_cascade=cv2.CascadeClassifier('fire_detection.xml')
cap=cv2.VideoCapture(1)          ex = ey = eh = ew = 0
while True:      ret,img=cap.read()      print(state)
if state:        #Start Automatic Mode
GPIO.output(5,GPIO.LOW)      gray=cv2.cvtColor(img, cv2.COLOR_BGR2GRAY)
fire=fire_cascade.detectMultiScale(gray, 4, 4)
 #Fire detect with haar cascade
nums = 0  fin = 0
cv2.rectangle(img, (310,230), (330, 250), (0,255,0), 2)
for (ex,ey,ew,eh) in fire:
cv2.rectangle(img, (ex,ey), (ex+ew, ey+eh), (255,0,0), 2)    #Highlight detected fire
roi_gray=gray[ey:ey+eh, ex:ex+ew]
roi_color=img[ey:ey+eh, ex:ex+ew]
GPIO.output(3,GPIO.HIGH)        #Initiate Water Spray
sleep(0.1)              GPIO.output(3,GPIO.LOW)
sleep(0.1)                  cv2.imshow('img',img)
if not state:    #Manual Mode
GPIO.output(5,GPIO.HIGH)
cv2.rectangle(img, (310,230), (330, 250), (0,255,0), 2)
cv2.imshow('img',img)
x, y = pyautogui.position()  #Location of cursor on screen
xsend = str((x*180)/xs)    #Move X coordinates
ysend = str((y*180)/ys)    #Move y coordinates
s1.write(xsend.encode())
      temp = str('x')
s1.write(temp.encode())
s1.write(ysend.encode())
temp = str('y')              s1.write(temp.encode())
s1.flush()                   k=cv2.waitKey(30) & 0xff
if k==ord('s'):                  #Toggle between modes
state = not state
elif k==ord('f'):                #Manual extinguisher deploy
GPIO.output(3,GPIO.HIGH)                sleep(1)
GPIO.output(3,GPIO.LOW) elif k==27:      End Program
 break    GPIO.cleanup()              cap.release()
cv2.destroyAllWindows()
```

7. Conclusion and Future Scope

A proposed system is able to extinguish fire before it reaches its destructive level. This system eliminates all the flaws and improves the damage limitation by raising an alarm. Further the Haar Cascade training used achieves accuracy of 70-75 % to detect fire. The pilot run with the training set classified sample as positive and negative images. An efficient method of fire combat is designed and developed using Machine learning technique provides the response time of 2-4 seconds. The performance of the cascade classifier depends on the competency of the ıing set. Further, it is observed that subjecting the classifier for more training improves the performance. ⁄ever, it must not be over trained. Over training the classifier would lead to overfitting. This noise and

imperfections in the training set will degrade the model. Thus optimal training is desirable. The mechanical actuation design proposed can traverse the entire volume of the room without leaving any blind spots. Further, controlling the turret remotely with an optical mouse provides a free moving experience to the user and carries out the actuation at satisfying pace with no evident latency. Provides faster response to fire breakouts. It is an efficient alternative fire combat system when fire brigade assistance is not available.

References:

1. Chityala, R., & Pudipeddi, S. (2014). Image processing and acquisition using Python. CRC Press.
2. Pajankar, A. (2017). Raspberry Pi Image Processing Programming: Develop Real-Life Examples with Python. Pillow and SciPy, India: Apress, 04.
3. Marwedel, P., & Engel, M. (2011, October). Embedded system design 2.0: rationale behind a textbook revision. In Proceedings of the 6th Workshop on Embedded Systems Education (pp. 9-16).
4. Membrey, P., & Hows, D. (2013). Learn Raspberry Pi with Linux. Apress.
5. Chen, T. H., Wu, P. H., & Chiou, Y. C. (2004, October). An early fire-detection method based on image processing. In 2004 International Conference on Image Processing, 2004. ICIP'04. (Vol. 3, pp. 1707-1710). IEEE.
6. Habiboğlu, Y. H., Günay, O., & Çetin, A. E. (2012). Covariance matrix-based fire and flame detection method in video. Machine Vision and Applications, 23(6), 1103-1113.
7. Chen, T. H., Kao, C. L., & Chang, S. M. (2003, October). An intelligent real-time fire-detection method based on video processing. In IEEE 37th Annual 2003 International Carnahan Conference on Security Technology, 2003. Proceedings. (pp. 104-111). IEEE.
8. Celik, T. (2010). Fast and efficient method for fire detection using image processing. ETRI journal, 32(6), 881-890.
9. Yamagishi, H. I. D. E. A. K. I., & Yamaguchi, J. U. N. I. C. H. I. (2000, October). A contour fluctuation data processing method for fire flame detection using a color camera. In 2000 26th Annual Conference of the IEEE Industrial Electronics Society. IECON 2000. 2000 IEEE International Conference on Industrial Electronics, Control and Instrumentation. 21st Century Technologies (Vol. 2, pp. 824-829). IEEE.
10. Privalov, G., & Privalov, D. (2001). U.S. Patent No. 6,184,792. Washington, DC: U.S. Patent and Trademark Office.
11. Cui, Y., Dong, H., & Zhou, E. (2008, May). An early fire detection method based on smoke texture analysis and discrimination. In 2008 Congress on Image and Signal Processing (Vol. 3, pp. 95-99). IEEE.
12. Jadhav, M. M., Durgude, Y., & Umaje, V. N. (2019). Design and development for generation of real object virtual 3D model using laser scanning technology. International Journal of Intelligent Machines and Robotics, 1(3), 273-291.
13. Makrand M. Jadhav, Shriram D. Markande. (2020). Performance Optimization of Polar Code Based OFDM Volte System Using Taguchi Method. International Journal of Advanced Science and Technology, 29(9s), 792 - 803.
14. Jadhav, M. M., Dongre, G. G., & Sapkal, A. M. (2019). Seamless Optimized LTE Based Mobile Polar Decoder Configuration for Efficient System Integration, Higher Capacity, and Extended Signal Coverage. International Journal of Applied Metaheuristic Computing (IJAMC), 10(3), 68-90.
15. A.O.Mulani and Dr.P.B.Mane, "Watermarking and Cryptography Based Image Authentication on Reconfigurable Platform", Bulletin of Electrical Engineering and Informatics, Vol.6 No.2, pp 181-187, 2017. DOI: 10.11591/eei.v6i2.651
16. Kulkarni P.R., Mulani A.O. and Mane P. B., "Robust Invisible Watermarking for Image Authentication", In Emerging Trends in Electrical, Communications and Information Technologies, Lecture Notes in Electrical Engineering, vol 394, pp 193-200, Springer, Singapore, 2017. DOI:10.1007/978-981-10-1540-3_20
17. Swami S. S. and Mulani A. O., "An efficient FPGA implementation of discrete wavelet transform for image compression", 2017 International Conference on Energy, Communication, Data Analytics and Soft Computing (ICECDS 2017), 2018, pp. 3385–3389
18. A.O.Mulani and Dr.P.B.Mane, "Area Efficient High Speed FPGA Based Invisible Watermarking for Image Authentication", Indian Journal of Science and Technology, Vol.9. No.39, Oct. 2016. DOI:10.17485/ijst/2016/v9i39/101888
19. A.O.Mulani and Dr.P.B.Mane, "An Efficient implementation of DWT for image compression on reconfigurable platform", International Journal of Control Theory and Applications, Vol.10 No.15, 2017.

Design Engineering

ISSN: 0011-9342 | Year 2021
Issue: 7 | Pages: 11479-11489

Design and Implementation of Resource Management Optimization Algorithm to improve QoS performance

Makarand Jadhav[1], Vivek Deshpande[2], Divya Midhunchakkaravarthy[3], Dattatray Waghole[4]

[1]Postdoctoral Fellow, Lincoln University College, Malaysia.
Associate Professor, NBN Sinhgad School of Engineering, Pune, Maharashtra (India),
makj123@yahoo.com

[2]Co-Supervisor, Lincoln University College, Malaysia.
Professor, Vishwakarma Institute of Information Technology, Pune, Maharashtra (India),
vsd.deshpande@gmail.com

[3]Supervisor, Lincoln University College, Malaysia,
divya@lincoln.edu.my

[4]Postdoctoral Fellow, Lincoln University College, Malaysia.
Associate Professor, JSPM's Jayawantrao Sawant College of Engineering, Pune, Maharashtra (India),
dattawaghole10@gmail.com

Abstract

In wireless communication, the physical layer handles radio propagation and other challenges unique to a wireless channel. Whereas, Media access control layer coordinates the access to the shared medium. This work carried out deliberates on physical as well as medium access control layers respectively. It aims to develop the algorithm to improve Quality of Service (QoS) for recommendation as well as allocation of a good channel in the presence of congestion in a dense environment. The performance of the algorithm is evaluated using network simulator NS2. The investigated algorithm focuses on improving the QoS performance of the network by throughput gain of 22.22 %, reducing packet dropping ratio by 4 %, and recommending a good channel based on the fitness function. The simulation result shows that the algorithm provides a 15% better packet delivery ratio in congestion and dense scenarios. In this paper, required QoS aimed at channel recommendation for communication using machine learning technique is achieved.

Keywords: ML, NS2, QoS, and QoE

1. Introduction

Wireless communication made revolutionary advancements in recent decades. Global System for Mobile cellular standard espoused for voice communications in 1992. A packet data network has shepherded a demand for pervasive data admittance. Successive generations of wireless standards

ISSN: 0011-9342 | Year 2021
Issue: 7 | Pages: 11479-11489

support the humorous data package to users. Further, 3G is said to be operator-centric. Whereas 4G is considered service-centric and 5G is user-centric. Resource management consists of three steps. The first step is resource allocation. It supports utilizing existing network resources. The second step is resource-leveling. It helps to realize unproductive resources. The third step is resource Forecasting. It allows predicting future resource requirements.

The key network QoS parameters are throughput, latency, jitter, packet loss, availability, and reliability. The data rate is expressed in bits/second. The tiniest throughput is guaranteed for specific services as well as applications. Whereas latency defines the delay between the data sent and received. On the other hand, jitter characterizes delay variation. Packet loss epitomizes data loss. This is a result of congestion. Availability assists to deliver services to the users with reliability.

This paper comprises five sections and contributes to the enhancement of QoS performance by proposing a resource optimization algorithm using a machine learning approach. Section two explicates the literature adopted for enhancing the performance of the 5G network. The third section presents the design of the proposed algorithm. The fourth section elaborates the result and discussion. Finally, the last section presents the conclusion followed by references.

2. Literature Survey

Currently, 3G and 4G have control of smart technology. With the increasing market demand for smart wireless technology, 5G will most likely become leaders in providing connectivity for various types of smart devices. Therefore, for today's wireless mobile communication systems, resource management is required based on fitness functions to enhance network performance.

In [1] the massive growth in mobile data traffic requires rigorous QoS requirements for 5G networks. Here, Radio Resource Management and innovative packet scheduling are proposed for bandwidth-hungry applications under dynamic network conditions. Further, reinforcement learning, as well as neural networks, is presented. It finds appropriate scheduling decisions. Smart cities are designed to adopt modern communication technology. Here, the role of various cognitive domains is explored in [2] to assure the best services of 5G and beyond 5G communications. In [3], a network slicing design is presented. It uses a fusion learning algorithm. A blend classifier to optimize deep belief and neural networks are proposed. It uses the glow-worm swarm method. In [4] a deep learning approach is proposed to replace the channel estimator. Here, links are scheduled for communication with the help of topographical locations. The reason is that the channel forte is a function of the path loss. A sum-rate optimal scheduling algorithm that provides fairness is suggested in [5]. This approach shows viable network efficacy results. A deep learning technique for a wireless network to achieve significant performance gain is offered in [5]. It reduces computations by 50%. Hence, it can solve network optimization complications effectually.

ISSN: 0011-9342 | Year 2021
Issue: 7 | Pages: 11479-11489

Optimization of QoS in wireless networks requires well-organized channel allocation schemes. A modified Erlang-B dynamic channel allocation scheme is explained in [7]. It can expand network performance. This approach improved capacity as well as the quality of experience. In the present pandemic situation, data demand, as well as plans, is improved with various broadband networks for smartphones [8]. But industry and researchers are adopting 5G network. It provides services with diverging and technically stimulating user necessities. However, the network configuration, management, and planning have tremendously become thought-provoking. In [9], a bioinspired solution is demonstrated that achieves optimality in computations.

Currently, resource management techniques using machine learning emerged as a boisterous way to achieve QoS performance. A work proposed in [11] with learning to optimize as well as manage available resources. An analysis of machine learning (ML) to enhance network performance and achieve acceptable QoS/QoE is defined in [12]. Machine learning is useful to extract as well as predict trends. In universal, interference is evaluated at the physical layer. Further, link superiority is predicted at the data-link layer. Whereas, traffic demand is estimated at the network layer. The utility of training and learning in communication is gaged in [13].

It finds applications in clustering, routing as well as base-station switching control. In the end, 5G in [15] purposes efficacy of network optimization. It helps to make use of the resources. This resulted in achieving better capacity and QoS. This paper aims in developing an algorithm to improve QoS for the allocation of a good channel using machine learning techniques in the presence of congestion in a dense environment. In this work, performance metrics considered are throughput, packet dropping ratio, and packet delivery ratio.

3. Design and Implementation of Resource optimization Algorithm

A mobile unit is called a node that communicates with the central station. This center station is located at the upper corner called a router or Data collector. The router is connected to the outer network through wireless or Fiber. A channel recommendation algorithm runs inside the wireless router. The application targeted is a Smart Factory as shown in Fig. 1 For a particular node, one channel is assigned for communications. Further, the router decides which channel is to be recommended for every node. The channel with the highest fitness i.e. having very good QoS is assigned first, followed in descending order. Data give and take policy happens with the recommended channel. This entire record is maintained to build the data when the channel is released. This record is useful next time for channel recommendation to build up a data log. The work regarding channel recommendation with and without machine learning techniques is proposed

Design Engineering
ISSN: 0011-9342 | Year 2021
Issue: 7 | Pages: 11479-11489

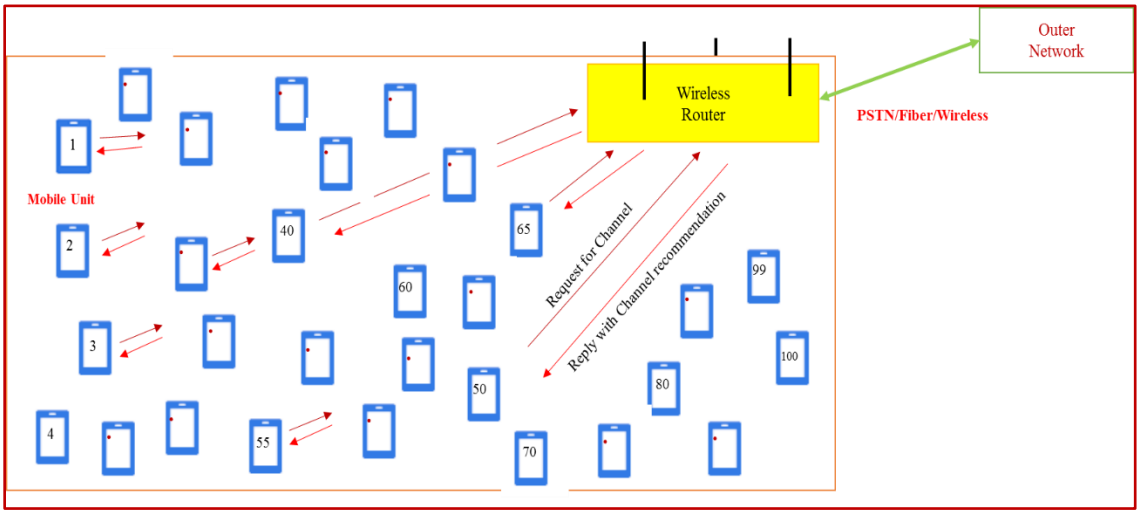

Fig. 1 Simulation Scenario for Smart Factory

. Simulations are carried out as per the settings shown in Table 1. The proposed algorithm is simulated using NS2.

Table 1. Simulation Parameters

Parameters	Particulars
Node Density	250
Node Speed	3 m/sec
Reporting Rate	50 packets/sec
Queue Length	100 packets
Energy	10 Joules
Packet Size	250 bytes
Simulation Area	1000 cm x 1500 cm
Simulation Time	50 sec
Channel Type	Mobile Nodes

Packet dropping ratio, packet delivery ratio, and throughput are used as performance metrics. They are observed against the changing size, the number of interfering nodes, and simulation time. Further, the effect of network congestion is studied. The metric evaluated is packet dropping ratio as well as throughput. The packet size, simulation time, and node density are rehabilitated in this simulation scenario.

ISSN: 0011-9342 | Year 2021
Issue: 7 | Pages: 11479-11489

4. Results and discussions

The general flow chart for Resource Management Optimization Approach to improve 5G Network performance is given in Fig. 2.

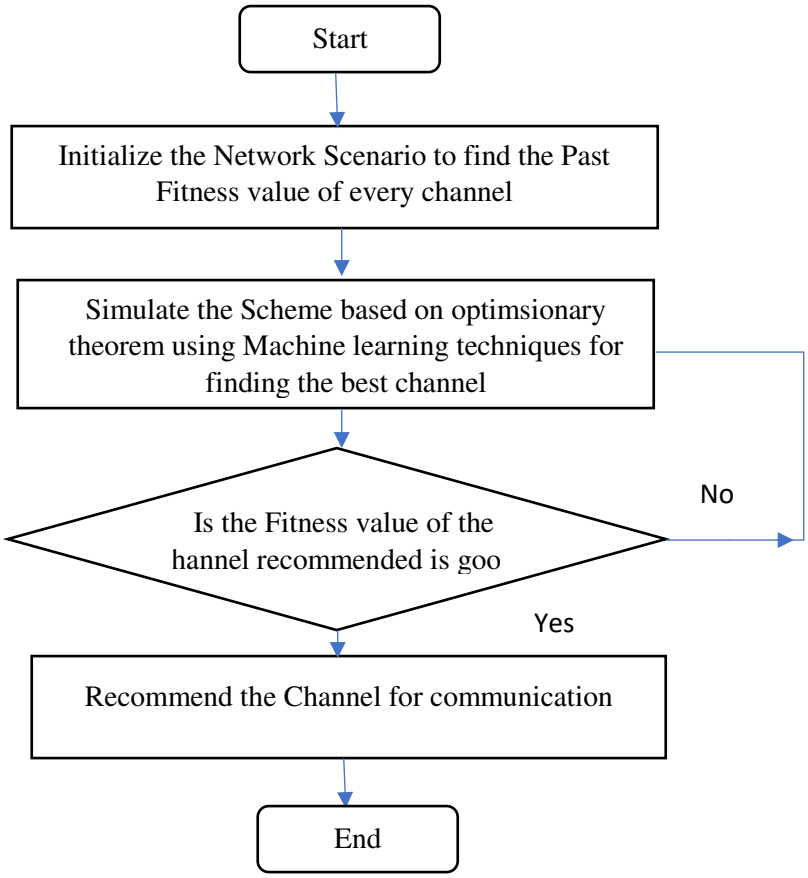

Fig. 2 Flowchart to evaluate network performance

The scheduling component is important at the access layer. It determines which users are active in a specified stint slot. Whereas, resource allocation is another mechanism at the physical layer of the wireless network. It assigns bandwidth as well as the power to the users. In this work, the experiment is to be done for channel selection based on QoS factors such as throughput, packet drop ratio, and Packet loss ratio.

A machine learning technique is designed and investigated for a 5G network. Packet dropping ratio and throughput are used as performance metrics. They are observed against the change in packet size, the number of nodes, and simulation time. Here, the size of the packet is altered in discrete steps. Fig. 3 and Fig. 4 illustrate the result of a change in packet size on considered performance metrics. A configuration of the algorithm and network setting is kept specifically for this experimentation. It is observed that changing the packet size is crucial in determining the

ISSN: 0011-9342 | Year 2021
Issue: 7 | Pages: 11479-11489

packet dropping ratio. The algorithm updates the channel recommendation table for subsequent channel allocation. This results to maintain a packet dropping ratio generally steady in the range of 7 to 18 %.

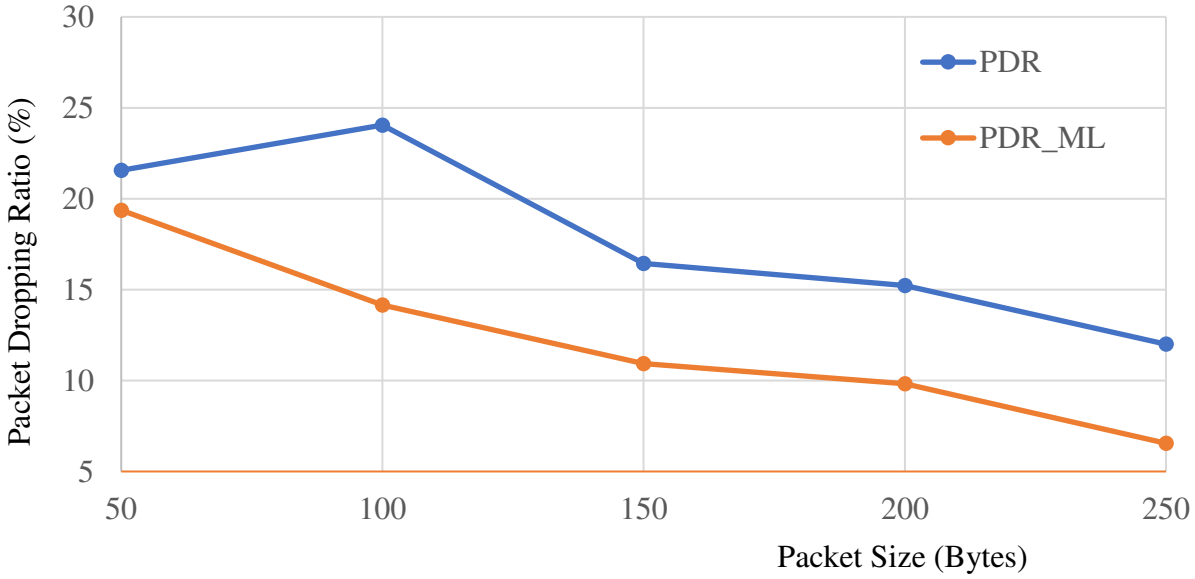

Fig. 3 Packet Dropping Ratio vs Packet Size

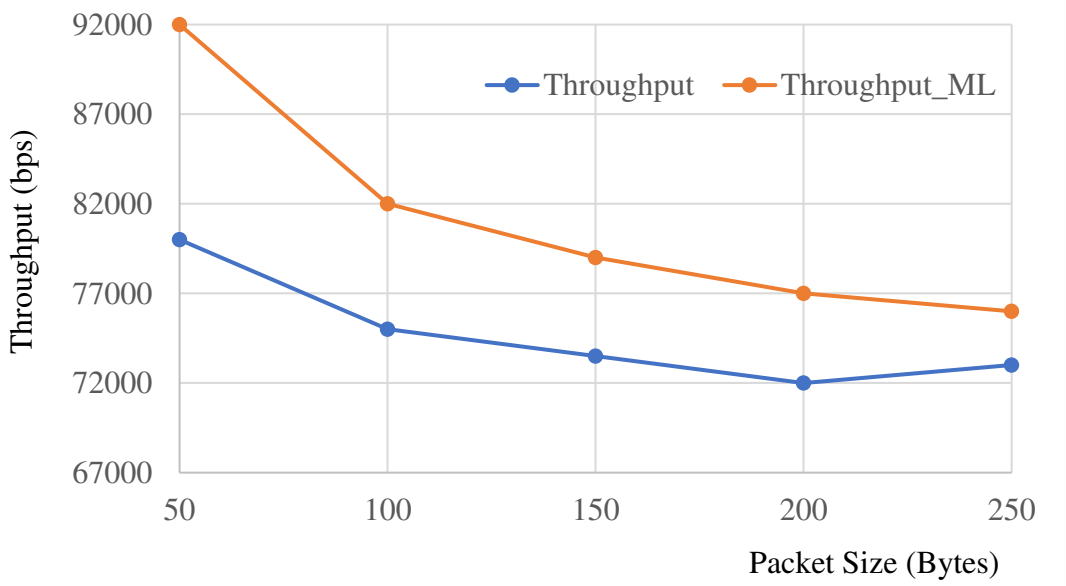

Fig. 4 Throughput vs Packet Size

Fig. 4 compares throughput with and without training the network for varying packet sizes. It is changed in distinct steps in the range of 50 to 250 bytes. The universal inclination is that an increase in the size of the packet decreases throughput. Thus, the proposed algorithm provides a

ISSN: 0011-9342 | Year 2021
Issue: 7 | Pages: 11479-11489

well-adjusted decrease in packet dropping ratio as well as throughput. It achieves a maximum 13.04 % improvement as compared with the network without training the network. A total of 65, 000 frames were transmitted. Thereafter, the packet loss ratio is evaluated. It is pragmatic that as the size of packet increases in distinct step in the range 50 to 250 bytes, decreases the total count of efficacious delivered packets. The algorithm had a total of 62,100 packets delivered at a packet size of 50 bytes as revealed in Fig. 5. The least gain achieved over with training is 9.73 %.

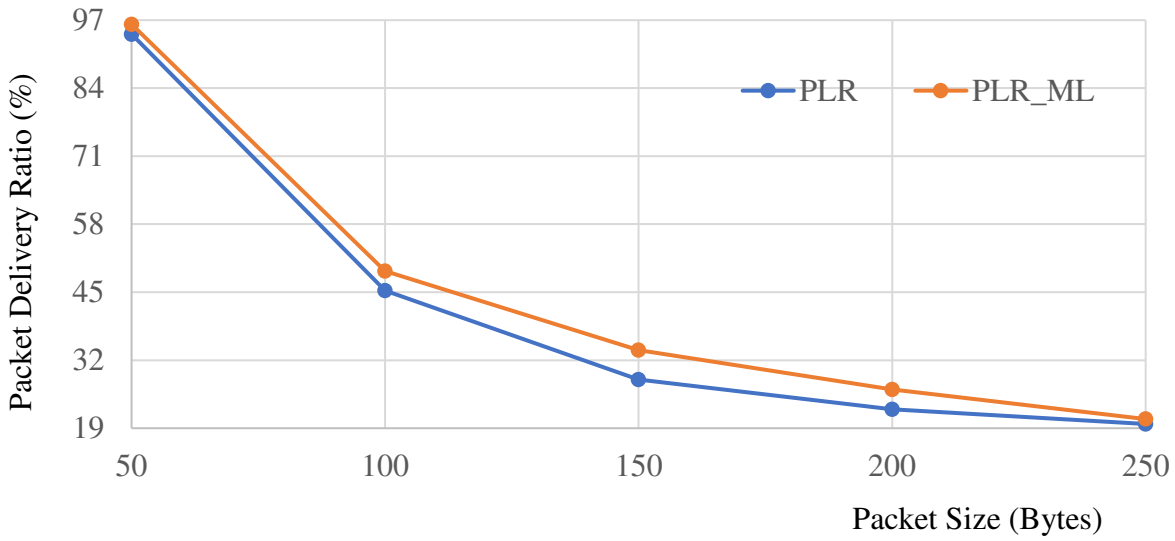

Fig. 5 Packet Delivery Ratio vs Packet Size

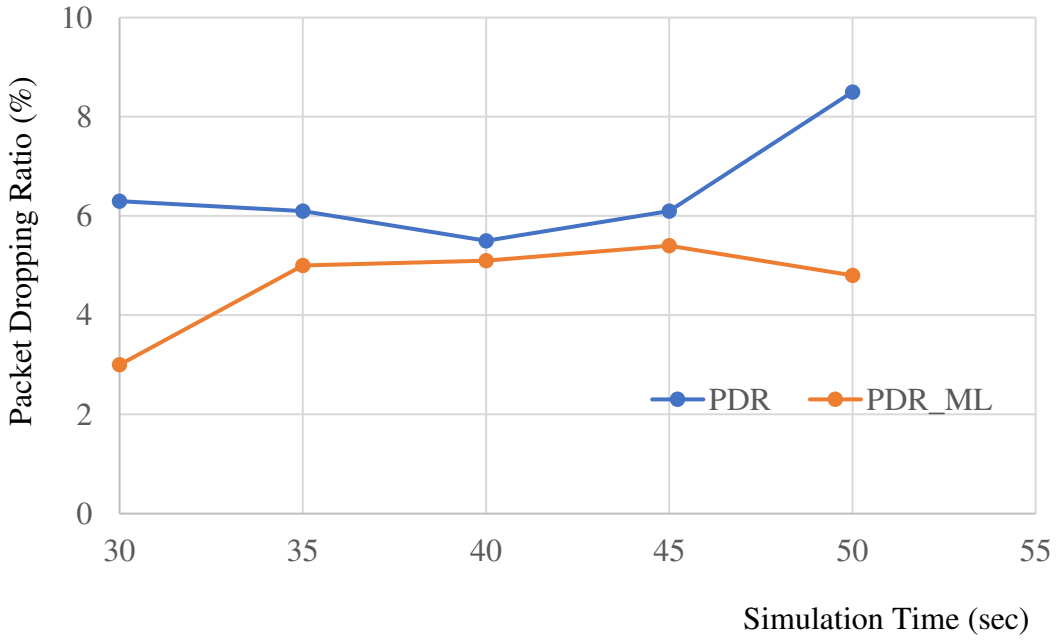

Fig. 6 Packet Dropping Ratio vs Simulation Time

ISSN: 0011-9342 | Year 2021
Issue: 7 | Pages: 11479-11489

Fig.6 shows packet dropping ratios with and without training the network against time. The packet dropping ratio starts with a modest 4 % with a machine learning algorithm. The dropping ratio shoots up and decreases thereafter. Fig.7 displays throughput with and without training the system. The throughput achieved increases steadily. A proposed data set used for training can recommend a good channel. It achieves a maximum throughput gain of 22.22 %.

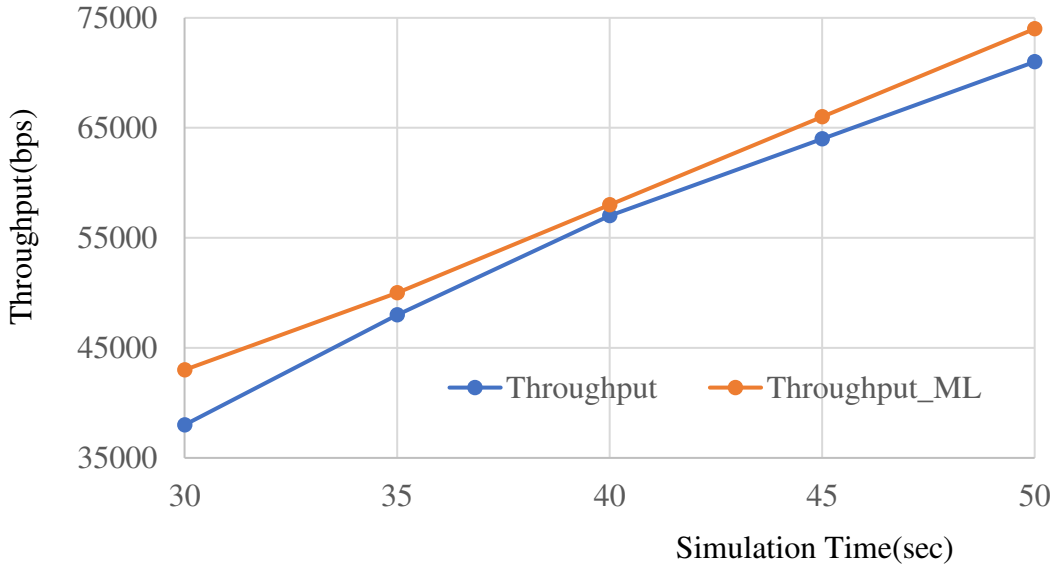

Fig. 7 Throughput vs Simulation Time

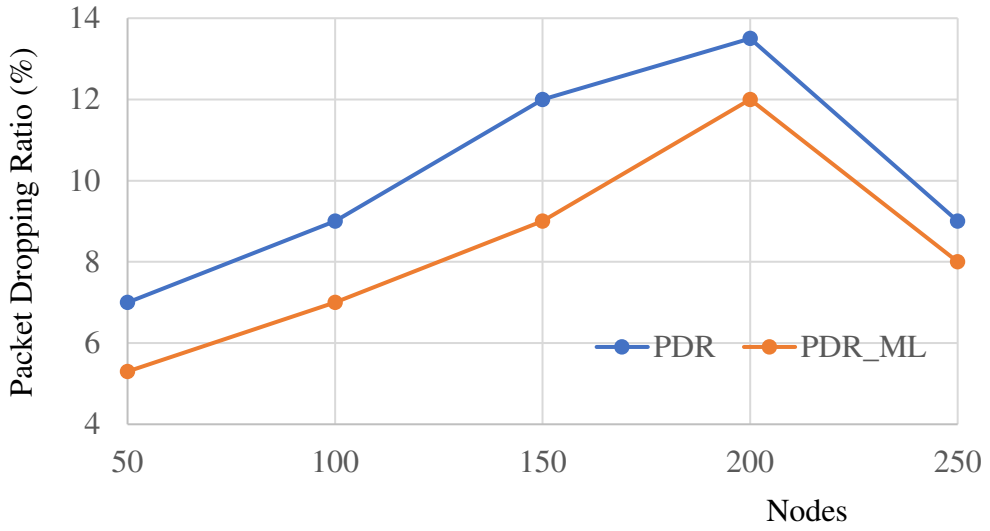

Fig. 8 Packet Dropping Ratio vs Nodes

ISSN: 0011-9342 | Year 2021
Issue: 7 | Pages: 11479-11489

Fig. 8 and Fig. 9 portray the consequence of node density to evaluate performance metrics. Here, nodes are increased again in a distinct range to measure packet drop ratio as well as throughput. In this simulation, 85,000 frames are transmitted. In general, node mobility increases the collision probability. A packet drop ratio perfectly maps to an equal reduction in throughput. This correlation occurs at the node density count equal to 200. The proposed algorithm can achieve a maximum packet drop ratio enhancement of 12.5 % at a node density of 250. Further, a throughput gain of 7.24 % is also achieved as compared to an algorithm without machine learning.

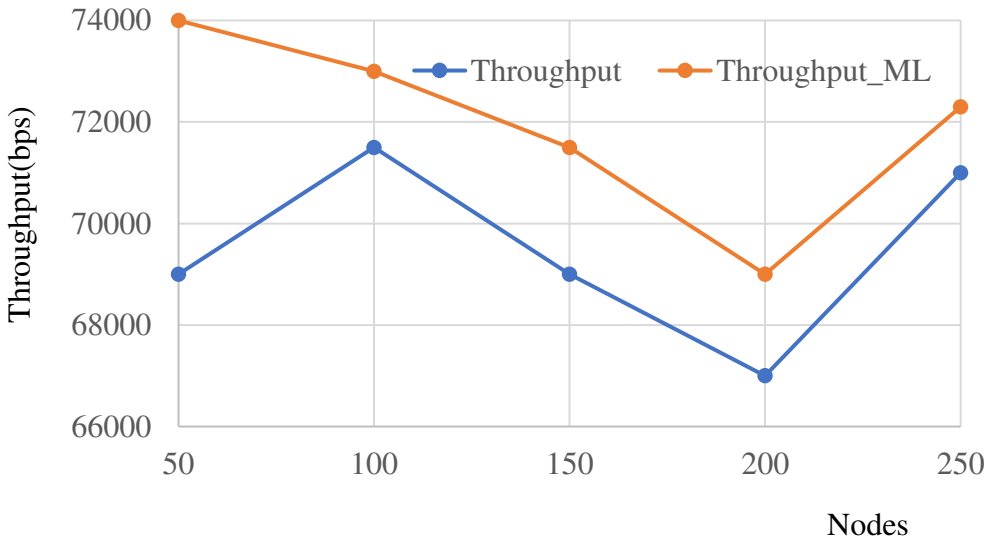

Fig. 9 Throughput vs Nodes

5. Conclusion

The key focus of the work is designing an algorithm to enhance the QoS performance of the network. The algorithm is implemented in a network simulator. The performance metric evaluated are packets drop ratio, packet loss ratio, and throughput. The investigated algorithm focuses on maximizing throughput. In this paper, a machine learning technique is proposed to train the network. For mobile nodes, though it keeps the highest throughput, its performance is at par as nodes density increases. It provides acceptable throughput as well as packet delivery for varying packet size, simulation time, and node density. The simulation result obtained for the presented scenario can attain improvement in Quality of Service by training the network for given traffic scenarios.

References

1. Comșa, I. S., Trestian, R., Muntean, G. M., & Ghinea, G. (2019). 5MART: A 5G sMART scheduling framework for optimizing QoS through reinforcement learning. IEEE Transactions on Network and Service Management, 17(2), 1110-1124.

ISSN: 0011-9342 | Year 2021
Issue: 7 | Pages: 11479-11489

2. Ullah, Z., Al-Turjman, F., Mostarda, L., & Gagliardi, R. (2020). Applications of artificial intelligence and machine learning in smart cities. Computer Communications, 154, 313-323.
3. Abidi, M. H., Alkhalefah, H., Moiduddin, K., Alazab, M., Mohammed, M. K., Ameen, W., & Gadekallu, T. R. (2021). Optimal 5G network slicing using machine learning and deep learning concepts. Computer Standards & Interfaces, 76, 103518.
4. Cui, W., Shen, K., & Yu, W. (2019). Spatial deep learning for wireless scheduling. IEEE Journal on Selected Areas in Communications, 37(6), 1248-1261.
5. Liu, L., Yin, B., Zhang, S., Cao, X., & Cheng, Y. (2018). Deep learning meets wireless network optimization: Identify critical links. IEEE Transactions on Network Science and Engineering, 7(1), 167-180.
6. Marne, H., Mukherji, P., Jadhav, M., & Paranjape, S. (2021). Bio-inspired hybrid algorithm to optimize pilot tone positions in polar-code-based orthogonal frequency-division multiplexing–interleave division multiple access system. International Journal of Communication Systems, 34(3), e4676.
7. Asuquo, D., Ekpenyong, M., Udoh, S., Robinson, S., & Attai, K. (2020). Optimized channel allocation in emerging mobile cellular networks. Soft Computing, 24, 16361-16382.
8. Santos, G. L., Endo, P. T., Sadok, D., & Kelner, J. (2020). When 5G meets deep learning: a systematic review. Algorithms, 13(9), 208.
9. Fu, S., Yang, F., & Xiao, Y. (2020). AI Inspired Intelligent Resource Management in Future Wireless Network. IEEE Access, 8, 22425-22433.
10. Jadhav, M. M., Dongre, G. G., & Sapkal, A. M. (2019). Seamless Optimized LTE Based Mobile Polar Decoder Configuration for Efficient System Integration, Higher Capacity, and Extended Signal Coverage. International Journal of Applied Metaheuristic Computing (IJAMC), 10(3), 68-90.
11. Shen, Y., Shi, Y., Zhang, J., & Letaief, K. B. (2019). LORM: Learning to optimize for resource management in wireless networks with few training samples. IEEE Transactions on Wireless Communications, 19(1), 665-679.
12. Kulin, M., Kazaz, T., De Poorter, E., & Moerman, I. (2021). A survey on machine learning-based performance improvement of wireless networks: PHY, MAC and network layer. Electronics, 10(3), 318.
13. Sun, Y., Peng, M., Zhou, Y., Huang, Y., & Mao, S. (2019). Application of machine learning in wireless networks: Key techniques and open issues. IEEE Communications Surveys & Tutorials, 21(4), 3072-3108.
14. Dattatray S Waghole, Vivek S Deshpande, “Characterization of wireless sensor networks for traffic & delay”, IEEE conf on Cloud & Ubiquitous Computing & Emerging Technologies, pp. 69-72, 2013.
15. Martin, A., Egaña, J., Flórez, J., Montalbán, J., Olaizola, I. G., Quartulli, M., ... & Zorrilla, M. (2018). Network resource allocation system for QoE-aware delivery of media services in 5G networks. IEEE Transactions on Broadcasting, 64(2), 561-574.

ISSN: 0011-9342 | Year 2021
Issue: 7 | Pages: 11479-11489

16. Dattatray S Waghole, Vivek S Deshpande, "Reducing delay data dissemination using mobile sink in wireless sensor networks", international Journal of Soft Computing and Engineering (IJSCE), vol 3 issue 1, pp. 305-308, 2013.
17. Jadhav, M. M. (2021). Machine Learning based Autonomous Fire Combat Turret. Turkish Journal of Computer and Mathematics Education (TURCOMAT), 12(2), 2372-2381.

Design Engineering

ISSN: 0011-9342 | Year 2021
Issue: 7 | Pages: 11470-11478

Position Aware Congestion Control (PACC) algorithm for Disaster Management System using WSN to improve QoS

Dattatray Waghole[1], Vivek Deshpande[2], Divya Midhunchakkaravarthy[3], Makarand Jadhav[4]

[1]Postdoctoral Fellow, Lincoln University College, Malaysia.
Associate Professor, JSPM's Jayawantrao Sawant College of Engineering, Pune, Maharashtra (India),
dattawaghole10@gmail.com
[2]Co-Supervisor, Lincoln University College, Malaysia.
Director, Vishwakarma Institute of Information Technology, Pune, Maharashtra (India),
[3]Supervisor, Lincoln University College, Malaysia
[4]Postdoctoral Fellow, Lincoln University College, Malaysia.
Associate Professor NBN Sinhgad School of Engineering, Pune, Maharashtra (India),
makj123@yahoo.com

Abstract

Because of its technical advancements in processors, communication, and low-power utilisation of embedded computing devices, WSN (Wireless Sensor Network) is currently the most widely used service in corporate and industry use. The wireless sensor network design is made up of nodes that monitor variables such as temperatures, humidity, pressure, location, vibration, and sound. These sensor nodes can be used in a variety of real-time applications to perform tasks such as smart monitoring, neighbouring node discovery, information transmission & storing, collection of data, target tracking, supervise and track, synchronisation, node mapping, and efficient routing among the base station and nodes. WSNs are currently being arranged in a more advanced manner. Congestion and collisions are the biggest problems in WSNs. To address this issue, the author introduced the PACC protocol, which contributes to the achievement of good QoS in WSNs such as latency, data delivery ratio, loss ratio, and network channel efficiency. PACC is invented with regression model of Machine learning to improve results. Applications such as patient monitoring systems and disaster management systems operate in real time. Congestion and traffic management are major challenges. This protocol aids in the resolution of this issue and improves network reliability.

Keywords: wireless sensor networks, sensor nodes, congestion and traffic, disaster management system.

Design Engineering
ISSN: 0011-9342 | Year 2021
Issue: 7 | Pages: 11470-11478

I. Introduction

A wireless sensor network is a collection of geographically dispersed distributed devices that use sensors to track physical and environmental variables. WSNs are made up of a variety of nodes that range in size from a few to hundreds or even thousands of node, which are connected to one or more sensors as desired. A sensor node is made up of a radio transceiver with an integrated antenna, a microprocessor for communicating with the sensors, and an energy source, which is typically a battery. The size of a sensor node can be tiny or large. Sensor nodes can range in price from a few hundred dollars to tens of thousands of dollars. A WSN's nodes communicate with a base station, also known as a sink. These massive numbers of nodes communicate wirelessly with one another and with the base station, and are able to sense data from their surroundings, store it, send it to neighbouring sensor nodes or the base station, and do calculations on it. WSN uses include physical security, air traffic control, environmental monitoring, healthcare monitoring, military, and others. Depending on the application, sensor networks might be very different.

The sensor node is a low-power wireless device that can be used for a variety of tasks. Sensor nodes are used in a variety of industrial settings. A cluster of sensor nodes collects data from the environment to meet specified application goals. Nodes can connect with each other thanks to transceivers. In a wireless sensor network, the number of sensor nodes might range from hundreds to thousands. Unlike sensor networks, ad hoc networks will have few nodes and no architecture.

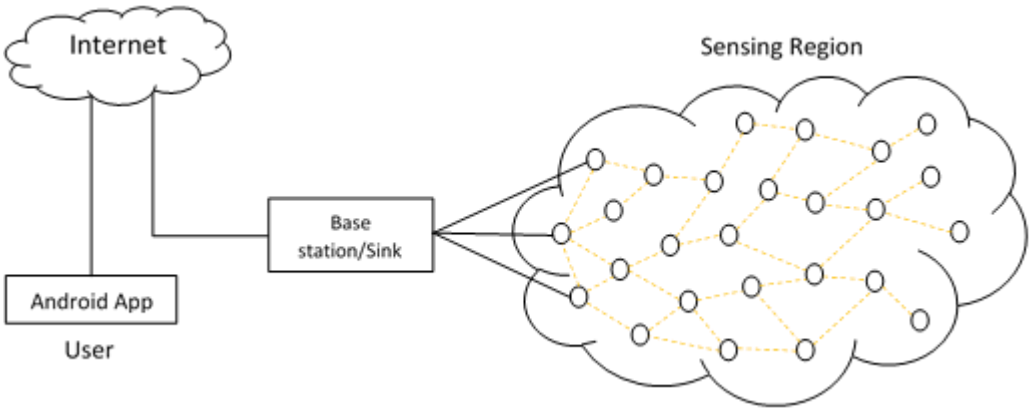

Fig.1 Architecture of Wireless Sensor Network

A wireless sensor network (WSN) is made up of one or more sink nodes and spatially distributed sensors (also called base stations). Sensors generate sensory data by continuously measuring physical elements like temperature, vibration, and motion. A sensor node can be a data source as well as a data router. A drain, on the other hand, receives data from sensors. Sensors must convey data to the sink(s) in an event monitoring application, for example, when they identify the occurrence of events of interest. To communicate with the end-user, direct connections, the Internet, satellite, or any type of wireless communication can be employed. The diagram depicts a typical WSN architecture shown in Fig. 1.

ISSN: 0011-9342 | Year 2021
Issue: 7 | Pages: 11470-11478

II. Literature Survey:

WSN congestion [1] may decrease the chances of a successful data transfer, decrease the quality of transmission service, and result in higher energy usage from new transmitting data. As a result, network congestion control measures must be managed. The PI queue congestion algorithm, PID queue congestion algorithm, PID queue congestion algorithm, and PI algorithm were simulated and compared in response to circumstances such as intermediate node congestion, severe performance deterioration, and high packet loss rate. as well as the PNPID algorithm It can be determined that, in most circumstances, the PNPID method can either stabilise or reduce the queue length at a position close to the expected value at various bit rates. The fluctuation of queue length is similarly low, indicating the PNPID algorithm's stability. The packet loss rate and waiting time of the PNPID method are improved when compared to the other three algorithms, demonstrating the PNPID algorithm's superior performance.

This research provided [2] a WSN reliability model that is generated automatically using the WSN architecture, as well as information on the routing methods employed and the mote's battery state. According to this paradigm, WSNs can fail in two places: connections and sensor nodes. The proposed models were evaluated using three scenarios. It was simple to show how the routing protocol, number of nodes in the area, and distance between these regions and the sink node all affect the region's reliability using these situations. In this paper, we studied at [3] the throughput and delay of wireless sensor networks using directional antennas. This study will look into the benefits of using directional antennas. Our findings apply to wireless ad hoc network latency investigations as well. We discovered that using directional antennas increases network throughput capacity while minimising multi-hop transmission delay. In reality, using directional antennas can minimise interference significantly, resulting in higher throughput. Additionally, directional antennas can increase transmission range, resulting in fewer hops.

III. Proposed PACC Algorithm for Smart Disaster management

The general flow chart for PACC algorithm is given in Fig. 2.

ISSN: 0011-9342 | Year 2021
Issue: 7 | Pages: 11470-11478

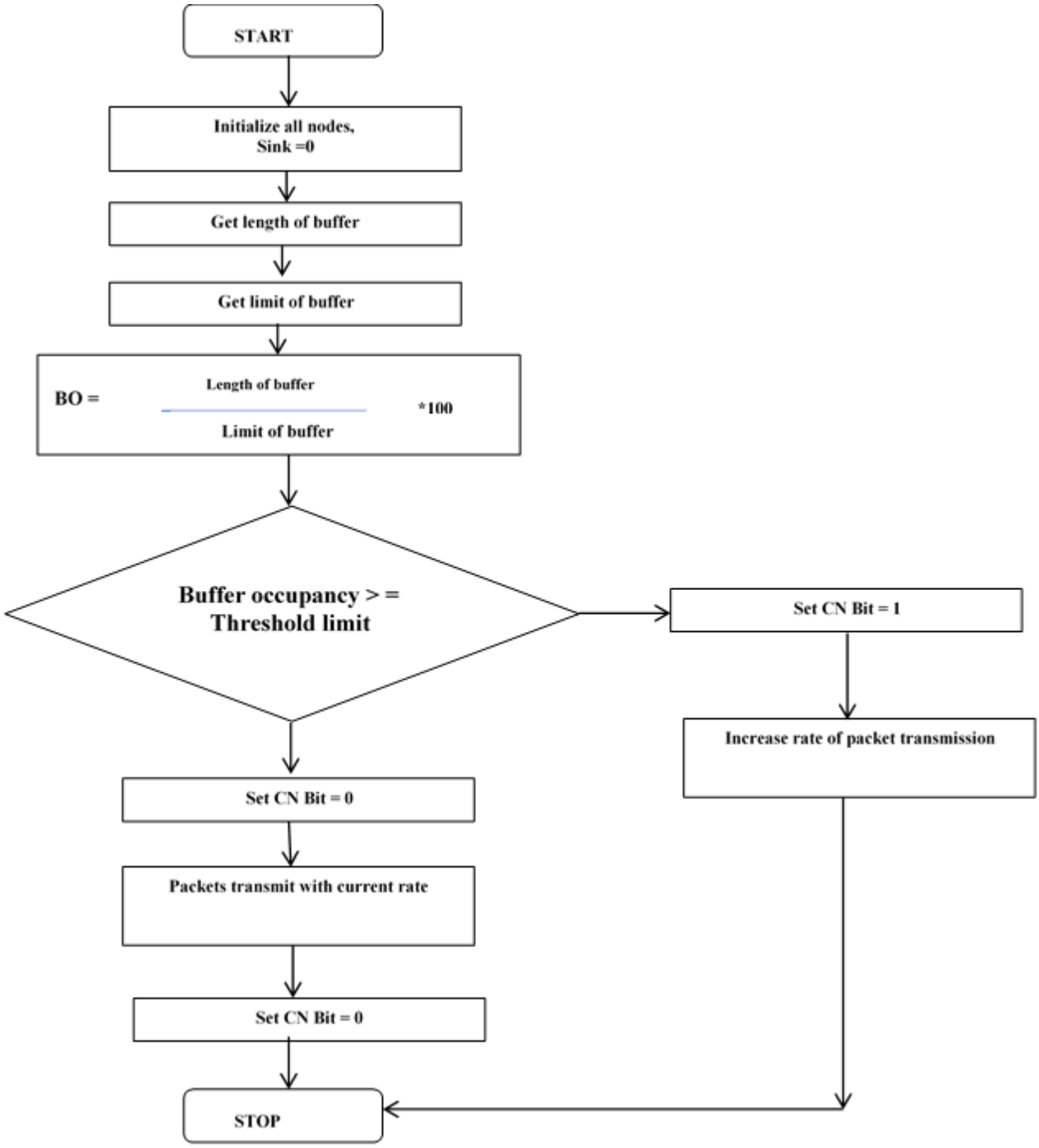

Fig 2. Flowchart: PACC technique

Result Analysis: -

Tool Used	NS2
Number of nodes	30
Packet Size	50,100,150,200,250

ISSN: 0011-9342 | Year 2021
Issue: 7 | Pages: 11470-11478

Reporting Rate	10 packets/sec
Routing Protocol	AODV
MAC Protocol	CSMA,TDMA, 802.15.4 (ZigBee), PACC (With ML)

1. Average PDR for Packet size

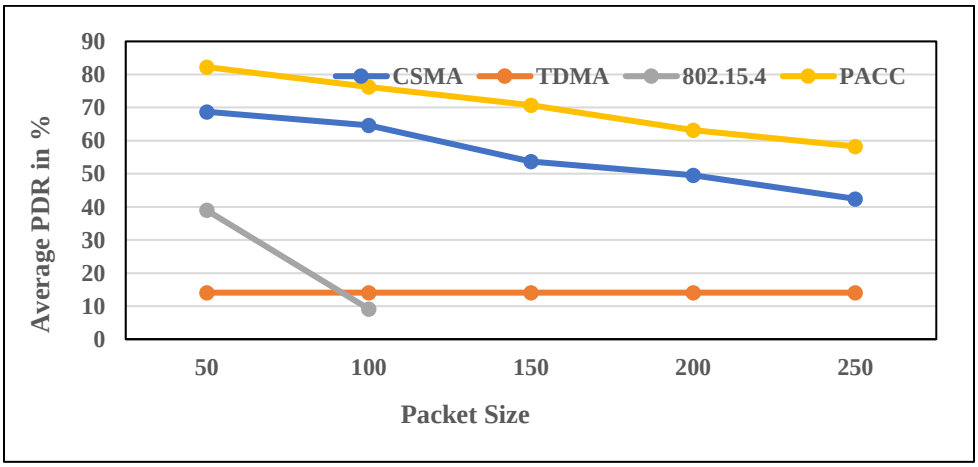

Figure 3. Average PDR for Packet Size

The average PDR for packet size in bytes is shown in Figure 3.In wireless sensor networks, a large number of packets successfully transmitted determine PDR. When compared to other protocols, PACC performs better. It achieves 10 to 16 percent better results than CSMA protocols and 30 to 55 percent better PDR results than ZigBee and TDMA protocols. An adaptive reporting rate management mechanism in the PACC protocol aids in increasing the packet delivery ratio in wireless sensor networks. The congestion notification bits (CN Bits) in each node's buffer are used by PACC. After the buffer surpasses the buffer's threshold value, the congestion notice bit is set. PACC increases the reporting rate for data packets to the sink node automatically. As a result, PACC's results are superior to those of other protocols. PACC initially outperforms for PDR while the packet size is 50 bytes, but as the packet size is increased to 250 bytes, the performance of the all-protocol drops. The 802.15.4 MAC returns results for packet sizes of 50 and 100 bytes. It doesn't deliver results after the 100-byte packet size since the node can only transmit the 100-byte packet size packet to the sink node.

ISSN: 0011-9342 | Year 2021
Issue: 7 | Pages: 11470-11478

2. Average PLR for Packet Size

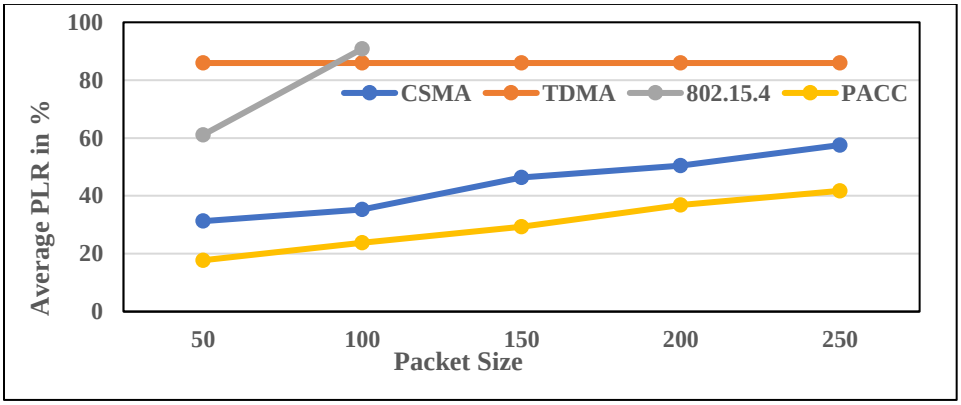

Figure 4. Average PLR for Packet size

The average PLR for packet size in bytes is shown in Figure 4. PACC adjusts the current reporting rate of nodes based on network conditions or congestion. When the congestion notification bit is set, the packet transmission rate from source to destination is increased. The PACC MAC Protocol can handle packets of up to 50 bytes. However, when the packet size changes between 50 and 250 bytes, the PLR's performance deteriorates. Congestion rises in accordance with the increase in packet size. However, the PACC protocol has a packet loss ratio that is 12 to 16 percent better than CSMA and 34 to 59 percent better than ZigBee and the TDMA protocol.

3. Average Delay for Packet Size

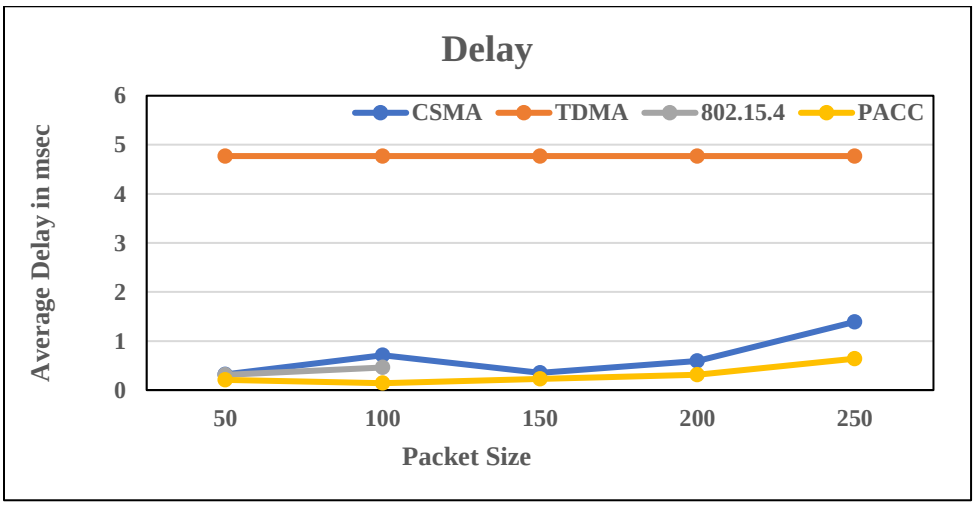

Figure 5. Average Delay for Packet Size

Figure 5 depicts the average EE latency as a function of packet size in bytes. An EE delay is the average time it takes to move packets from one point to another. The speed at which packets are transmitted from one point to another is affected by network congestion and traffic. The PACC

ISSN: 0011-9342 | Year 2021
Issue: 7 | Pages: 11470-11478

protocol achieves a lower average delay, and node congestion notification alerts the user when the packets' buffers are full. PACC automatically increases the rate of data transmission from the source to the sink node, resulting in a low average EE delay parameter when compared to other protocols When compared to other algorithms, it produces a 10 to 12 percent superior result. When compared to the TDMA protocol, PACC provides 40 to 50% better outcomes for the delay. Initially, the PACC protocol has a minimum delay of 50 bytes packet size, but after that, the packet size varies from 50 to 250 bytes, and the PACC protocol's delay grows somewhat.

4. Average Throughput for Packet Size

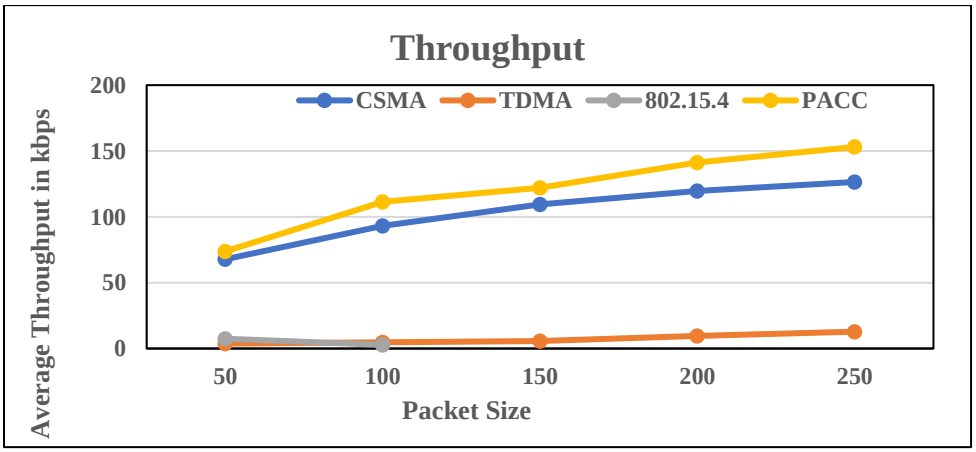

Figure 6. Average Throughput for Packet Size

Figure 6 shows the average throughput by packet size. PACC is a protocol for controlling the RR. For packet transmission to the sink node, the PACC protocol uses the appropriate communication channel. The performance of PACC is superior to that of other algorithms. When compared to the CSMA protocol, it performs 12 to 15% better and 24 to 54 percent better than ZigBee and the TDMA algorithm.

IV. Conclusion

PACC is a WSN MAC that uses "position aware congestion control." A network congestion handling algorithm is proposed. The PACC protocol's operation is dynamic, depending on network congestion and node buffer occupancy. WSN performance is influenced by congestion at the node and link levels. PACC's performance was evaluated and compared to that of Zigbee, CSMA, and TDMA protocols. The PACC's average PDR performance against packet size is better than that of other protocols. PACC outperforms CSMA by ten to twenty-two percent, TDMA by 37 to 64 percent, and ZigBee by 35 to 72 percent. For packet sizes 50 and 100 bytes, PACC's average PLR performance is 10 to 21% better than CSMA, 29 to 58 percent better than TDMA, and 42 to 71 percent better than 802.15.4. PACC has been found to have a higher average throughput than protocols. It has an average throughput of 8 to 12 percent higher than CSMA, 28 to 61 percent higher than TDMA, and 25 to 46 percent higher than 802.15.4. The PACC protocol's EE delay

ISSN: 0011-9342 | Year 2021
Issue: 7 | Pages: 11470-11478

performance is shown to be 12 percent better than CSMA, up to 5% better than ZigBee, and 48 to 52 percent better than TDMA. As a result, the PACC protocol's overall performance is excellent, and it is effective in attaining QoS in WSN. Future study is needed to enhance parameters such as control overheads and energy usage using PACC in relation to WSN, as well as to create a hybrid MAC protocol to meet all QoS criteria.

Reference:

[1] E. F. Ahmed Elsmany, M. A. Omar, T. Wan and A. A. Altahir, "EESRA: Energy Efficient Scalable Routing Algorithm for Wireless Sensor Networks," IEEE Access, vol. 7, pp. 96974-96983, 2019, doi: 10.1109/ACCESS.2019.2929578.

[2] W. Wu, N. Xiong and C. Wu, "Improved clustering algorithm based on energy consumption in wireless sensor networks," in IET Networks, vol. 6, no. 3, pp. 47-53, 5 2017, doi: 10.1049/iet-net.2016.0115.

[3] Deepak Mehtra,Sharad Saxen,"MCH-EOR: Multi-objective Cluster Head Based Energy-aware Optimized Routing algorithm in Wireless Sensor Networks",Sustainable Computing: Informatics and Systems, Vol.28, 2020

[4] K. Haseeb, N. Islam, A. Almogren and I. Ud Din, "Intrusion Prevention Framework for Secure Routing in WSN-Based Mobile Internet of Things," IEEE Access, vol. 7, pp. 185496-185505, 2019, doi: 10.1109/ACCESS.2019.2960633.

[5] Dattatray S Waghole, Vivek S Deshpande, “Characterization of wireless sensor networks for traffic & delay”, IEEE conf on Cloud & Ubiquitous Computing & Emerging Technologies, pp. 69-72, 2013.

[6] M. Premkumar, T.V.P. Sundararajan,"DLDM: Deep learning-based defense mechanism for denial of service attacks in wireless sensor networks", Microprocessors and Microsystems, Vol.79, 2020

[7] V. Bibin Christopher, J. Jasper,"Jellyfish Dynamic Routing Protocol with Mobile Sink for Location Privacy and Congestion Avoidance in Wireless Sensor Networks", Journal of Systems Architecture, July 2020

[8] Dattatray S Waghole, Vivek S Deshpande, “Reducing delay data dissemination using mobile sink in wireless sensor networks”, international Journal of Soft Computing and Engineering (IJSCE), vol 3 issue 1, pp. 305-308, 2013.

[9] S. Anitha, P. Jayanthi, V. Chandrasekaran,"An Intelligent Based Healthcare Security Monitoring Schemes For Detection Of Node Replication Attack In Wireless Sensor Networks", Measurement, 2020.

[10] Thomas Haakensen and Preetha Thulasiraman,"Enhancing Sink Node Anonymity in Tactical Sensor Networks using a Reactive Routing Protocol", IEEE, 2018

[11] Jadhav, M. M. (2021). Machine Learning based Autonomous Fire Combat Turret. Turkish Journal of Computer and Mathematics Education (TURCOMAT), 12(2), 2372-2381.

ISSN: 0011-9342 | Year 2021
Issue: 7 | Pages: 11470-11478

[12] Roberto Milton Scheffel, Antônio Augusto Fröhlich,"FT-TSTP: A Multi-Gateway Fully Reactive Geographical Routing Protocol to Improve WSN Reliability", IEEE, 2018

[13] Yang, X., Chen, X., Xia, R., & Qian, Z. (2018). Wireless Sensor Network Congestion Control Based on Standard Particle Swarm Optimization and Single Neuron PID. Sensors, 18(4), 1265.

[14] Marne, H., Mukherji, P., Jadhav, M., & Paranjape, S. (2021). Bio-inspired hybrid algorithm to optimize pilot tone positions in polar-code-based orthogonal frequency-division multiplexing–interleave division multiple access system. International Journal of Communication Systems, 34(3), e4676.

[15] Dâmaso, A., Rosa, N., & Maciel, P. (2014). Reliability of Wireless Sensor Networks. Sensors, 14(9), 15760–15785.

[16] Dai, H. (2009). Throughput and delay in wireless sensor networks using directional antennas. 2009
International Conference on Intelligent Sensors, Sensor Networks and Information Processing (ISSNIP).

[17] Jadhav, M. M., Dongre, G. G., & Sapkal, A. M. (2019). Seamless Optimized LTE Based Mobile Polar Decoder Configuration for Efficient System Integration, Higher Capacity, and Extended Signal Coverage. International Journal of Applied Metaheuristic Computing (IJAMC), 10(3), 68-90.

IJCRT.ORG ISSN : 2320-2882

INTERNATIONAL JOURNAL OF CREATIVE RESEARCH THOUGHTS (IJCRT)

An International Open Access, Peer-reviewed, Refereed Journal

Design Modification and Fatigue Life Analysis of Pressure Vessel Filter Tube Sheet

Mr. Suraj Gaikwad[#1], Prof. Ravikant K. Nanwatkar[*2]

[#]*Department of Mechanical Engineering, STES's NBNSSOE, Pune, Savitribai Phule Pune University, India*

***Abstract*— tubesheet in pressure vessel use to filter the natural gas during mining process for many petroleum industrial applications. During this process the natural gas contains many contaminating elements with sulphur as main ingredient, which can combines with sand or other carbon elements to create harmful effects of particulate impurities like slogging, clogging, fouling on the surface of the tubesheet. These impurities creates chemical reaction with tubesheet surface material which are normally made up of steel or ceramics. During working condition, the layer of clog is deposited on the filter tubes sheet surface and tubes. This clog layer creates increase in pressure inside the vessel. Once this pressure level exceeds the acceptable value, the filter tube sheet are cleaned either weekly or monthly basis. But this cleaning process needs to stop the entire plant working till the end of complete removal of clog, this creates reduction in efficiency parameters in terms of cost. In the present work design of pressure vessel filter tubesheet is performed on the basis of working conditions. Further it has been modified as per the corrections and suggestions given by end user. Number of holes for filtration and its pattern have been calculated on basis of modified design to get effective filtration with maximum efficiency. Another solution in terms of replacing filter unit has been proposed with which is divided into two sections and after every 4 to 5 seconds other section of tubesheet receives a back pressure of one seconds and washes out the other part of filter tubes. This modification in cleaning process gives efficient results without shutting down the plant production. Since it is a regular cycle so its needs to be shut down the plant once a year for full clean-up. This modification in working cycle creates cycling loadings on the tubesheet i.e. reverse pressure for cleaning and forwards pressure for working of pressure vessel. This compressive and tensile forces creates fatigue on the tubesheet and reduction in its fatigue strength. Therefore this tubesheet needs to analyse with modified concept for reduction in stresses and improved fatigue life. Dynamic analysis has been performed to evaluate fatigue life with modified thickness with dense meshing to get effective solution with respect to change in thickness of tubesheet.**

***Keywords*— FEA Analysis, filter tube sheet, transient analysis, Fatigue life evaluation, fouling.**

I. INTRODUCTION

This project deals with the analysis and determination of the fatigue life of the tube sheets which are widely used in the filters as main supporting elements of the filter tubes with variation in thickness. The application of the filters which is considered in this project is of petro chemical industries. The specific application analysed deals with the natural gas filtering immediately after it is mined. A tube sheet is a plate, sheet, or bulkhead which is perforated with a pattern of holes designed to accept pipes or tubes, are used to support and isolate tubes in heat exchangers and boilers or to support filter elements. Depending on the application, a tube sheet may be made of various metals or of resin composites or plastic and covered in a cladding material which serves as a corrosion barrier and insulator and may also be fitted with a galvanic anode. Tube sheets may be used in pairs in heat exchange applications or singularly when supporting elements in a filter. Perhaps the best known use of tube sheets is as supporting elements in heat exchangers and boilers. These devices consist of a dense arrangement of thin walled tubes situated inside an enclosed, tubular shell.

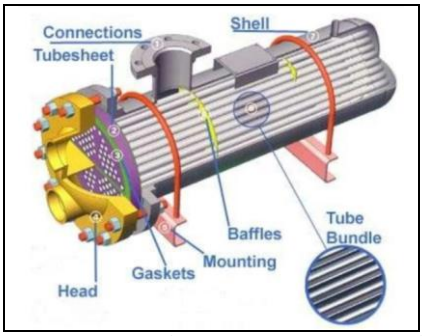

Figure1: General Assembly of Pressure Vessel & Pattern of tubesheet

Tubes are supported on either end by sheets which are drilled in a predetermined pattern to allow the tube ends to pass through the sheet. The ends of the tubes which penetrate the tube sheet are expanded to lock them in place and form a seal. The tube arrangement forms a contained unit between the tube sheets. The tube sheets are then bolted to flanges inside the hell extends beyond each tube sheet and is sealed, thereby forming two closed chambers on the non-tube ends of eets. This creates an arrangement where the exchanger consists of two separate end chambers joined by tubes through an isolated space between the tube sheets. Heated fluid is then passed from one end chamber to the other tubes where cold fluid in the cavity between the tube sheets absorbs the heat energy. The design of tube sheets is a se and complex process; the exact number of tubes needs to be established and a pattern of holes calculated to

spreads them evenly over the tube sheet surface. Large exchangers may have several thousand tubes running through them arranged into precisely calculated groups or bundles. Sheet design and production is largely automated these days with computer-aided design software performing the calculations and the tube sheet drilling done on computer numerical control machines. Tube plates or tube sheets have rows of holes with diameter of 'D' and pitch 'P'. The material remaining between these holes are called ligament and the cross-sectional area of the ligament compared to the area in a normal unpierced cross section of width 'P' is called ligament efficiency. In other words, Stress Concentration Factor (SCF) is defined as the ratio of maximum principal stress □1 in the stressed model to the nominal stress applied at the boundary of the plate (□nom). As tubesheet plays a vital role in design and analysis of the pressure vessel it should be carefully studied for various loads and working conditions. The thickness of the tubesheet varies directly to the costing and procurement of various component of pressure vessel. Thicker tubesheet results in longer tube length inside the tubesheet that do not take part during working operations. The primary aim of this project is to evaluate the fatigue life design of tubesheet by determining and analyzing the effects of instant back pressure for cyclic loadings using Finite Element Analysis, the diameter, thickness and other design parameters are studied for given mechanical and working parameters for efficient and safe performance of the pressure vessel. This project work includes various design calculations using standard ASME codes for pressure vessel. A mathematical modeling has been prepared by considering tubesheet as a flat plate with center hole, for verifying the designed and FEA solution. Further dynamic and transient analysis has been done with FEA software ANSYS for evaluating the fatigue life of the tube sheet.

A. *Problem Definition*

Tube Sheet filters is cleaned by applying back pressure, and the pollutants are then collected at the opposite end of the vessel. Industrial filters do this operation once a month. However, in a Coal gas plant, the level of impurities is high, and this results in dense clogging of the filters within 5 days, and severe damage is caused to the filter and assembly due to the heavy built up of pressure as the tube get clogged. To tackle this problem, an instantaneous back pressure mechanism has been developed, which delivers 5 seconds of back pressure after 14 seconds of front pressure. This de-clogs the filters and reduces chances of pressure built up. However, due to back pressure, the stress profile in the filter changes from tensile to compressive, creating possibility of fatigue.

B. *Objectives of the Project:*

- Design of filter tubes heat and other related component on basis of working parameters.
- Design validation and modification as per end user.
- Mathematical modeling for validation of FEA methodology for the project.
- Dynamic Analysis with TET and HEX elements of FEA to evaluate efficient option for further transient analysis.
- Fatigue life analysis using various possible boundary conditions with respect to variation in tubesheet thickness.
- Evaluation of optimized thickness of tubesheet considering stresses, deformation and applied working pressure.

C. *Methodology:*

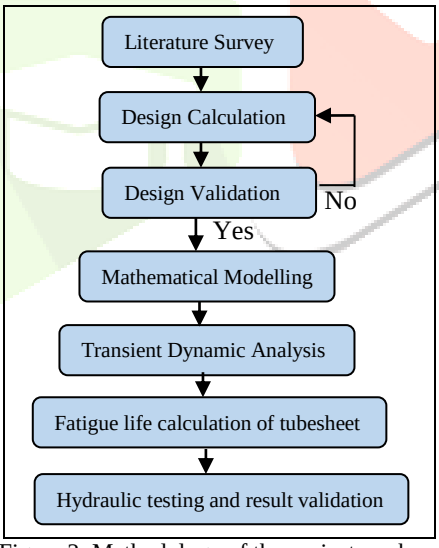

Figure 2: Methodology of the project work

II. LITERATURE SURVEY

W.J. O'Donnell [1] has described the method for calculating the stresses and deflection in the perforated plates with a triangular penetration pattern. Many different sets of effective elastic constants for perforated materials having a triangular penetration pattern have been proposed. The Paper concluded with Effective Elastic constants for both plane stress and bending loads for any plate thickness (H/R > 4) and preposition of complete structural design criteria for perforated plates. **D.L. Kaap, M.A. Sprague, et.all. [2]** describes a finite element benchmark for the dynamic analysis of perforated plates with a square penetration pattern using finite element dynamic analysis which agrees that Experimental and theoretical effective stiffness values for tube sheets with stiffness values determined from FE deflection analysis of statically loaded perforated plates. **Ming-Jia Li, Song-Zhen et.all. [3]** Summarized the development of the simulations and experimental studies for the fouling, erosion and corrosion of heat exchangers. The prediction models and methods, the simulations with these models and relevant experiments of fouling, corrosion were introduced. **Kalepesh D. Shirode, Dr. S.B. Rane et.all. [4]** investigated the optimized tube sheet with different methodologies by comparisen of design and analysis of tubesheet thickness by using UHX code of TEMA standerds. From the design methodolgies it is found that both standerds are based on different theroy of also found that FEA analysis results are closed to exact solution and these results can be accepted with a resonable

degree of accuracy. **Kotcherla Sriharsha, Venkata Ramesh et.all. [5]** Elaborated the strength analysis of a typical tube to tube sheet joint in shell and tube heat exchanger. In the work the joint between tube and tube sheet joint in shell and tube heat exchanger is designed and analysed using ANSYS, for the combination of admiralty brass and steel as tube and tube sheet materials respectively. **Ravivarma.R, Azhagiri. Pon [6]** analysed required to assess integrity of Tubesheet are analysis for operating pressure loads and transient thermal analyses together with mechanical loads, for static and dynamic analysis. **R.D. Patil 2013[7]** has worked on the stress analysis of plate perforated by holes in square inch pattern. In this paper, for in plane loading a 4 x 4 pattern of hole i.e. 16 holes arranged in square pattern and subjected to uniaxial tension is considered. The stress distribution changes with the change in ligament efficiency for any given type of loading. Therefore effect of ligament efficiency on stress concentration factor was studied for uniaxial loading condition. **Naik Shweta [8]** has worked on the shape optimization and designing an optimal thickness for filter sheet assembly components for maximum economy. This paper describes a method for calculating stresses and deflections in perforated plates with a triangular penetration pattern. Average ligament stresses are obtained from purely theoretical Considerations but effective elastic constants and peak stresses are derived from strain measurements and photo elastic tests. Hydro test was taken with and without the filter weights and results were taken. Finite Element Analysis Validation shows that efficiency of Filter sheet can be increased by increasing number of tubes and still maintaining Factor of Safety 5. **Dr. Enrique Gomez, Mr. Roberto Ruiz et.all. [9]** focused on stress analysis of heat exchanger tube sheet with a misdrilled hole or irregular or thin elements and A stress analysis is described for a nuclear steam generator tube sheet with a thin or irregular ligament associated with a misdrilled hole using the rules of ASME B&PV Section III and Non-Mandatory Appendix A, Article A-8000 for Stresses in Perforated Flat Plates. The analysis is applied to an actual, non-parallel misdrilled hole and compared to a parallel misdrilled hole. **L.K. Zhu, L.J. Qiao, X.Y. Li [10]** analysed the tube sheet cracking in slurry oil steam generators Tubesheet cracking is a severe problem in the oil refinery industry with consequences of shortened service life and increased costs. Analysis of the tube-sheet cracking shows that the cracks always occurred in the shortest tube-tube ligaments. The residual contact stresses concentrated near the oil-side expansion joints where the cracks initiated. **N. Merah,A.Al-Aboodi, A. N. Shuaib et.all. [11]**worked on a 3-D finite element (FE) model of a tube-tubesheet joint was used to determine displacement and stress distributions along the axial direction of roller expanded tube-tubesheet joint and to evaluate the combined effects of large initial clearance and strain hardening of tube material on interfacial pressure and tube deformation. An appreciable difference is observed at with over tolerances where the 3-D model predicts cut-off clearances (clearance at which the interfacial pressure starts to drastically drop) which are about 30% lower than those predicted by the axisymmetric models. **Minshan Liu, Qiwu Dong, XinGu, [12]** proposed that the waste heat boiler acts effectively to a kind of heat exchanger. The numerical analysis and experimental research are carried out to obtain the stress of the new type Ω-tubesheet in waste heat boiler and the stress distribution of Ω-tubesheet. It is indicated that the stress state of the Ω-tubesheet can be enhanced by changing the conventional whole-circle tubesheet into the composed structure to both the high and low temperature tubesheet. **R. A. Newby, G. J. Bruck et.all. [13]**Worked on Optimization of Advanced Filter Systems for hot gas particulate filter technology. Ceramic barrier filters have reached a near-commercial status for IGCC and PFBC applications, their reliability and maintainability is still a concern. This test experience has focused the issues and has helped to define advanced hot gas filter design concepts that offer higher reliability and availability. **Arthur P. Boresi and Richard J. Schmidt [14]** focused loading condition and its stress distribution for different shapes and location of applied forces with different boundary conditions. Work Results for large elastic deflections of circular plates, that is, for maximum deflections that are large compared to the plate thickness i.e. Stresses and Deflections in Flat Circular Plates with Central Holes. In the case of large deflections, direct tensile forces (tractions), though small for deflections less than half the plate thickness, become relatively large for deflections greater than the thickness.

III. DESIGN AND MATERIAL SELECTION

A. Conventional vs proposed filtration method:

During conventional processing of cleaning operation of tubesheet whole plant is shut down for a period of week or month time which creates lost in production and economical aspect.to avoid this proposed Method as shown in figure is comprises in four parts of time cycle. The newly designed compartments are divided into two compartments as shown in figure after every 5 seconds one of the compartments receives a back pressure of 1 second, and cleans the filter tubes. This ensures cleaning without stopping the plant, plus since this is in regular cycles, plant shutdowns for full clean-up are needed only once a year. During filtration process the compressed gas is passed through the gas inlet chamber to the Filter elements. This gas is collected at the top of the filter compartment. Blow pipes with nozzles are provided for providing the back pressure and clean the filter elements. A compressed air supply is provided for creating a high intensity back pressure. The process of creating back pressure is divided into 12 second of cycles for cleaning number of chambers. The process repeats itself over and over again. However one of the crucial components is the filter sheet itself. This sheet stress reversals from positive to negative and is susceptible to fatigue.

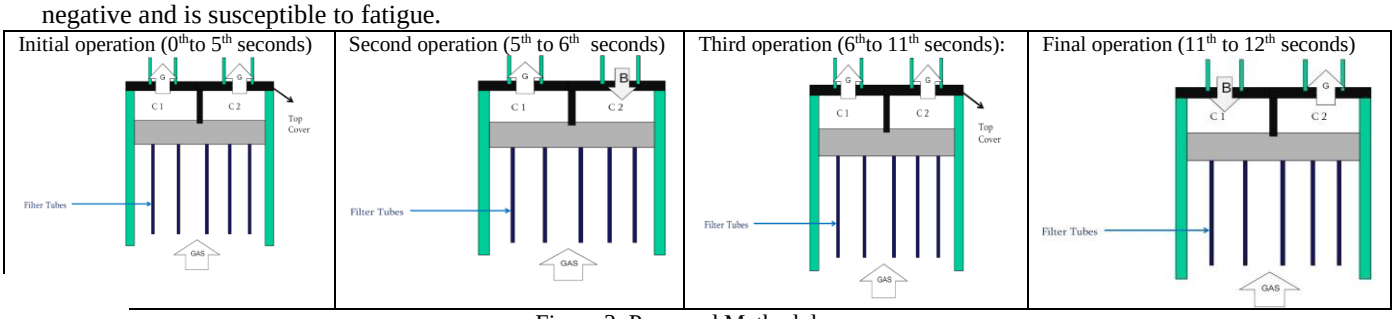

Figure 3: Proposed Methodology

B. Material Selection

Materials are selected according to the following criteria.

1) Corrosive or noncorrosive service
2) Contents and its special chemical/physical effects
3) Design condition (temperature)
4) Design life and fatigue affected during the plant life
5) Referenced codes and standards
6) Low temperature service
7) Wear and abrasion resistance
8) Welding and other fabrication processes

The material taken for tubesheet is SGR 590, as per the specifications of ASME codes. During analysis and testing of tubesheet of pressure vessel in this case the material used is SA 516 GR70 having following properties,

TABLE I
Properties of the tubesheet material

Carbon, max 0.5" and under	Manganese 0.5"	Tensile strength in ksi	Yield strength in ksi
0.27%	0.85-1.20%	70-90	38

C. Design parameters:

TABLE III
Tubesheet Parameters for Design Calculations (Instant Back Pressure)

Sr. No.	Parameter Description	Notations	Given Value
1	**Internal Pressure**	P	0.14 MPa
2	**External Pressure**	P_0	Atmospheric
3	**Process Volume**	V_p	126 cu m
4	**Expected Stagnant Volume**	V_s	Not Specified
5	**Buffer Volume Requirement**	V_b	Not Specified
6	**Tube Porosity Volume**	T_p	70
7	**Tube Length**	T_L	5.5m
8	**Radius of tube sheet**	r	2m
9	**Tube Diameter**	d	0.15m

A 5% Gap will be maintained on the Tube Sheet radius to allow for welding. Tubes arrange to form a 60^0 Equilateral Triangle.

TABLE IIIII
Designed values of various parameters for tubesheet

Tube sheet volume	11.945 x 10^6	**Area pertaining to material removed**	993.31 mm^2	**Tube volume**	15393.804 mm^3
Tubesheet thickness	150mm	**Thickness of Shell and head**	2mm	**No of holes**	544
Nozzle thickness	306mm	**ligament efficiency**	0.16	**Load on bolt**	417745.99
Reinforcement pad	478 mm.	**Length of hub**	0.12"	**Length of shell**	355.6mm
No of bolts	24	**Bolt area required**	20.887in^2		

IV. EXPERIMENTAL ANALYSIS

A. FEA ANALYSIS (Transient Dynamic Analysis)

1) The final modified dimensions are as follows:-
   - Thickness of Tubesheet – 150 mm
   - Ligament Efficiency – 0.16
   - Number of Holes on the tubesheet - 490
2) Boundary Conditions for Convergence in tubesheet analysis:
   - Case 1: self-weight and gravity acting downwards.
   - Case 2: gravity acting downwards and design load (0.16 Mpa) acting in opposite direction of gravity.
   - Case 3: gravity acting downwards and back pressure (0.16 Mpa) acting in the direction of gravity.
   - Case 4: both positive and negative pressures acting on it.

Tubesheet was analysed for above mentioned cases by changing the element types. Tetrahedron Elements and Hexdominent Elements were used to get the maximum deflections and maximum stresses. Analyses were carried out varying the number of nodes and the size of elements. Rise of 50000 nodes was kept in every proceeding analysis. Highest number of nodes for analysis was selected as 3, 50,000 nodes. The maximum deflection and maximum stresses with respect to the number of nodes were plotted on the graphs. From these graphs the element size for which the stress values were highest was selected for the further Transient Dynamic Analysis.

TABLE IV
Comparative Analysis of HEX and TET element

Boundary conditions	TET element		HEX element	
	Max Deformation	Max stress	Max Deformation	Max stress
Tubesheet analysis with self-weight and gravity acting downwards	38.074	0.8212	45.794	0.8290
Tubesheet analysis with gravity acting downwards and design load (0.16 Mpa) acting in opposite direction of gravity.	35.272	0.7150	122.23	2.3752
Tubesheet analysis with gravity acting downwards and back pressure (0.16 Mpa) acting in the direction of gravity	100.4	2.1186	106.13	2.1186
Tubesheet analysis with both positive and negative pressures acting on it.	61.76	1.0276	74.207	1.0381

As shown in above table TET element gives more accurate results compared to HEX element.

nt Dynamic Analysis of Filter Tube Sheet for Multiple Cycles

nt analysis of tubesheet was performed using 1, 00,000 nodes value for multiple cycles. Below figure shows the onditions for single cycle under which the tube sheet was dynamically analysed with respect to time.

The top and bottom faces of Tube sheet were divided into two parts from centre and were named as Top A, Top B, Bottom A, Bottom A, Bottom B respectively. The circular plate was fixed at the circumference.

1) *Boundary Conditions*

- **0 – 5 Seconds:** - Pressure of 0.14 Mpa was applied on the left bottom half face whereas 0.145 Mpa was applied on the right top half face of the tubesheet.
- **5 – 6 Seconds:** - No pressure was applied on any of the surface.
- **6 – 11Seconds:** - Pressure of 0.14 Mpa was applied on the right bottom half face whereas 0.145 Mpa was applied on the left top half face of the tubesheet.
- **11 – 12Seconds:** - No pressure was applied on any of the surface.

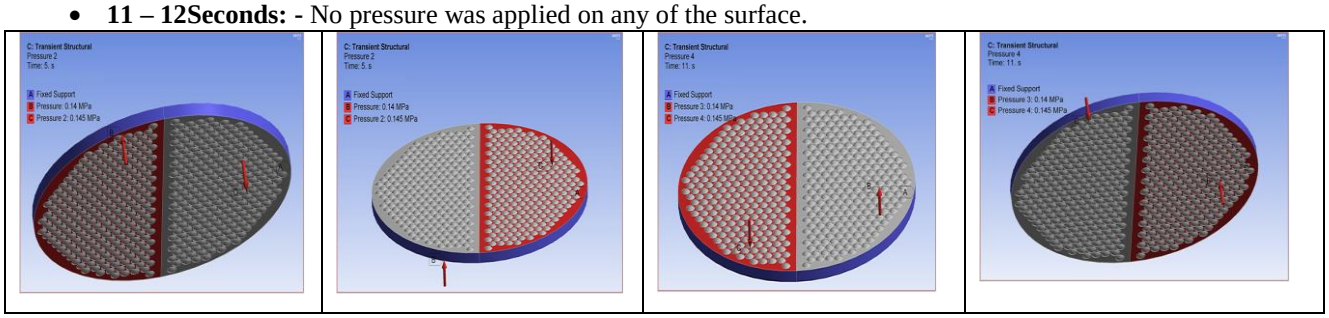

Figure 4: Time Cycle analysis using FEA

2) *Results of Transient analysis:*

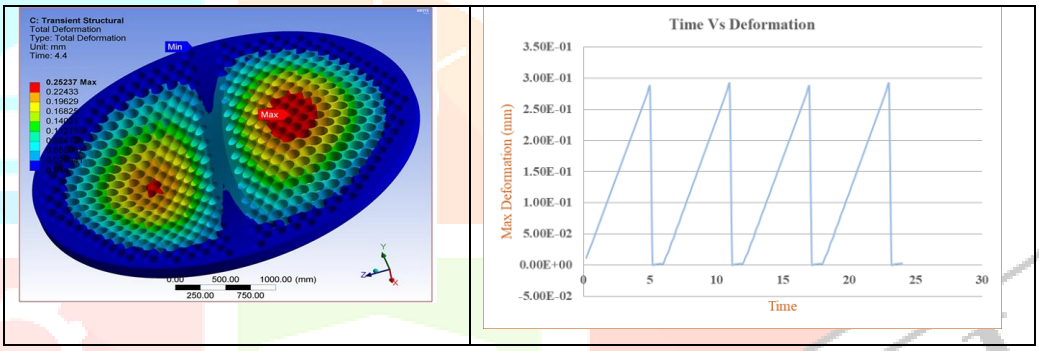

Figure 5: Transient Analysis Results with 100000 nodes for multiple cycles,

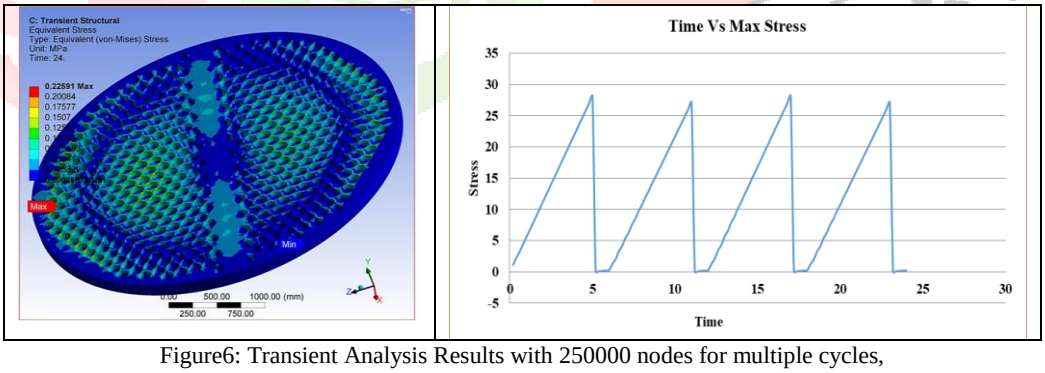

Figure6: Transient Analysis Results with 250000 nodes for multiple cycles,

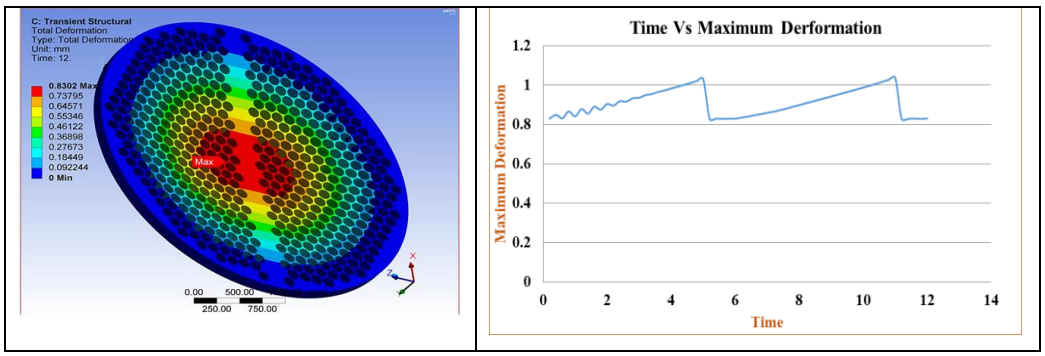

Figure7: Transient Analysis Results with 250000 nodes for single cycles,

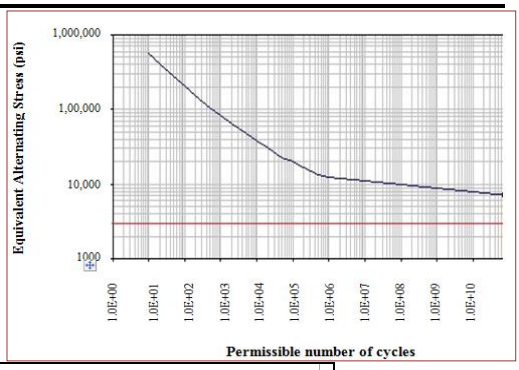

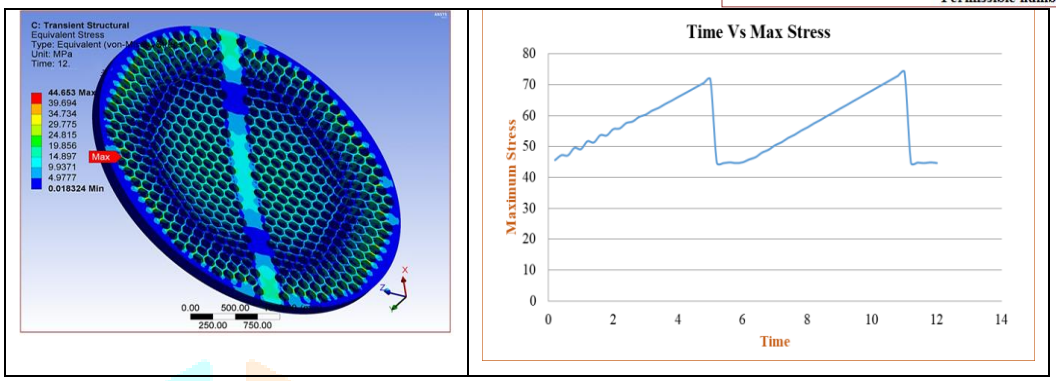

Figure8: Transient Analysis Results with 250000 nodes for every half cycles,

C. Fatigue Life Calculations For Tube Sheet

Cyclic Data

dS_{pk}– Range of Primary + Secondary + Peak = 27 N/mm^2 = 3916.30899 Psi

K_f – Fatigue Strength reduction factor = 2.50

m – Material constant used for the fatigue knock down factor = 3.00

n – Material constant used for the fatigue knock down factor = 0.20

S – Material Allowable Stress = 20015.207 Psi

S_y – Material yield Strength = 38426.29823 Psi

T_{av}– Average Cycle temperature = 150

E_t – Modulus of Elasticity at T_{av} = 29030000

Fatigue Penalty Factor

S_{ps} = 3* S or 2* S_y……(Whichever is maximum)

S_{ps}= 76852.59646

K_{ek} 1 = 1

K_{ek} 2 = 1+ (1-n) / (n (m-1)) (dS_{pk} / S_{ps} – 1) = -0.89808

K_{ek} 3 = 1 / n = 5

K_{ek} = if (dS_{pk}<S_{ps}) then K_{ek} 1

Therefore, K_{ek} = 1

Figure9: Fatigue life cycle graph for 150 mm thickness tubesheet

Permissible cycle life

$S_{alt}K$ = (K_f * K_{ek} * dS_{pk}) / 2

$S_{alt}K$ = 4895.386 Psi ……. Alternating stress in Tube sheet

$S_{alt}K$ = 33.7525 N/mm^2

It can be observed that for the calculated value of alternating stress i.e. 4895.386 psi, the model can sustain for more than E^{11} number of load cycles. Hence the tube sheet can sustain the alternating stress for infinite life. In this case the transient dynamic analysis of tubesheet was carried out for different loading conditions and for different thickness of tubesheet. Below are the results of the analysis in terms of fatigue life of the Tubesheet.

- **Tubesheet with 150mm thickness and 1,00,000 nodes:-**
  Maximum deformation – 0.252 mm
- **Tubesheet with 150mm thickness and 2,50,000 nodes:-**
  Maximum deformation – 1.0372 mm
  Fatigue Life – 1.0E11 number of cycles

D. Experimental Validation

1) All new product equipment shall be tested at 2.5 times the operating pressure using Hydro test.
2) The Hydro test shall have slow built up of pressure, from base pressure to test pressure over a period of 120 min.
3) The equipment shall be maintained at test pressure for 30 min.
4) The pressure shall be gradually reduced to base pressure within a period of 45min.
5) After test, all components shall be subjected to NDT (Non Destructive Test), as below

   Visual Inspection-No surface irregularities must be present.

   Pre Dyed components should have no loss of dye due to leakage.

   Ultra Sonic Testing – Post Test, internal damage shall get amplified if any, and shall be recorded in an Ultra Sonic Test.

6) The test performance of the assembly should be completely elastic; this shall be verified by checking the dimensions of product for any permanent yield.

Hydro Test Condition

1) Working fluid: Water with Anti Scaling Additives
2) Test Pressure: 2.5 x 0.07 MPa
3) Leak Inspection: Sensors (LDR) on the top side of Filter Assembly.
4) Method: Visual Inspection on top side after completion of test.
5) Remark: Simultaneous testing of all 7 chambers was done.

Test Execution Details

1) Begin Time: 09.00 hrs
2) Base Pressure: 0 MPa (Empty vessel)
3) Peak Pressure Time: 11.00 hrs
4) Peak Pressure: 0.175 MPa
5) Pressure relief begins Time: 11.30 hrs

Visual Inspection Details

1) No leak observed on Top Side of Assembly
2) No visible damage observed after test.
3) Plug Adhesion intact after test.

Auditors Remarks:

1) Code requirements have been met by the analysis.
2) The Mesh is satisfactorily fine enough to generate accurate results.
3) The boundary conditions were inspected.
4) The maximum Stress in Filter sheet is 32 MPa, however nominal value if calculated is much lower, it satisfy FOS is 5.
5) Gasket plate shows peak pressure of 34 MPa. However it is observed to significant stress raiser due to vicinity of contact and relatively less thickness of the plate compared to the other components.
6) Material Non Linearity may not be modelled in future analysis as it will have negligible effect on accuracy and unnecessary increases solution time.
7) FEA processing has been done in line with requirements of SA 516 GR70, FEA and the component maintains a FOS greater than 5 for the current boundary conditions.

The tubesheet was checked for the maximum deformation under the fluid pressure of 0.173 Mpa, and working at 27^0C. The holes of tubes were blocked with the help of GR 3084 Plugs. To measure the deformation (LC 4C1 X) HBM type of Strain gauge was located at the centre of the Filter Tubesheet. The table below shows the values of deformation obtained analytically as well as experimentally and the percentage of error.

TABLE V
Experimental Vs FEA Analysis Results

Sr. No.	Test	Max Deformation in mm by FE Analysis	Max Deformation in mm by Measurement	% Error
1	Hydro Test at 0.173 Mpa Pressure	4.3903	4.9	10.4%
2	Under self-weight and gravity condition at 0 Mpa	0.82867	0.86	3.64%

Improvements in Design and Scope of Project

Following are the parameters where there is a scope of improvement.

a. Changing the material used for the Tubesheet
b. Reducing the number of filter holes in the tubesheet.
c. Changing the pattern of holes in the tubesheet.
d. Changing the cycle time of pressures and checking it for fatigue life.
e. Changing the thickness of the tubesheet and checking it for the required life.

Out of the above scopes only one was carried out for analysis purpose. In improvement the thickness of the tubesheet was reduced and checked for the fatigue life, following results were obtained in the transient analysis with varying thickness,

TABLE VI
Result analysis of transient FEA for variation in thickness.

Conditions of Analysis	Maximum Deformation (mm)	Fatigue Life
Tubesheet with 150mm thickness and 1,00,000 nodes	0.252	1.0E+10
Tubesheet with 150mm thickness and 2,50,000 nodes	1.0372	1.0E+11
75mm thick tubesheet with extreme loading conditions	7.3413	1.0E+08
75mm thick tubesheet with real load conditions	6.3733	1.0E+08

V. CONCLUSION AND FUTURE SCOPE

A. *Conclusion*

The project deals with the determination of the fatigue life of tubesheet which is one of the major components in industrial filter vessels. The tubesheet have to sustain the static load of the filter tubes as well as the self-weight due to gravity. In the study a new system exerting back pressure was implemented due to which the tubesheet was under alternating causing the tubesheet to undergo fatigue. To increase the accuracy of results the convergence analyses were ed with different boundary conditions to get the proper number of nodes and element size for further analysis. ;ence analysis gave the following conclusion:-

a) 2.5 Lakh nodes should be used for the further transient analysis as the value of stress is maximum for 2.5L nodes for different boundary conditions.
b) Hexdominent Element should be used as it shows quality meshing results.

Transient dynamic analyses were performed on the tubesheet to check the maximum deformation and stresses at various instant of time during the load cycle. A transient analysis performed on the tubesheet with 1 Lakh nodes concluded that the deformation at the end of every load cycle is reaching its initial value and only one complete load cycle is sufficient for further analyses. Further the transient dynamic analysis of tubesheet with 2.5 Lakh nodes was performed to get the maximum deformation and maximum stresses in the tubesheet. Using the maximum stress values the fatigue life of tubesheet was calculated which came out as infinite life. Further the improvement in project was suggested as the reduction of tubesheet thickness to 75mm form 150mm. The fatigue life under extreme condition for tubesheet came out as finite life but under real loading conditions the life was infinite which proved that the tubesheet with 75mm thickness can be used for the current application. The summarized conclusions are listed below,

1) Design calculations of pressure vessel has been verified by customer end and modified as per ASME section VIII.
2) Triangular (30°) and Rotated triangular (60°). A triangular (or rotated triangular) accommodates more tubes than square (or rotated square) pattern. Triangular layout produces high turbulence. A triangular layout pattern is limited to use in clean services on the shell side.
3) Square (90°) and Rotated square (45°). It is usual practice to use square layout pattern for dirty services on shellside.
4) Proposed mathematical model of circular plate with hole suggest that finite element procedure for the tubesheet of pressure vessel is acceptable.

B. Future Scope

Following are the parameters where there is a scope of improvement.

1) Finite element procedure is best suitable process for pressure vessel analysis; further this process can be applied using various different FEA elements with fine meshing and transient analysis.
2) Further analysis can be done for different components of the pressure vessel such as shell, flange, support etc for evaluating the results to improve efficiency and life of the pressure vessel.
3) Changing the material used for the Tubesheet – Comparatively stronger material can be used and analyzed for the fatigue life. The thickness of tubesheet required in this case will be comparatively less.
4) Reducing the number of filter holes in the tubesheet. – Reducing the number of holes may increase the ligament efficiency of the tubesheet.
5) Changing the pattern of holes in the tubesheet- Different patterns of holes may give different ligament efficiencies and the optimum pattern could be evaluated after analysis.
6) Changing the cycle time of pressures and checking it for fatigue life.

REFERENCES

[1] *"Design of Perforated Plates"*W.J. O'Donnell, B.F. Langer; Journal of Engineering for Industry; Trans. ASME;Volume 84 (August 1962); Paper no.61-WA-115.

[2] *"A finite element Benchmark for the Dynamic Analysis of Perforated Plates with a Square Penetration Pattern",*D.L. Kaap, M.A. Sprague, R.L. Engelstad; Fusion Technology Institute University of Wiscons;UWFDM-1034 May 1997.

[3] *"Comparisen and Design and Analysis of Tubesheet Thickness by using UHX code of ASME and TEMA standerds",*Kalepesh D. Shirode, Dr. S.B. Rane, Mr. Yashawant Naikinternational journal of mechanical engineering and technology (IJMET), ISSN 0976-6359,volume-4, issue-4, july-august 2013, pp 105-117.

[4] *"Strength Analysis of Tube to Tubesheet Joint in Shell and Tube Heat Exchanger"*Kotcherla Sriharsha, Venkata Ramesh Mamilla and M.V. Mallikarjun in International Journal of Science, Engineering and Technology Research (IJSETR), Volume 1, Issue 4, October 2012, ISSN: 2278-7798.

[5] *"Finite Element Analysis of a Tubesheet with considering effective geometric properties through design methodology validated by Experiment",* Ravivarma.R, Azhagiri. Pon, International Journal of Computational Engineering Research (IJCER), ISSN (e):2250-3005, volume-4, Issue-4, April 2014.

[6] *"An Approch to Finite element Analysis of Boiler Tubesheet"*R.D. Patil, Dr. Bimlesh Kumar,American Journal Of Engineering Research(AJER),e-ISSN:2320-0847, p-ISSN:2320-0936,Volume-2, Issue-8, PP-8-11.

[7] *"Thickness and Shape Optimization of Filter"* Naik, Shweta, Global Journal of Researches in Engineering; Mechanical and Mechanics Engineering; Volume-13; Issue-1;Version-1.0;Year-2013.

[8] *"ASME Section III Stress Analysis of a Heat Exchanger Tubesheet with a Misdrilled Hole and Irregular or thin ligaments"*Dr. Enrique Gomez, Mr. Roberto Ruiz, Mr. Robort M. (CON) Wilson, proceedings of the ASME 2013 pressure vessels and piping conference PVP 2013 July 14-18, 2013 paris, France.

[9] *"Analysis of the Tubesheet Cracking in Slurry Oil Steam Generators"*L.K. Zhu, L.J. Qiao, X.Y. Li, B.Z. Xu, W. Pan, L. Wang, Alex A. Volinsky;ELSEVIER science directory journal, engineering failure analysis 34(2013) 379-386.

[10] *"3-D finite element analysis of roller-expanded heat exchanger tubes in over-enlarged tubesheet holes"*N. Merah, A. Al-Aboodi, A. N. Shuaib, Y. Al-Nassar in article; Appl Petrochem Res (2012) 1:45-52; DOI 10-1007/s 13203-011-0005-z.

[11] *"Stress Analysis of Tubesheet in waste Heat Boiler"*Minshan Liu, Qiwu Dong, XinGu, journal of pressure equipment and systems 4(2006) 48-51;Thermal Energy Engineering Research Centre of Zhengzhou University, Zhengzhou 450002, China,

[12] *"Optimization of Advanced filter system"*R. A. Newby, G. J. Bruck, M. A. Alvin, T. E. Lippert,Westinghouse Science & Technology Centre;WorkedUnder Contract Number DE-AC26-97FT3300703 August 20, 1997 - April 1998.

vance Mechanics of Materials" Arthur P. Boresi, Richard J. Schmidt, John Wiley & sons, Inc; sixth edition.

essure Vessel Design Manual" Dennis Moss, ELSEVIER publications, third edition.

essure Vessel Design" Guides and Procedures, P.V. Engineering.

*STI Guidebook Series - Vol. 4 to ASME Section VIII Div. 1 for Pressure Vessels"*Bruce E. Ball, Will J. Carter,Third on (Covering 2001 Edition of ASME Section VIII Div. 1).

[17] Giglio M. 'Fatigue Analysis of Different types of Nozzles' [Journal] // International Journal of Pressure Vessels and Pipings.
[18] Liu Minshan 'Stress analysis of Ω-tubesheet in waste heat boiler' [Journal]. - [s.l.] : Journal of Pressure Equipment and Systems, 2006.
[19] Myung Jo Jhung Jong Chull Jo 'Equivalent Material Propeties of Perforated Plate with Triangular or Square Penetration Pattern For Dynamic Analysis' [Journal]. - [s.l.] : Nuclear Engineering and Technology, 2006. - Vol. 62.
[20] Nandagopan O. R. 'Non Linear Behaviour of Perforated Plate with Lining' [Journal]. - [s.l.] : Defense Science Journal, 2012. - Vol. 62.
[21] R. D. Patil & Dr. B. Kumar 'An Approach to Finite Element Analysis of Boiler Tubesheet' [Journal]-[s.l.] : American Journal of Engineering Research, 2013 - 08 : Vol. 02.
[22] 2010 ASME Boiler and Pressure Vessel Codes Section VIII Division II.

Analysis and Simulation of Hybrid Energy Storage System for Electric Vehicle

Ravikant K. Nanwatkar[1], Dr. Deepak S. Watvisave[2]
[1]*Ph.D. scholar, Department of Mechanical Engineering, SCOE, SPPU, Pune, India*
[2]*Associate Professor, Department of Mechanical Engineering, Cummins COEW, SPPU, Pune, India*

Abstract **- The continuous increase in demand of efficient energy storage for automobile sector and with controlling mechanism to rise in environmental issues leads to adoption of hybrid energy storage system. This hybridization can be battery and internal combustion engine or battery with supercapacitor to meet the energy and power requirement demands. Electric mobility deals with use of electric energy in automobile sector but problem lies in using pure electric battery-based vehicle are less power density at higher torque requirement as well thermal runaway for longer run. Many renewable energy sources like wind, wave and solar energy which can be used to generate electricity for charging electric vehicle batteries. Some conventional batteries like lead acid have drawbacks of increased in weight and size optimization for efficient energy storage system. Also, by using hybridization of internal combustion engine with battery, still dependency on petroleum fuel and its environmental effects will not be controlled. Therefore, selecting option of hybrid energy storage system of lithium-ion battery and supercapacitor can be an efficient option to meet the requirement of energy and power during working cycle. The structural design of battery and supercapacitor hybrid system consists of high-capacity battery-type electrode and a high-rate capacitive electrode; its proper design will provide improvement in performance, reduction in cost, safer working conditions and environmental friendliness. The proposed work basically focuses on hybrid energy storage system for light vehicle. A comparative analysis of various hybridization is studied in this paper with case study involving simulation using MATLAB / Simulink software. Main idea in this work is use of convertor to be worked as a controlled energy system for maintaining the high voltage of the supercapacitor when it exceeds the battery voltage for at most of driving conditions. At smooth running conditions battery will provide the necessary amount of energy to propel the vehicle, when requirement of power density is less and energy density is more. At starting phase and inclination road when power requirement is more compared to energy density supercapacitor will work. This system will increase the life of the battery and reduction in weight of vehicle as the batteries are sized to ensure many constraints like start up, acceleration, braking and energy recovery.**

Index Terms **- Electric vehicles, lithium-ion batteries, Supercapacitor, Hybrid Energy Storage System, Simulink.**

I.INTRODUCTION

Electric mobility is the field in which all street vehicles that is powered by an electric motor and primarily gets their energy from the power grid. This includes purely electric vehicles, vehicles with a combination of electric motor and a small combustion engine and hybrid vehicles that can be recharge via the power grid. The basic source of fuel supply to electric Vehicle is Electrical Energy which significantly reduces CO2 emission. This electricity can be generated from many non- conventional energy resources which help to decrease in use of fossil fuels. Various rechargeable batteries can be an efficient option for replacing conventional energy sources and to reduce its unwanted effects. Among all Lithium battery is a type of rechargeable battery that have metallic lithium as an anode. The batteries have a high energy density, no memory effect and low self-discharge but with drawback, of a flammable electrolyte, and if damaged or incorrectly charged can lead to explosions and fires.

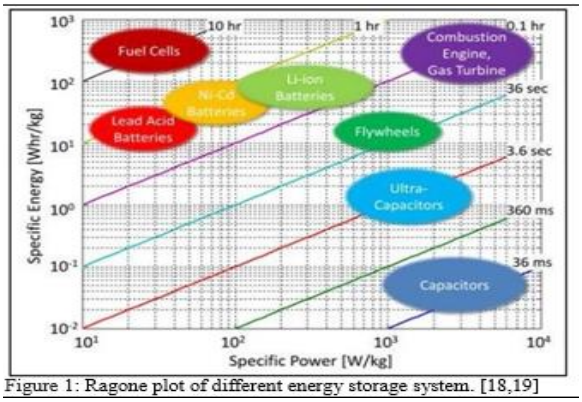

Figure 1: Ragone plot of different energy storage system. [18,19]

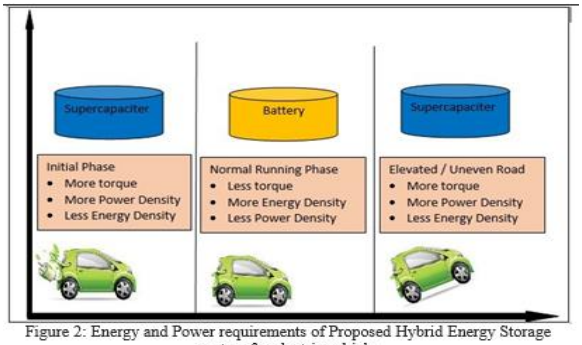

Figure 2: Energy and Power requirements of Proposed Hybrid Energy Storage system for electric vehicle.

Various hybrid combinations are used in electric vehicles like, pure battery based electric vehicle, hybrid electric vehicle, plug in hybrid electric vehicle. Etc. the design of efficient energy storage system and its thermal management is critical issue. In battery-based energy storage system, battery with higher power density is required to meet the power demands. As a solution for this, the size of battery can be increase but it will raise the issue of increase in cost and thermal management in high power load as well as cold temperature conditions. In addition to that some issues related to the balancing of cells of battery as without balancing system, the individual cell voltages tend to drift apart over time. This tends to decrease the capacity of the total pack during operation results in failure of the total battery system during high rate of charge and discharge conditions. In addition to these issues, the application where instantaneous power input and output is required i.e. the applications where batteries suffering from frequent charge and discharge operations adversely affect the life of battery. All of above problems can be resolved by Hybrid energy storage system in which Supercapacitor is to combine with batteries to achieve better overall performance. As shown in figure 1, this is because, supercapacitor has more power density but lower energy density compared to batteries.

Table 1: Comparison of Li-ion supercapacitor with other Energy storage system [5]

Energy Storage Device	Energy Density	Power Density	Cycle life
HESS of Li-ion	10-20	900-9000	>100000
Li-ion Battery	100-265	100-265	300-500
EDLC (Supercapaciter)	2-8	500-5000	>100000
Li-acid battery	30-50	100-200	200-300
Ni-MH battery	60-120	250-1000	300-500
Zinc-bromide battery	85-90	300-600	2000

Therefore during higher power requirements i.e. start and peak power phase supercapaciter will work and during smooth running conditions batteries will work for supplying energy requirements which will surely increase the life of battery. Therefore, the basic idea, in this work is to use best features of both devices. The high life cycle and power density of supercapaciter will be use to improve the battery life and optimize use of energy density so that there will be significant reduction in cost of battery as well CO2 emission. This hybridization should be such that it should be equipped with high power as well as high energy density. Basically, there are two ways for this hybridization as shown in figure.

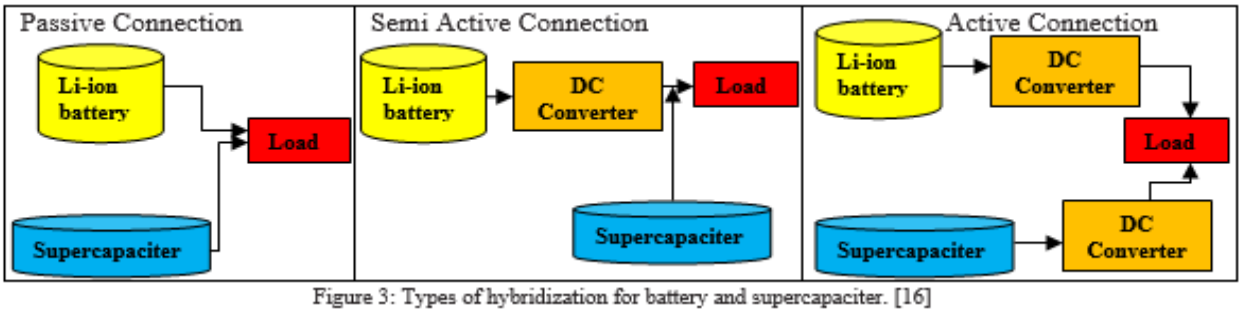

Figure 3: Types of hybridization for battery and supercapaciter. [16]

First is passive type in which battery and supercapacitor is directly connected to DC bus. It has advantages like, high peak power capability, higher efficiency and longer battery life cycle etc. but has a drawback of unachievable system optimization as there is no power management mechanism to govern the power sharing between battery and super capacitor. Whereas in active type, battery and super capacitor are connected to DC-bus via DC-DC converter. It has advantages of design flexibility, acquiring higher power capacity, less voltage variation and reduction in weight but with disadvantage of increase in cost of DC- DC converter. Other possible hybridization can be other types of batteries as mentioned above with either supercapacitor or internal combustion engine. Other type of energy storage can

be fuel cell which can be future aspect in automobile field. The proposed works is based on analysing different hybrid combination specifically for light weight applications like two-wheeler. Various types of earlier work related to this is explained in literature survey.

II. LITERATURE REVIEW

Marek Michalczuk et.al. [1] In 2012 has presented HESS for a small urban electric car with lithium batteries and Ultracapacitors. They Worked on Energy recovery through regenerative braking and the results are simulated using Matlab /Simulink PLECS toolbox. Jian Cao et.al. [2] In 2012 experimented on HESS with PSAT (The Power System Analysis Toolbox) with a smaller dc/dc converter which acts as a controlled energy pump for maintaining an inflated amount of ultracapacitor compared to the battery at driving conditions. Further work proposed on the analysis of the HESS efficiency parameters at high- voltage conditions and Sizing of the dc/dc converter versus the Ultracapacitors. Rebecca Carter et.al. [3] Worked on novel HESS of lead acid battery and supercapacitor using regenerative breaking. The availability of energy from regenerative braking and the characteristics of the supercapacitor were considered as impact factors. With decreasing peak battery current supercapacitor were found to be effective. Further modifications can be done by increasing the supercapacitor operating voltages to enable energy content to be maintained while reducing equivalent series resistance. A. Ostadi et.al. [4] 2013 worked on various literature related to HESS of battery and supercapacitor by connecting it to DC sources to meet energy and power demands of the vehicle including energy management issues. Qualitative analysis through literature review reveals that the partially decoupled configuration with the ultra-capacitor unit directly connected to the DC bus and battery unit connected via a bidirectional DC-DC converter is the most promising interfacing topology in EV/HEV applications. Seyed Hamidi et.al. [5] In 2015 worked on Lithium-ion batteries and Ultracapacitor for network applications with variant materials for cathode, anode and lithium-ion battery that results in a variety of output performance characteristics along with equivalent electrical circuit. Their proposed work relates Lithium-ion and ultracapacitor for high power density with extensive discharge demand application to improve issues encountered in Lithium-ion batteries like high production cost, high sensitivity for thermal runaway. Clemente Capasso et.al. [6] 2016 worked on HESS with Na-Cl batteries & EDLC using a Controlled DC/DC bi-directional power Converter. Further work proposed on Simulation & experimental study with HESS having lithium-ion and ultracapacitor. Wenhua Zuo et.al. [7] 2017 worked on various combinations of HESS with a high capacitive battery and rated capacitive electrode. Further works remained on BSH with aqueous high voltage window and integrated 3D electrodes /electrolyte architecture. Anuradha Herath et. al. [8] 2018 worked on charging and discharging algorithm of battery and supercapacitors as per its acceleration and deceleration conditions. The novel system is capable of reducing the strain on the batteries while extending the range of the vehicle compared to the conventional battery electric vehicle. Mahdi Soltani et.al. [9] 2018 worked on Lithium-ion capacitors which can be used as a high-power storage unit for MLTB (Millbrook London Transport Bus) driving cycle. Further work remained to optimize the LiC and LiB unit for a lower cost, size, a higher energy and power density. Lip Sawa et.al. [10] 2018 worked on HESS with Lithium-ion batteries and ultracapacitor model to evaluate the thermal and electrical performance parameters for different driving cycles. The simulation results in improved dynamic stress, better thermal performance for peak power demand the better life span of battery and reliability of HESS. The remained work is set up formation for electric propulsion system test bench to validate the simulation results and to incorporate the intelligent energy management system in the model. Md. Arman Arefin et.al. [11] 2018 worked on Simulations of HESS with battery and supercapaciter taking two basic scenarios into consideration: fresh cells and half-used battery cells. The simulations showed that the lower the temperature is, the higher the hybrid system efficiency becomes. Hybridization with regenerative breaking not only increases the efficiency of the energy storage system but it also increases the power train efficiency and the battery lifespan. This HESS gives advantages of reduction in battery aging, maximum battery current and the number of executed cycles and increase in power preserving capacity of the system with increase in battery maintenance interval. Lia Kouchachvili et.al. [12]

2018 worked on battery and supercapaciter HESS by coupling the battery with a supercapaciter, which is basically an electrochemical cell with a similar architecture, but with a better capability rate and cyclability. Basic principal was supply of excess energy by supercapaciter when battery won't be able to so. Configurations, design, and performance of HESS had been discussed with active, semi active and passive types of HESS. Various applications area of HESS like mobile charging stations, racing cars, has been discussed with different batteries and supercapaciter combinations, related issues and future aspects. Immanuel N. et.al. [13] 2019 proposed a novel topology of hybridizing battery, supercapaciter and hybrid capacitor for optimum utilization of energy in electric vehicles. This paper deals with the combination of both supercapaciter and hybrid capacitor with the battery thus addressing the problem of the lack of autonomy between two recharge points in supercapaciter. The prospects of using a multiple-input DC-DC converter was also analysed. Electric vehicle profile obtained by experimental analysis were used for verification with the proposed ides of the project. The application of the novel hybridization of the three energy storage devices can be extended to other applications having a load profile with high crest factors. S Devi Vidhya et.al. [14] 2019 presented the modelling, design and power management of HESS for a three wheeled light electric vehicle under Indian driving conditions. The HESS includes Li-ion battery and Ultracapacitor combined with a bi-directional converter in order to get efficiency parameters. The HESS in this project work shows efficient results towards improving the life of battery and supercapaciter. Simulations were carried out in MATLAB/Simulink environment to verify the effectiveness of the proposed control strategy with modelled system components of three-wheeled light electric vehicle. The power split validation in this work were done experimental prototypes of HESS. A.Bharathi Sankar et.al. [15] 2019 presented a smart power converter to for electric bicycle which is powered by a battery and super capacitor hybrid combination. In this work an assembly of a rear hub motor onto a normal geared bike powered by a lead acid battery pack is introduced. A super capacitor module was connected in parallel to the battery pack via a custom-made Arduino controller-based power converter which arbitrates power between the battery and super capacitor. Experimental results show an improvement in the up-hill acceleration of the bicycle as a direct result of the power converter being responsive enough to harvest the extra current from the high power complementary super capacitor module avoiding deep discharges from the battery to improve the battery life. The maximum speed remained unchanged. The main battery pack was shielded from high discharge currents to enhance its life cycle. Walvekar, A et.al. [16]

2020 worked on hybridization of li-ion battery and supercapaciter for two-wheeler electric vehicle. In this paper, the effect of different topologies of HESS and effect of degree of hybridization is analysed w.r.t. current profile, voltage profile and State of Charge (SOC). Results show that use of HESS for Electric two-wheeler in place of only battery decreases, the Peak/RMS Current experienced by the battery with corresponding improvement in battery life.

III.PROPOSED MODEL

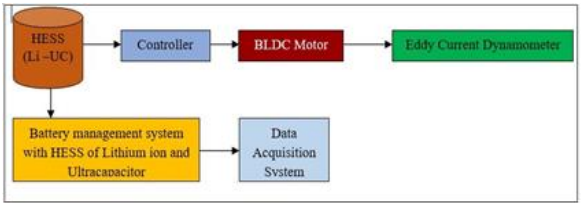

Figure 4: Proposed model of hybridization of lithium ion battery and supercapacitor

Dynamics of Motorcycle:

Here, the motion of motorcycle and their components due to applied forces in running conditions are discussed. This includes balancing, steering, braking, acceleration, suspension and induced vibration on the vehicle body. The various forces acting on two-wheeler bike including the driver, has been categorised into external and internal. The external forces are due to gravity, inertia, ground contact and atmospheric conditions whereas internal forces are caused due to bike rider and interaction between the components of the vehicle body. The mathematical modelling of electric vehicle's mechanical behaviour is studies considering it as two-wheeler and the performance limiting parameters viz. state of charge, variation of current and voltage according to battery parameters. Finally, the Simulink model of the e-vehicle is performed using Matlab/Simulink. The

mechanical model performed here on assumptions that motorcycle as a rigid body with rider to be static on motorcycle, so that centre of gravity is constant during driving conditions. The motorcycle body is subjected to aerodynamic drag force, rolling resistance and the component of the weight force caused by the angle of inclination to the road surface (Fp). Considering all these forces the free body diagram of two-wheeler is as shown in figure.

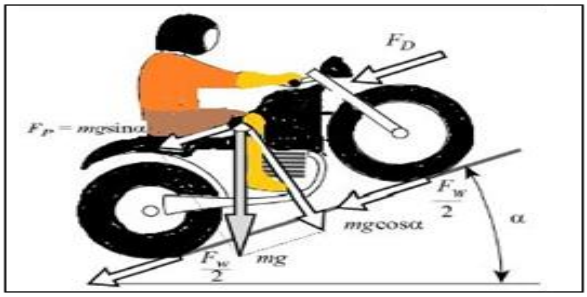

Figure 5: Drag forces acting on the motorcycle. [17]

The rolling resistance can be considered as 2% of the weight, which is considered as negligible for sum of resistance forces. If ρ is the air density coefficient, C_D is the drag coefficient, A is the frontal area of the motorcycle and V is the linear velocity, the drag force acting on the motorcycle centre is (F_d) can be calculated by,

$$F_d = \frac{1}{2}\rho C_D A V^2 \quad \ldots\ldots\ldots\ldots\ldots 1)$$

The resistive force caused by a slope of the road is given by,

$$F_R = m.g.\sin\alpha \quad \ldots\ldots\ldots\ldots\ldots (2)$$

Where, m = 220 kg Approx. (considering racing bike two wheeler), g = acceleration due to gravity = 9.81m/s^2, α is the angle of inclination to the road surface. The effect of sum of resistive forces applied on the motor shaft is given by following equation where, Tm is total resistive force, r_w is the total radius of wheel and tire and N is the ratio of number of teeth of front and rear sprockets.

$$T_m = \frac{r_\omega}{N}[m_g \sin\alpha + \frac{1}{2}\rho C_D A V^2] \quad \ldots (3)$$

The change in linear momentum of the motorcycle and pilot, given by following equation, can be seen as a linear force Fi being applied on the motorcycle centre of gravity.

$$F_i = m\ddot{x} \quad \ldots\ldots\ldots\ldots\ldots\ldots\ldots (4)$$

The equivalent torque applied on the rotor shaft is given by,

$$T_{im}^r = \frac{\ddot{\theta}_r}{N}\frac{mr^2\omega}{N} = \frac{\ddot{\theta}_r\, mr^2\omega}{N^2} \quad \ldots\ldots (5)$$

Converting above equation in terms of the angular acceleration of the rotor shows that the equivalent moment of inertia of the motorcycle applied at the rotor shaft is,

$$J_m = \frac{mr^2\omega}{N} \quad \ldots\ldots\ldots\ldots\ldots\ldots (6)$$

The effect of both wheels' angular momentum is mathematically described as the concentration of both wheels momentum on the rear wheel. The torque resulting from the variation of the wheels' angular momentum is given by,

$$T_{im}^\omega = j_\omega \ddot{\theta}_\omega \quad \ldots\ldots\ldots\ldots\ldots\ldots (7)$$

In the rotor, this torque can be determined by following equation, where the equivalent inertia of the wheels applied on the motor shaft is,

$$T_{im}^\omega = \ddot{\theta}_r \frac{j_\omega}{N^2} \quad \ldots\ldots\ldots\ldots\ldots\ldots (8)$$

For simplification, the wheels are modelled as disks of homogeneous density, thus, the moment of inertia of each is determined with following equation, where the subscripts wf and wr are used to refer to the front and rear wheels. In this case, the radius of both wheels are equal, $r_{\omega f} = r_{\omega r} = r_\omega$

$$J_{\omega f} = \frac{1}{2} m_{\omega f} r_{\omega f}^2$$

$$J_{\omega r} = \frac{1}{2} m_{\omega r} r_{\omega r}^2 \quad \ldots\ldots\ldots\ldots\ldots\ldots (9)$$

The motorcycle geometry can be characterized by the wheelbase p, the height of the centre of gravity h and the distance between the centre of gravity and rear wheel axle b, see figure,

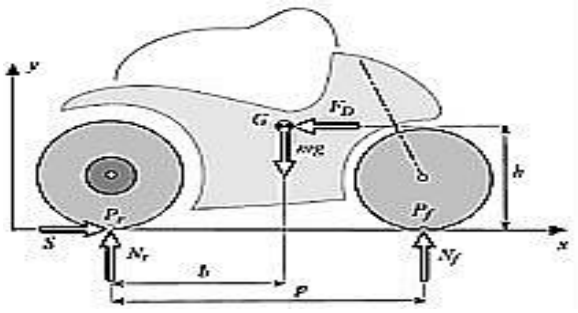

Figure 6: Motorcycle geometric parameters. [17]

The weight of the motorcycle is shared between both wheels and the opposite force that the ground exerts on each wheel is called normal force Nr for the rear wheel and Nf for the front wheel. In steady state, the normal force acting on each wheel is given by,

$$N_f = mg\frac{b}{p}$$

$$N_r = mg\frac{(p-b)}{p} \quad \ldots\ldots\ldots\ldots\ldots\ldots (10)$$

In transitory rectilinear motion, i.e. accelerating or braking, a load transfer occurs between wheels, which is proportional to the accelerating or braking force. During acceleration, the normal force acting on each wheel is given by,

$$N_f = mg\frac{b}{p} - S\frac{h}{p}$$

$$N_r = mg\frac{(p-b)}{p} + S\frac{h}{p} \quad \ldots\ldots\ldots\ldots\ldots\ldots (11)$$

$$S = T_{em}^{r}\frac{N}{r_{\omega}}$$

Where,

During braking, there is a load transfer from the rear wheel to the front wheel, characterized with by,

$$N_f = mg\frac{b}{p} + F_B\frac{h}{p}$$

$$N_r = mg\frac{(p-b)}{p} - F_B\frac{h}{p} \quad \ldots\ldots\ldots\ldots\ldots\ldots (12)$$

Where, $F_B = F_{BF} + F_{BR}$ is the braking force applied by the ground on the rear wheel, F_{BR}, and on the front wheel F_{BF}. Both when accelerating and braking the maximum linear force applied by one tire on the road is given by,

$F_{Bmax} = F_{BFmax} + F_{BRmax}$ ……. (13)

$\leq \mu_f Nf + \mu_r Nr$……(14)

$S_{max} \leq \mu_r Nr$

Where μ_f and μ_r are the front and rear wheel traction coefficients. These are considered equal, $\mu_f = \mu_r = \mu$. The value of μ is not given by the tire manufacturers. For the case of the racing tires, the values ranged from μ = 1:1 to μ = 1:5. Hence, the value μ = 1:3 was considered a good approximation. For this value of the traction coefficient, the maximum braking and acceleration forces are given by F_{Bmax} = 2904:72 Nm and S_{max} = 2904:72 Nm

The maximum braking force applied by the tires on the road is limited to either the slip condition or the flip over condition (complete loss of rear tire traction). Considering the traction coefficients of slick tires on a racetrack, maximum braking is generally limited by the flip over of the motorcycle. Moreover, the braking force distribution among front and rear brakes varies with the traction coefficient and tends to increase on the front tire while decreasing on the rear tire as μ increases. This is due to the previously described load shift to the front of the motorcycle when braking. The distribution of braking force among the wheels can take values higher than 90% for the front wheel and less than 10% for the rear wheel in a case where $\mu \leq 1$. The flip over of the motorcycle happens when the normal force on the rear tire becomes null and all the braking force is being applied on the front wheel. In this case, the braking force is given by,

$$F_B = mg\frac{(p-b)}{h} = 2255.63\text{Nm} \quad \ldots\ldots\ldots (15)$$

This value corroborates that for this particular motorcycle, braking is limited by the flip over of the motorcycle and not by the tire slippage.

Similarly to the braking limits, acceleration can also be limited either by the point at which the normal force on the front wheel is null (wheelie) or the point at which the rear tire slips. Again it is less common for rear tire slippage to happen on a race environment, nevertheless, both situations are considered. The traction force required to lift the front wheel is given by,

$$S = mg\frac{b}{h} = 2255.63\text{Nm} \quad \ldots\ldots\ldots\ldots\ldots\ldots (16)$$

As with the case of braking situation, the maximum traction force is limited by the wheelie situation.

The dynamics involved in a motorcycle turning are highly complex. For the sake of simplicity, the simplifications used here are,

1. The motorcycle runs along a turn of constant radius at constant velocity (steady state conditions)
2. The gyroscopic effect is negligible
3. The cross section of the tires is null

The maximum velocity in a turn is given by,

$$V_{max} = \sqrt{\tan\varphi_i g R_c} \quad \ldots\ldots\ldots\ldots\ldots\ldots (17)$$

Where φ_i is the lean angle, R_c is the radius of the curve, g is the acceleration of gravity and V is the motorcycle linear speed. This demonstrates the fact that the maximum turn speed is not affected by the mass, but by the turn geometry and the maximum lean angle.

The actual lean angle is measured from the upright position, resulting in an approximate value of 52º. Even though this represents but a gross estimate of the real lean angles, it serves to prove that a maximum value of 50º of lean angle is be an adequate approximation.

Experimental analysis

Simulation for electric vehicle to evaluate the battery parameters is proposed here. The simulation has been carried out using MATLAB / Simulink considering Hybridization of lithium ion battery which is initially charged 100% and Supercapaciter as an energy source and following input parameters,

Table 2: EV parameters for simulation

Nominal voltage of lithium ion battery	48 V	Mass of vehicle	220 kg
Rated Capacity	48Ah	No of wheels per axle	2
Rolling radius of tire	0.3 m	Horizontal distance from front axle to CG	1.4 m
Rated vertical load	3000 N	Horizontal distance from rear axle to CG	1.6 m
Peak longitudinal force at rated load	3000 N	CG distance above ground level	0.5 m
Slip at peak force at rated load	10%	Frontal area	$2m^2$
Carrier (C) to driveshaft (D) teeth ratio	4	Drag coefficient	0.25
Follower (F) to base (B) teeth ratio (NF/NB)	2	Air density	$1.18kg/m^3$
No-load speed	7500 RPM	Rated speed (at rated load)	5000 RPM
Rated load (mechanical power)	5KW	Rated DC supply voltage	50V

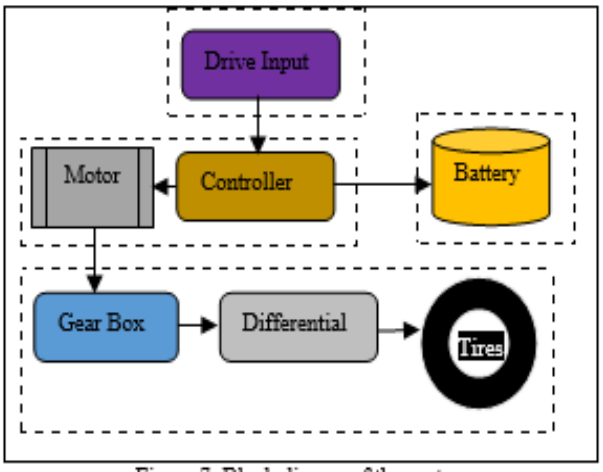

Figure 7: Block digram of the system

Figure 7: Block digram of the system

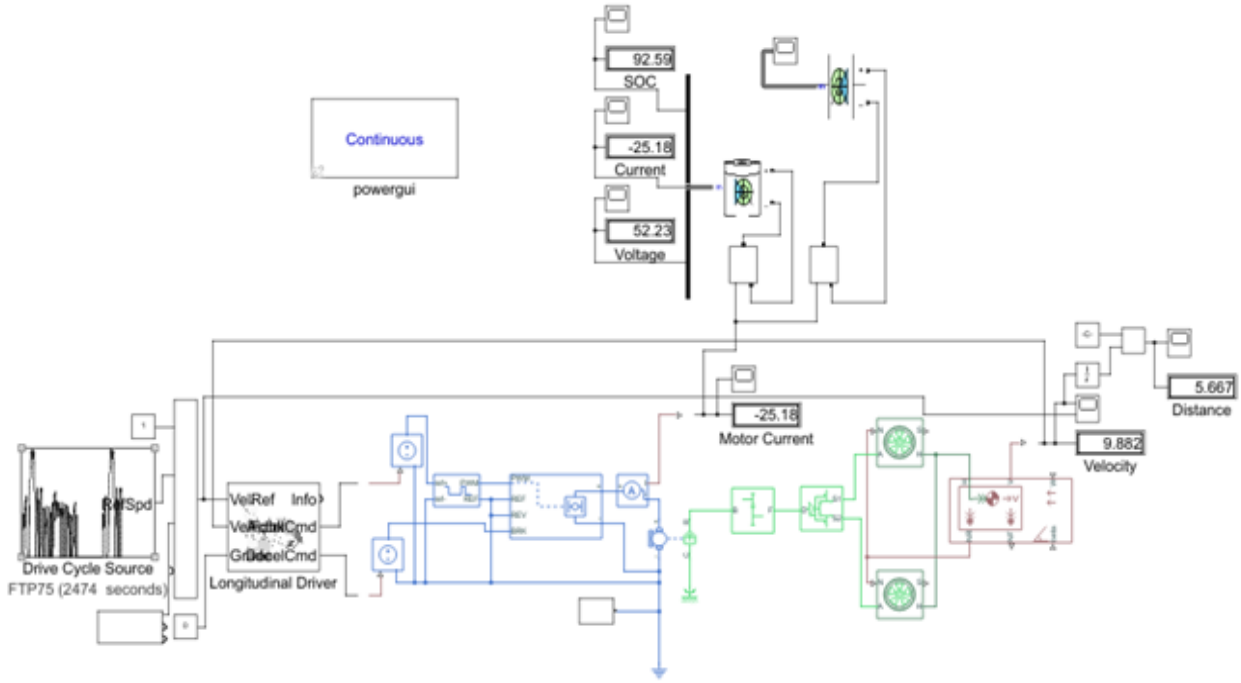

Figure 8: Simulink model of Electric Vehicle

Observation Results:

Initially battery was charges 100%. Comparing FTP 75 cycle of 2474 seconds, following results were obtained,

Battery state of charge – 85.17%

Current - -25.13 A
Voltage – 52.29 V
Velocity – 9.865 Km / hr
Distance Travelled – 5.664 Km.

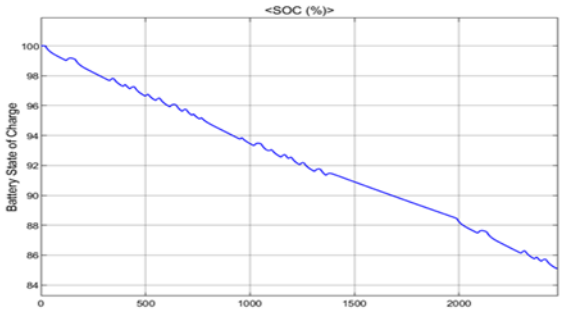

Figure 9: Battery SOC Vs time

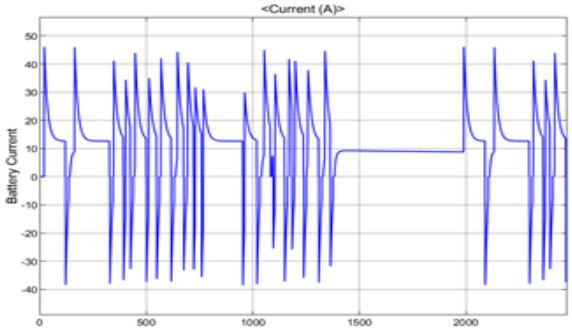

Figure 10: Battery current Vs time

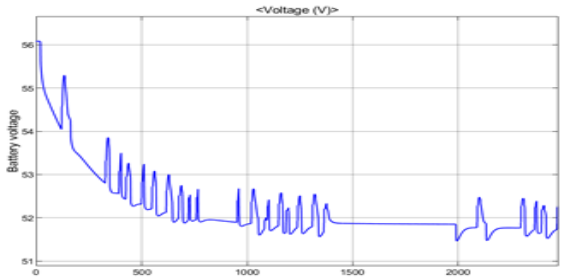

Figure 11: Battery Voltage Vs time

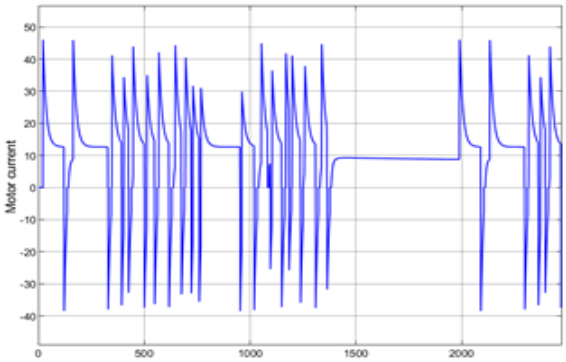

Figure 12: DC Motor current Vs time

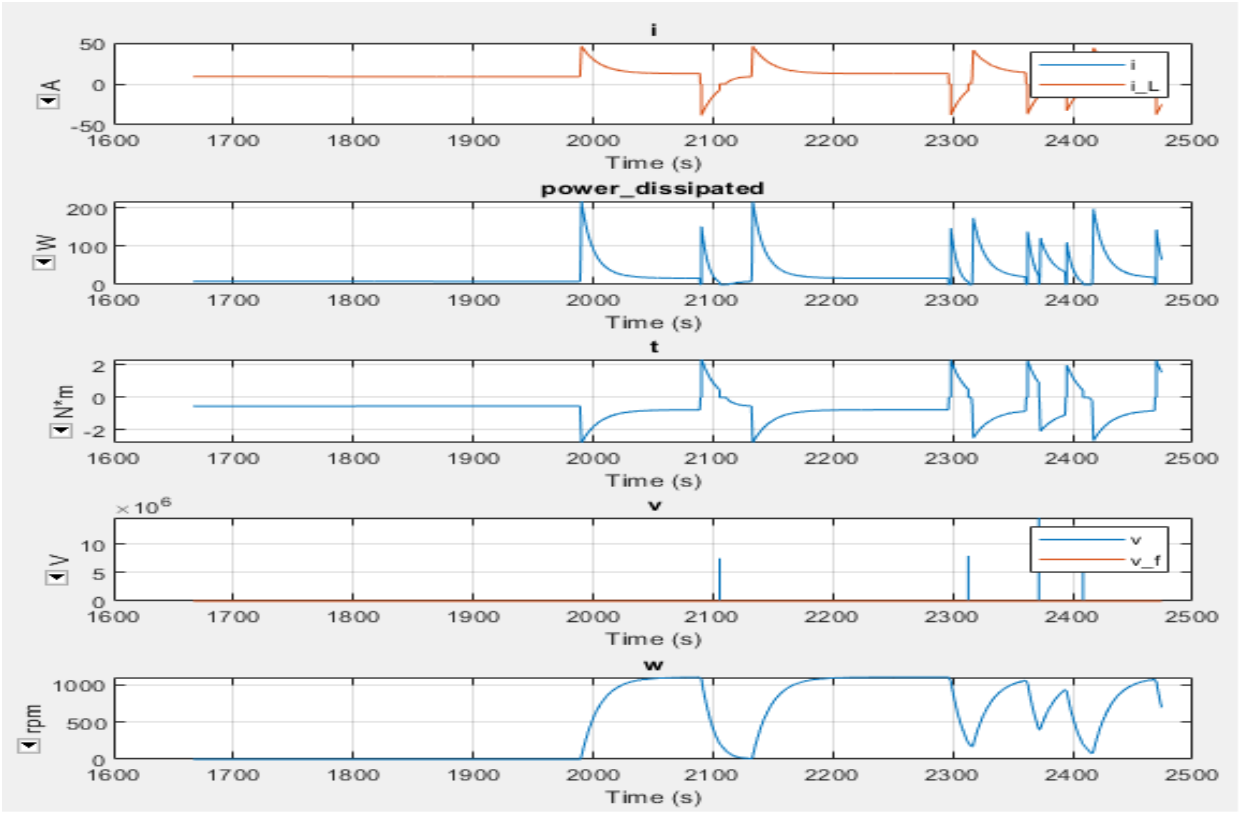

Figure 13: Variation of DC motor parameters Vs time

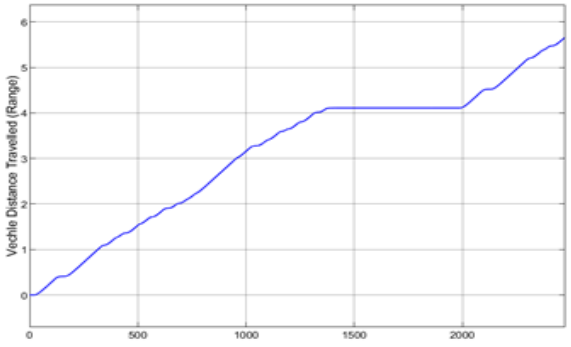

Figure 14: Distance covered by vehicle Vs time

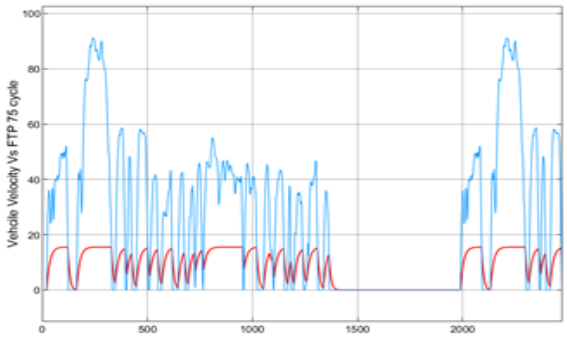

Figure 15: Distance covered by vehicle Vs time

V.CONCLUSION AND FUTURE SCOPE

Conclusions:

- Literature Survey showed much work needs to be performed on implementation of electric vehicle and its hybridization related to its structural and thermal investigations as per road and transportation conditions.
- Mechanism needs to analyse for activation of supercapaciter during high power density requirements and battery during high energy density requirements. Also the shorter discharging time of supercapaciter needs to work upon for effective hybridization.
- Proposed HESS can be worked on active as well as passive for getting effective structural optimized solution.
- Simulation of electric vehicle shows graphical representation of variation in different parameters of electric vehicle and it seems that, battery state of decreases linearly w.r.to. Time. Battery and DC motor current shows interrupted step response and voltage decreases interruptedly w.r.to time. Distance covered by vehicle shows increasing linear relation for first 1300 seconds, for next 700 seconds it is constant whereas again increase linearly further till completion of cycle.
- In this analysis FTP 75 cycle is considered for comparative analysis with proposed EV, the graphical representation of which shows necessity of modification in input parameters to match with the required cycle.

Future scope:

- Further analysis can be done for different motors and controllers performance.
- EV paraemters can be further modefied for paramters meting with the required FTP 75 cycle.
- Further comparative analysis can be done for different batteries and other energy sources.
- We can make hybridization of battery and solar panel, battery and supercapaciter, battery with internal combustion engine also for analysis the behaviour of different battery performance with its hybrdiaztion for getting effective energy storage system for electric vehicle.

REFERENCE

[1] Mahdi Soltani, Joris Jaguemont, Peter Van den Bossche, Joeri van Mierlo and Noshin Omar, “Hybrid Battery/Lithium-Ion Capacitor Energy Storage System for a Pure Electric Bus for an Urban Transportation Application” in applied science article, 2012, pp.1-19.

[2] Jian Cao and Ali Emadi, IEEE Transactions on Power Electronics, “A New Battery/Ultracapacitors Hybrid Energy Storage System for Electric, Hybrid, and Plug-In Hybrid Electric Vehicles”, Volume 27, No. 1, January 2012, pp.122-132.

[3] Rebecca Carter, Andrew Cruden, IEEE transactions on vehicular technology, “Optimizing for Efficiency or Battery Life in a Battery/Supercapacitor Electric Vehicle”, May 2012, 61(4):1526-1533.

[4] A. Ostadi, M. Kazerani et.all. In IEEE transactions IEEE Transportation Electrification Conference and Expo (ITEC), “Hybrid Energy Storage System (HESS) in vehicular applications: A review on interfacing battery and ultra-capacitor units” 2013, pp.275-281.

[5] Seyed Ahmad Hamidi, Emad Manla, and Adel Nasiri, “Li-Ion Batteries and Li-Ion Ultra capacitors: Characteristics, Modelling and Grid Applications” in IEEE transactions, 2015, pp.4973-4979.
[6] Clemente Capasso, Ottorino Veneri, “Integration between supercapacitor and ZEBRA batteries as the high-performance hybrid storage system for electric vehicles” in Science directory ELSEVIER publication, 2017, pp. 2539-2544.
[7] Wenhua Zuo, Ruizhi Li, Cheng Zhou, Yuanyuan Li, Jianlong Xia, and Jinping Liu “Battery-Supercapacitor Hybrid Devices: Recent Progress and Future Prospects” in Advanced Science News publication, 2017, pp.1-21.
[8] Herath, Pasan Gunawardena, “Conversion of a Conventional Vehicle into a Battery-Supercapacitor Hybrid Vehicle” in American Journal of Engineering and Applied Sciences, a science publication article 2018, pp.1178-1187.
[9] Mahdi Soltani, Jan Ronsmans et.al., July 2018 Applied Sciences 8(7):1176, “Hybrid Battery/Lithium-Ion Capacitor Energy Storage System for a Pure Electric Bus for an Urban Transportation Application”2018, pp.1-19.
[10] Lip Sawa, Hiew Poona, in ELSEVIER science direct journal ICAE 2018, “Numerical modelling of hybrid supercapacitor battery energy storage system for electric vehicles”, 2018, pp.2751-2755.
[11] Md. Arman Arefin, Avijit Mal, Journal of Mechanical and Energy Engineering, Vol. 2(42), No. 1, “Hybridization of battery and ultracapacitor for low weight electric vehicle”, 2018, pp. 43-50.
[12] Lia Kouchachvili, Wahiba Yaïci in ELSEVIER journal of power sources 374, “Hybrid battery/supercapaciter energy storage system for the electric vehicles”, 2018, pp. 237-248.
[13] Immanuel N. Jiya, Nicoloy Gurusinghe et.all., Indonesian Journal of Electrical Engineering and Computer Science Vol. 16, No. 2, November 2019, “Hybridisation of battery, supercapacitor and hybrid capacitor for load applications with high crest factors: a case study of electric vehicles” pp. 614~622
[14] S Devi Vidhya and M Balaji, in Measurement and Control 2019, Vol. 52(9-10), “Modelling, design and control of a light electric vehicle with hybrid energy storage system for Indian driving cycle”, pp. 1420–1433.
[15] A.Bharathi Sankar, R.Seyezhai, in WSEAS TRANSACTIONS on POWER SYSTEMS E-ISSN: 2224-350X, Volume 14, 2019, “Super capacitor/Battery based Hybrid Powered Electric Bicycle” pp.156-162.
[16] Walvekar, A., Bhateshvar, Y et.all. In SAE international US, ISSN 0148-7191 in 2020, “Active hybrid energy storage system for electric Two-wheeler”. pp.1-6.
[17] Vittore Cossalter, “Motorcycle dynamics”, Second English edition 2006.
[18] Thomas Reddy, Handbook of batteries. McGraw-Hill Professional; 4th edition, 2010.
[19] Scott J. Moura, Jason B. Siegel, Donald J. Siegel, Hosam K. Fathy, and Anna G. Stefanopoulou, "Education on vehicle electrification: Battery Systems, Fuel Cells, and Hydrogen," in IEEE Vehicle Power and Propulsion Conference, 2010.

NOVATEUR PUBLICATIONS
INTERNATIONAL JOURNAL OF INNOVATIONS IN ENGINEERING RESEARCH AND TECHNOLOGY
[IJIERT] ISSN: 2394-3696 Website: ijiert.org
VOLUME 8, ISSUE 6, June. -2021

"DESIGN AND MANUFACTURING OF PROTECTION CAP FOR STUB SHAFT USING PLASTIC INJECTION MOULDING"

Malhar Mahajan
Dept. of Mechanical Engineering NBNSSOE, Pune, India
mahajan.malhar1099@gmail.com

Atharva Joshi
Dept. of Mechanical Engineering NBNSSOE, Pune, India
atharva.jo2@gmail.com

Rohan Kshirsagar
Dept. of Mechanical Engineering NBNSSOE, Pune, India
rohan.ksgr007@gmail.com

Shrihari Khatri
Dept. of Mechanical Engineering NBNSSOE, Pune, India
khatrishrihari@gmail.com

Dr. Arun Thakare
Dept. of Mechanical Engineering NBNSSOE, Pune, India
arun.thakare@sinhgad.edu

ABSTRACT
In most industries, the product is manufactured at one place while assembled at another location. So, during transportation and handling, from manufacturing to assembly plant the part might get damaged, due to which it will not fit to assemble, leading to a big loss for the company. To avoid this, the part needs to be protected. By manufacturing of product using Plastic Injection Moulding (PIM), it will protect the part during transportation and handling. Considering strength as one of the important properties of the part, injection moulding is best suited for the mass production of plastic parts. Hence, injection moulding is most widely used in the local industries. This paper gives an insight into the Plastic Injection Moulding process from designing to manufacturing of the product, with certain process parameters that need to consider while designing for the selection of optimum material for the product.

Keywords: Plastic Injection moulding, Mass Production, Optimum Material.

INTRODUCTION:
The most common methods of manufacturing plastic parts include Extrusion, Injection moulding, Blow moulding, Casting, etc. However, injection moulding is most widely used in the local industry as it is suitable for mass production. In the plastic injection moulding process, plastic products are produced by forcing the resins made of plastic materials by application of high pressure into a mould (hollowed-out block cavity) where it is cooled, allowed to solidify, and after that taken out from the mould by opening cope and drag part of the mould. The solidified material ejected from the mould results in the final product. Objects having complicated shapes and geometries can be easily manufactured by using a plastic injection moulding process with great dimensional accuracy.[1] The cooling process in plastic injection moulding is of great importance as it plays a crucial role in determining both the production rate and part quality.[2]
In this project, a protection cap is being manufactured to protect the base of the stub shaft. Stub shaft is used in power transmission systems. It is a small rotating shaft that helps to transmit power from its place of generation to a location where it is applied to perform useful work. It allows side-load to the back of an engine while simultaneously preventing any load transmission back to the crankshaft. Considering the dimensions of the stub shaft a protection cap is manufactured by using plastic injection moulding. The main purpose of the protect the edges of the stub shaft during transportation from one location to another.

Another important parameter that needs to be considered is costing of the process. Higher cost of material will result in an expensive product. Hence, the selection of material should be considered to fulfil the requirements of the customer.[3] Fig. (1) shows a vertical plastic injection moulding machine.

Fig. 1 – Injection Moulding Machine

LITERATURE SURVEY

R. M. Khan et al.[1] , In this paper author studied and identified the factors which are considered to manufacture a product with minimum defects. It is concluded that to control defects in manufactured product selection of proper geometry and process parameters are important.

Y. C. Lam et al.[2] **,** This paper states the importance of a cooling system in plastic injection moulding. CAE (Computer - Aided Engineering) technology is adopted for the optimization of the cooling systems in plastic injection moulding. From a case study, the authors have concluded that the genetic algorithm and CAE stimulation is efficient in a cooling system. It results in a high production rate and good production quality.

P. K. Mulge et al.[3] , This paper gives a brief review on optimization of process parameters used in plastic injection moulding by using Taguchi's methodology. Taguchi's techniques are most widely used in industry to save cost, reduce experimental time, and improve the quality of the manufactured products.

G. Singh et al.[4] , In this paper author reviewed and concluded that controlling process parameters leads to improve quality of the product. The two most commonly occurring defects in plastic injection moulding are warpage and shrinkage. The use of recyclable and eco-friendly raw materials is highly beneficial for the environment and society.

K. Jain et al.[5] , This paper highlights the causes of defects in plastic injection moulding components. The product quality of components mainly depends on the selection of material, mould design, setting process parameters, and cooling system. In plastic injection moulding, residual stresses lead to the formation of shrinkage in components. By using Taguchi's approach shrinkage defects can be minimized which helps to reduce the warpage of components.

S. Kitiyama et al.[6] , This paper states various process parameters of the plastic injection moulding process to minimize the weld lines and the importance of clamping force to improve the quality of the moulded product. By using numerical simulation, factors such as mould temperature, melt temperature, injection time, etc. were optimized for the smooth manufacturing process.

M. Kroon et al.[7] , In this paper author investigated fracture mechanical properties of Low-Density Poly-ethylene (LDPE) using both analytical and experimental methods. The Author also discussed various grades of polyethylene (PE) according to their mechanical behaviour.

P. K. Bharati et al.[8] , This paper focuses on various process parameters and approaches used for plastic injection moulding. Various approaches used are mathematical models, Taguchi method, fuzzy logic, case-oning (CBR), finite element method (FEM), non-linear modelling, etc. These approaches help to ıe process in the best possible way.

P. D. Kale et al.[9] , This paper gives a brief review of, how the runner system affects the quality of the product and the complete injection moulding process in detail. From this paper, author observed that improper runner system causes burn mark, warpage, weld lines in the product. From this paper, author concluded that replacing the cold runner system with a hot runner system reduces the defects in the product also helps in scrap reduction.
R. A. Yadav et al.[10] , In this paper methods of optimization in the plastic injection moulding process and various process parameters are reviewed. The Strength and weakness of various approaches such as Taguchi method, Artificial Neuron Networks (ANN), Case-Based Reasoning (CBR), Genetic Algorithms (GA), etc. are addressed in this paper. By adopting these approaches various factors in manufacturing such as cost, quality, and time can be controlled.
Dr, A. R. Ahamed et al.[11] , In this paper author focused on critical factors involved in the plastic injection moulding process. Some critical factors include melt temperature, injection pressure, cooling time. Taguchi and ANOVA techniques were used to find the effects of melt temperature, injection pressure, and cooling time of plastic materials.
X. P. Dang et al.[12] , In this paper author discussed basic steps for optimization of plastic injection moulding process parameters. The author mainly focuses on simulation based optimization and introduced two robust techniques for optimizing mould parameters, which include direct numerical optimization and metamodel based optimization. The author concluded that the direct GA optimization method is the best choice for low non-linear problem.
S. J. Liu et al.[13] , In this paper author gives a brief review on the manufacturing of thermoplastic components by novel water-assisted injection moulding technology. To optimize various process parameters during manufacturing such as melt temperature, mould temperature, etc. The author used Taguchi orthogonal array design method for the precise manufacturing of component. The author concluded that the parts produced by assisted injection moulding method have shortened cycle time as compared to other assisted injection moulding processes.

PROBLEM STATEMENT

Design and manufacturing of protection cap for stub shaft using injection moulding methodology. The major challenge is to come up with an optimum design to match customer requirements in a cost efficient way and to select the best supplier for rawmaterials and ensure smooth manufacturing to match customer demand.

METHODOLOGY

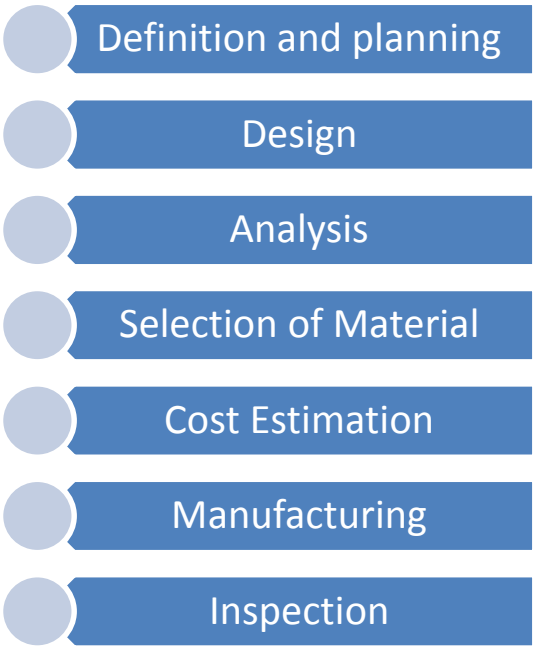

Fig. 2 – Methodology

- **Definition and Planning:** Discussion of the problem statement and further planning.
- **Design:** To design the part as per the dimensions of the stub shaft.
- **Analysis:** To carry out analysis to select best suited material.
- **Selection of material:** Based on the analysis result, selection of precise material.
- **Cost Estimation**: To predict the cost of the resources required to complete the product within the project scope.
- **Manufacturing**: To manufacture the product by using an automatic machine.
- **Inspection**: To inspect the final product by considering good quality, accuracy and precision to fulfil customer's requirements.

EXPERIMENTAL WORK

Design of Stub shaft

- A stub shaft is a small rotating shaft made of mild steel (M.S) used in power transmission systems.
- The main purpose of the protection cap is to protect the edges at the base of the stub shaft.
- From the sketch below it is observed that:
- The maximum diameter of the base of the shaft – 89.7mm
  The width of the shaft – 26.5mm
  The length of the shaft – 144.5mm
- From the fig. (3) the 3-D sketch of the stub shaft is shown which helps in determining the centre of gravity of the stub shaft.

Fig. 3 – 3D Model of the stub shaft

DESIGN OF PROTECTION CAP

- Design for manufacture (DFM) is a process in which the product is designed by the design engineer to achieve the best possible results to meet customer's requirements.
- The product which is being designed is a protective cap that is used to protect the base of the stub shaft.
- In the fig. (4), a 2-D sketch of the Protection cap is shown which is designed on solid works as per the dimensions of the stub shaft.
- The internal diameter of the cap is equal to the maximum diameter of the base of the stub shaft.
- While designing, a flange of 97 mm is provided for easy fitting and removal of the cap from the base of the stub shaft.
- For cost optimization, the minimum required thickness and width of the cap should be taken under consideration.
- As per the calculations, the thickness and width of the cap were 1.5 mm and 16 mm respectively.

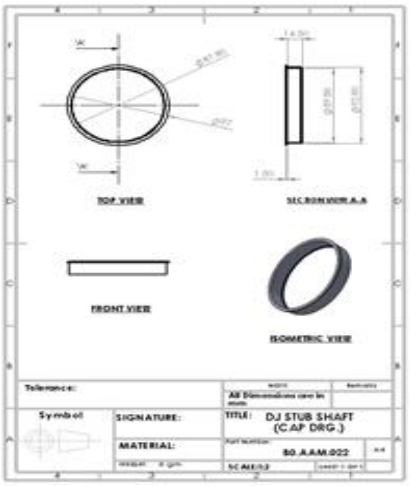

Fig. 4 – Design of the cap

PROPERTIES OF MATERIALS

The common materials used in plastic injection moulding are:
Nylon-6, Polyvinyl Chloride, Polypropylene, Low-Density Polyethylene, etc.
Few properties of the above materials need to be considered while the selection of material is given in the table below-
Table (1) shows the mechanical properties of different materials. By considering these properties, an analysis will be carried out to select the best suited material for the cap.

Table – 1 Mechanical Properties of material

PARAMETER		**MATERIAL**		
	NYLON-6	PVC	PP	LDPE
Modulus of Elasticity (N/mm^2)	3500	3230	1450	449
Tensile strength, yield ($N/mm^{2)}$	186	50	369	64.8
Hardness	82	83	83	56.0
Mould Temperature (^oC)	95	70	91	65.66
Tangent Modulus ($N/mm^{2)}$	792.52	729.05	947.62	305.5

RESULT AND DISCUSSION

Modelling

Modelling is the first step towards analysis. It acts as a link between designer and manufacturer to create a 3D prototype of the product that is to be manufactured. The fig. (5) shows the 3D model of the protection cap which is modelled on ANSYS Workbench. The cap is designed on software as per the dimensions of the base of the stub shaft.

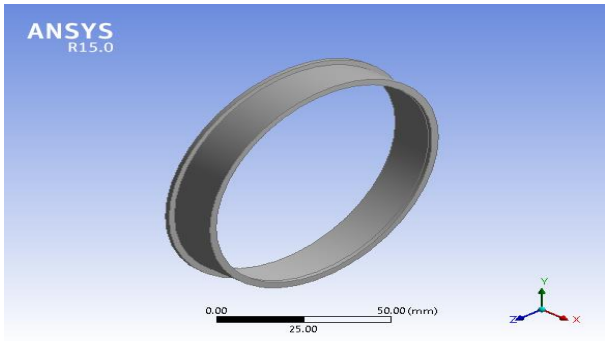

Fig. 5 – 3-D Model of Cap

Analysis

The analysis of the 3D model of a protection cap was carried out on ANSYS Workbench R15.0. The material properties like young's modulus, Poisson's ratio, tangent modulus and other mechanical properties were defined for all the materials. After meshing of the cap, boundary conditions were applied to carry out the analysis.

Meshing

Meshing or discretization is defined as dividing the body into a finite number of smaller elements to increase the accuracy up to the maximum possible extent. For the protection cap, fine meshing was done which created 15555 nodes and 7405 elements.

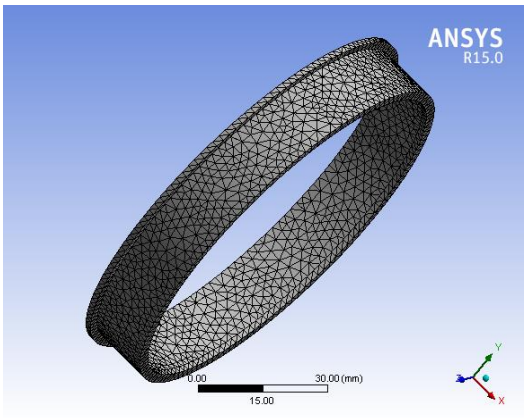

Fig. 6 – Fine meshing of cap

Boundary Condition

The value of variables such as force, displacement, temperature, etc. specified on the boundaries of the body or structure is called boundary conditions. The Boundary condition is an important factor of mathematical modelling. They help in determining the flow of the problem which leads to a unique solution. As the cap is resting on its base, the fixed support is applied at the base. A Remote point is a point in which boundary conditions can be applied from outside of the body. The significance of remote point is, the force that is applied on the point is equally distributed over the surface of the body. To apply the remote force, it is necessary to calculate the C.G of the body. Fig. (7) shows a web projected from a remote point to the targeted surface.

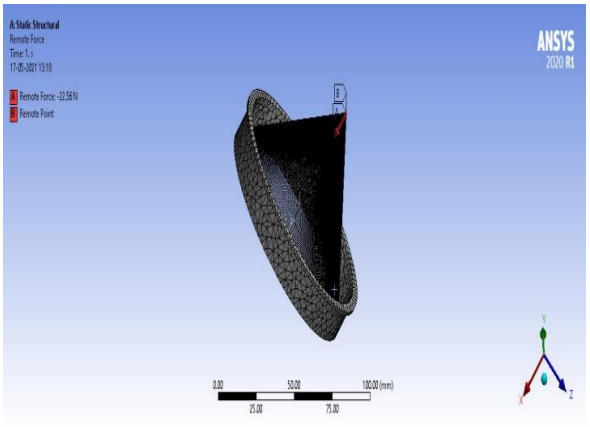

Fig. 7 – Remote force applied on the cap

Results and selection of material

LDPE

A. Deformation

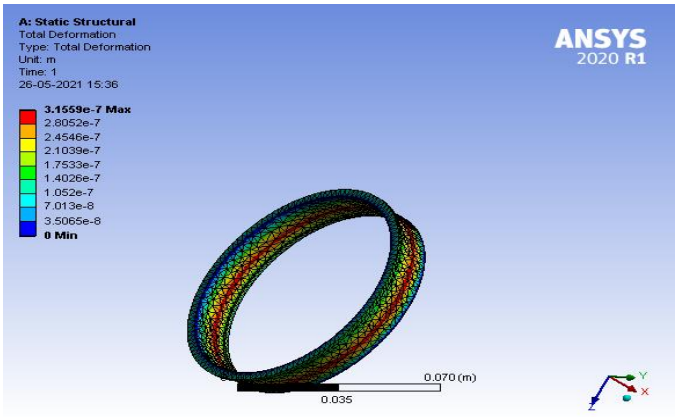

Fig. 8 – Total Deformation of LDPE

B. Stress

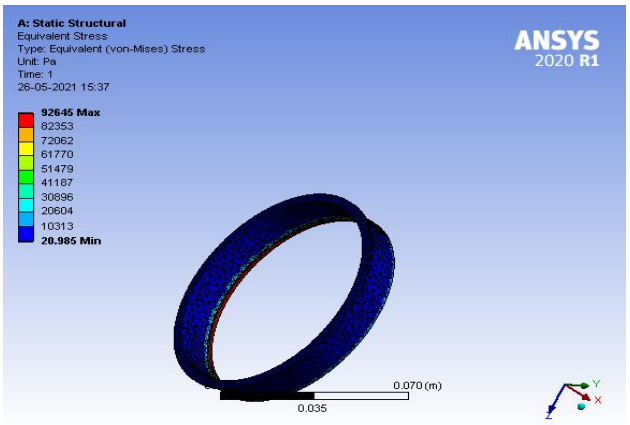

Fig. 9 – Equivalent Stress of LDPE

- From the above figures, the deformation of the cap under a certain load and stress induced on the cap is shown.
- Table (2) shows a comparison of various materials concerning to different parameters.

Table 2 – Comparison of Materials

Parameters	LDPE	PVC (FLEXIBLE)	PP	NYLON-6
Stress (N/m^2)	92645	83495	83096	83561
Cost (Rs)	120	115	140	260
Mould Temperature (^oC)	65	70	91	95
Young's Modulus (N/mm^2)	449	3230	1450	3500
Ultimate Compressive strength (N/m^2)	$6.5*10^7$	$2.5*10^7$	$4*10^7$	$5.5*10^7$

Analytical Calculation of Stress:

$\sigma = F/A$

where,

F = Load acting on the body in Newton.

= 22.56 N

A= Cross sectional area in mm2
=278.973 mm2
σ = Stress acting on body.
= 80.868 KN/m^2

The following scale shows variation in property of different materials for selection of optimum material.

HARDNESS

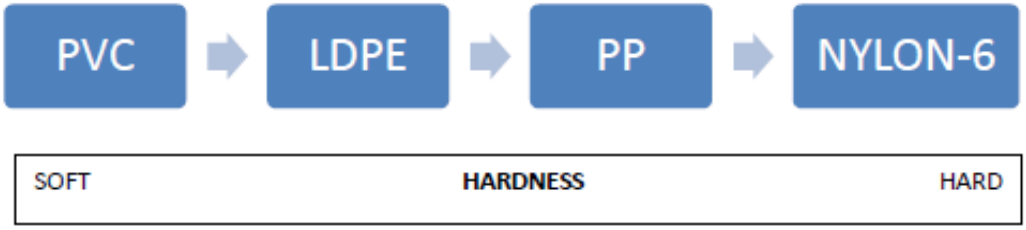

COSTING

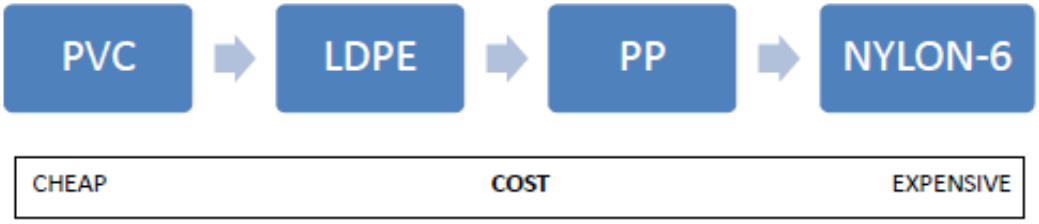

WEIGHT

FLEXIBILITY

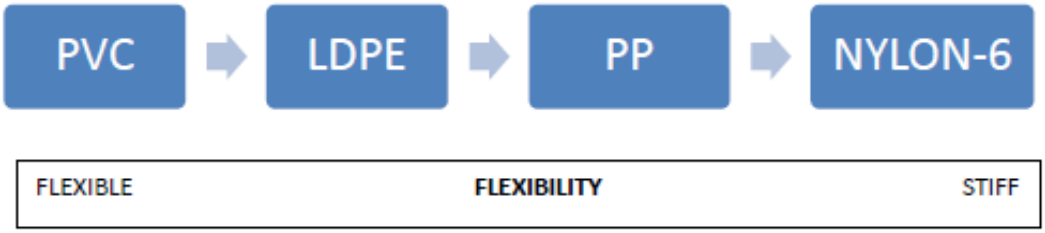

From charts, a comparison of different materials concerning various parameters is shown. To select the optimum material for the cap all the parameters must meet the customer requirement. The cap material must the stress induced due to the force acting on the cap and at the same time, it must be cost-effective.

1. STRESS: Analytical value of stress-induced in the cap is calculated in the analytical stress calculation section. So, by comparing the actual value and the experimental value the best-suited material can be selected for the cap. The actual value of stress-induced in the cap due to force is 80.868 KN/m^2. This is the minimum value of stress the cap should withstand.

2. DEFORMATION: The deformation values of all compared materials are almost equal. Therefore, these values will not be considered as the main comparing parameter for the selection of material.

3. MOULD TEMPERATURE: Mould temperature has a profound effect on the final properties of the product. The actual surface temperature of the mould is called the mould temperature. Perfect mould temperature results in the reduced unit cost of plastic product and improves the quality of the moulded product. The higher the mould temperature, the higher will be the cooling time which will indirectly increase the cycle time of the product. Therefore, the mould temperature should be as low as possible.

4. COST: Cost is one of the important parameters that need to be considered while the selection of material. The increasing cost of material gradually increases the final cost of the product. Failing to control the cost of the product results in less demand for the product in a competitive market. Hence the selected material should be cost-efficient and should have good mechanical properties which match the requirements of the product.
Considering the above parameters, the mould temperature of LDPE is lowest as compared to other materials which reduce the product ejection time resulting in an increased production rate. Similarly, in costing the price of PVC is lowest as compared with other materials but it does not fulfil the demands of some mechanical properties required for the cap. Hence the second-best cost-efficient material i.e., LDPE is considered. From table (2) the experimental values of stresses of all materials meet the maximum value of stress-induced. Therefore, by considering all the above parameters LDPE is the best-suited material for manufacturing of Protection cap.

Cost Estimation

Cost estimation is one of the important parameters which need to be considered while manufacturing any product. It gives a brief idea about the inventory cost as well as the production cost of the product. Table (3) shows the expected final cost of the cap.

Table 3 – Cost Estimation

Sr. No.	Component	Weight	Raw Material	R/M Cost/Kg	Material Cost	Labour Cost	Over Head Cost	Profit @ 15%	Total Rate
1	Dia 87.8 Cap	200 Grams.	LDPE	Rs. 120/-	2.60	0.55	0.20	0.50	3.85

By calculating the weight of the material per Kg required for the production, the material cost can be calculated. The Production cost primarily involves Labour cost and Cycle time. The complex design of the part tends to increase the production cost, which can be minimized by advanced mould designs. By using a recycled form of material, the cost of the product can be minimized. It possesses the same plasticity as that of the virgin material and the cost is 30% less than the raw material which is one of the main advantages of using recycled material. Whereas the cost of the cap can also be reduced by reducing the cycle time of the process, which can be done either by using automatic machines which will indirectly reduce the labour cost or by improving the process parameters. Apart from the production and material cost, the profit parameter is included for the growth of the company. By combining all the discussed parameters, the final cost of the cap is estimated.

Manufacturing

Plastic injection moulding process manufacture's products that have good dimensional accuracy, high quality and better dimensional stability. Factors that affect the quality of the moulded product depend on Design of product, Mould design, Machine performance and efficiency. The basic requirements of injection moulding are plasticization, injection and moulding. Plasticization is a prerequisite which ensures the quality of moulded
d helps to meet the requirements of moulding. Sufficient speed and pressure must be maintained
cting the molten material into the mould. At the same time to sustain the high pressure generated

inside the cavity, there must be sufficient clamping force. Thus, the clamping device and injection device play a major role in the injection moulding machine.

Basic steps of manufacturing

In the following figure, the basic steps of the plastic injection moulding process are shown:

Step 1 – Mould Closing: Mould cavity consists of two parts: Cope and Drag. For the product to be manufactured, both parts of the mould are in a closed position to avoid the spillage of material during the injection.

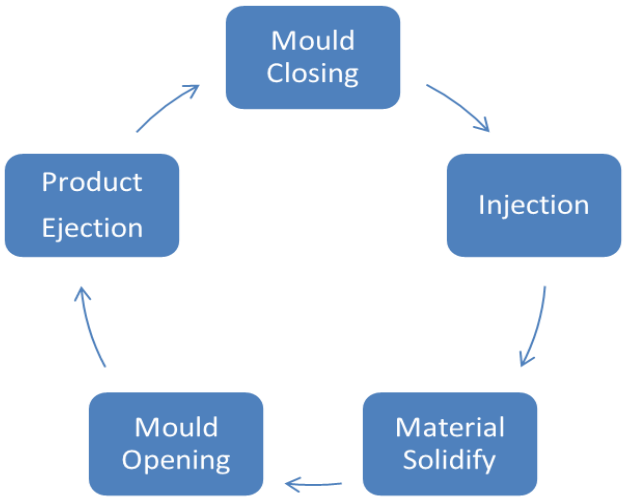

Fig. 10 – Manufacturing Process

Step 2 – Injection: The resins are fed into the hopper which passes through the barrel in which heating coils are located. This results in the melting of material and the molten resins are dosed through a nozzle at high pressure into the mould cavity.

Step 3 – Material Solidify: The injected material is kept inside the mould for a certain period of time to solidify. Also, water cooling channels are provided for effective solidification of the material.

Step 4 – Mould Opening: After the Solidification of material inside the cavity, the mould is opened for ejection.

Step 5 – Product Ejection: After ejection of product from the cavity, post-processing is done to get the final-product.

Horizontal injection moulding machine

Horizontal injection moulding machine is most widely used in plastic fabrication companies. The two main units of this machine are the clamping unit and the injection unit. Both these units lie on the same horizontal centerline.

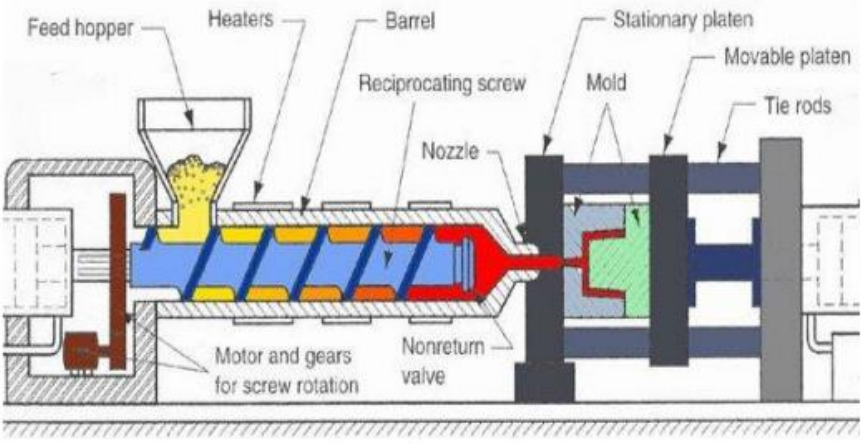

Fig. 11 Horizontal Injection Moulding Machine [3]

Fig. (11) shows a schematic diagram of a horizontal plastic injection moulding machine. The Clamping unit, injection unit and drive unit are the main units of the machine. When the molten resins are injected into the mould cavity at high pressure it results in high forces which may lead to the opening of the mould to avoid this, the clamping unit is used to keep the mould in a closed position by the use of clamping devices. Low clamping force may result in material spillage or deformed shape of the product. The function of the clamping unit is to hold, close and open the mould during the operation. The purpose of the injection unit is to inject molten granules into the mould cavity using injection nozzles. Power to perform injection and clamping operations is provided by the drive unit. Parameters considered in mould designing are runner system, gate location, sprue design, selection and location of the cooling channel.

The plastic resins are fed into the hopper either manually or by an automated system. Then the resins flow under gravity through the barrel into the heating chamber. The reciprocating screw extends from the hopper to the injection chamber. Heating bands are provided along the length of the screw which melts the plastic. Due to the reciprocating motion of the screw, the molten plastic gets injected into the mould cavity. The plastic flows into the mould cavity through the sprue, runner and gate. From the injection nozzle, the molten plastic flows through the sprue into the runner, which then directs the plastic into the mould cavity through the gate. The cooling channel is used for rapid cooling to reduce the manufacturing cycle time. When the plastic gets solidified the mould opens and the final product is ejected.

CONCLUSION

From this paper, it is concluded that a protective cap of optimum material is manufactured to satisfy customer requirements. The manufactured cap fulfils the requirement of protecting the edges of the stub shaft while transportation and handling. Considering the mechanical properties of the cap, to make the cap cost-effective and of good quality, low-density polyethylene (LDPE) is the best-suited material for the protection cap. Earlier, while transportation and handling the edges of the stub shaft were used to get damaged which led to a big loss for the company. However, the protection cap served the purpose of protecting the edges of the stub shaft, which minimizes the loss for the company. Although plastic injection moulding is a complex process, the product can be manufactured with lesser defects by controlling the process parameters.

ACKNOWLEDGEMENT

The authors acknowledge Mr. Arvind Ravetkar Akshay Firms who provided expertise and insight about the injection moulding process that greatly assisted the project work.

REFERENCES

1) Khan.R.M , Acharya .G, (2016) “Plastic Injection Molding Process and Its Aspects for Quality: A Review” 3(4):66-70 ISSN: 2394 - 658X
2) Lamy.y.c, Zhaiy.l.y, Taiy.k and Foky.s.c, (2004) “An evolutionary approach for cooling system optimization in plastic injection moulding”, vol. 42, no. 10, 2047–2061
3) Mulge.P.K , Dr Kalashetty.S.S, “A Brief Literature Review on Optimization of Plastic Injection Moulding Process Parameters for Various Plastic Materials by using Taguchi’s Technique” (2019) Vol. 8, Issue 07, ISSN: 2278-0181
4) Singh.G, Verma.A, (2016) “A Brief Review on injection moulding manufacturing process”, ICMP
5) Jain.K, Kumar.D, Kumawat.S, (2013) “Plastic Injection Molding with Taguchi Approach – A Review”, Vol. 2, Issue 5, ISSN No 2277 - 8179.
6) Kitayama. S, Tamada. K, Takano. M, Aiba. S, (2018) “Numerical optimization of process parameters in plastic injection molding for minimizing weldlines and clamping force using conformal cooling channel” , https://doi.org/10.1016/j.jmapro.2018.04.007
7) Kroona. M, Andreasson. E, Petersson. V, Olssond.P, (2018) "Experimental and numerical assessment of the work of fracture in injection-moulded low-density polyethylene", https://doi.org/10.1016/j.engfracmech.2018.02.004
8) Bharti. P. K, (2010) “Recent methods for optimization of plastic injection molding process – A ective and literature review" Vol. 2(9), 4540-4554

9) Kale.P.D, Darade.P.D and Sahu.A.R " (2020) A literature review on injection moulding process based on runner system and process variables", doi:10.1088/1757-899X/1017/1/012031
10) Yadav.R.A, Joshi.S.V, Kamble.N.K " (2012) "Recent Methods for Optimization of Plastic Injection Molding Process - A Literature Review" Volume 3, Issue 12, ISSN 2229-5518
11) Dr Ahamed.R, Dr.Dawood.S, Karthikeyan.R, (2013), "Designing and Optimizing the Parameters which affect the Molding Process using Design of Experiment", Volume 1, Issue 2, pp.116-122, ISSN:2347-5188
12) Dang.X.P, (2014) "General frameworks for optimization of plastic injection molding process parameters" http://dx.doi.org/10.1016/j.simpat.2013.11.003
13) Liu.S.J, Chen.Y.S, (2003) "The manufacturing of thermoplastic composite parts by water-assisted injection-molding technology" doi:10.1016/j.compositesa.2003.10.006

A Fundamental Study of Financial Performance With Reference To Hindustan Lever Ltd. And Procter & Gamble Ltd.

Dr. *Prakash V. Pise*

Assistant Professor

NBN Sinhgad School of Management Studies Ambegoan BK, Pune

E-mail:Prakash.pise532@gmail.com

Cell No: 9011067318

Abstract:

Financial performance is one of the most pivotal functional areas of management as the effectiveness of a business enterprise significantly depends on the efficient utilization of its financial resources. The growth potential of an enterprise also depends on its financial success as a major portion of investment funds of an ongoing business comes from its retained earnings. The importance of financial management has greatly enhanced during the last decade due to continue inflation. It has had a tremendous effect on the financial operations of manufacturing sector, power and energy sector, service sector and also retail sector. High interest rates have pushed up the cost of capital in the retail sector. High interest rates have pushed up the cost of capital in the retail sector. At the same time, it has increased the need of financial resources for operating of retail functions. Today working capital requirements and financial outlays on replacement, modernization and expansion have greatly increased in this sector. Consequently, financial managers are faced with the problem of raising additional financial resources. Their task has been made more difficult by the government policy of restricting the supply of loanable funds. The tasks of financial manager is more difficult but at the same time more important and more challenging for the financial managers of retail sector.

Key Words: *Financial Performance, Profitability Management, Working Capital Management*

Introduction:

Concept of working capital:

Working capital refers to the cash a business requires for day to day operation ,or, more specifically , for financing the conversion of raw materials into finished goods, which the company sells for payment. Among most important items of working capital are levels of inventory, debtors and credits. These items are looked at for signs of a company's efficiency and strength.

According to Hoagland "working capital is descriptive of that capital which is not fixed. But the more common use of working capital is to consider it as the difference between the book value of the current assets and the current liabilities.

Concept of gross working capital:

In the broad sense, the term working capital refers to the gross working capital and represents the amount of funds invested in current assets. Thus the gross working capital is the capital is the capital invested in total current assets of the enterprise. Current assets are those assets which in the ordinary course of business can be converted into cash within a short period of normally one accounting year.

Gross Working Capital = Total Current Asset

Concept of net working capital: In narrow sense, the term working capital refers to the net working capital. Net working capital is the excess of current assets over current liabilities or say.

Net working capital = current assets – current liabilities.

Capital working capital may be positive negative.

Constituent of working capital:

Current assets	Current liabilities
Raw Materials	Sundry creditors
Debtors	Bank overdraft
Prepaid expenses	Short –term loans
Loan and advances	Provisions
Investment	
Cash and bank balance	

Current Assets: current assets are those which are either in the form of cash or can be converted into cash within a year. Current assets are important to business because they are the assets that used to fund day operations and pay ongoing expenses.

The main items that comprise current assets are.

1. Inventories: inventories represent raw material and components, work in progress and finished goods.

2. Trade debtors: trade debtors comprise credit sales to customers

3. Prepaid expense: these are those expenses, which have been paid for goods and services whose benefits have yet to be received.

4. Loan and advances: they represent loans and advances given by the firm to other firms for a short period of time

5. Investment: these assets comprise short –term surplus funds invested in govt. securities, shares and short –term bonds

6. Hard cash and bank sense of balance: these assets represent cash in hand and at bank, which are used to meeting operational requirement. One thing can be see here is that this current asset is purely liquid but not non productive.

Cash and bank sense of balance: these assets represent cash in hand and bank, which are used for meeting operational requirements. One thing you can see here is that this current asset is purely liquid but non productive.

Current liabilities: current liabilities from part of working capital that represent obligations which the firm has to clear to the outside parties in a short –period, generally within a year. It includes:

1. Sundry creditors: These liabilities trunk out of purchase of raw material on credit terms typically for a period of one to two months .
2. Bank overdraft: This includes withdrawals in excess of credit balance standing in the firm's current accounts with banks.
3. Short –term loans: short- term borrowing by the firm from banks and others from part of current liabilities as short –term loans.
4. Provisions: This includes provisions for taxation, proposed dividends and contingencies.

Concept of profitability Analysis:

The most important part of financial performance is profitability analysis. The tool analysis is required to calculate or test of earning capacity of the business. Profit is the oxen of every business. It is most important part for the survival of business. Profit is required for the continues growth in competitive business world. The most effective and efficient tool of profitability analysis is ratio analysis .Profit is f of two types operating and non-operating. We can said that profitability analysis create clear and rative position regarding the financial performance of the selected units.

Objectives of study:

The present study "A comparative study of Financial Performance of HUL and P&G.", has been designed to achieve the following objectives:-

(1) To analyses and evaluate the overall working capital management.
(2) To analyses and evaluate the overall profitability.
(3) To analyses and evaluate the trends in financial performance of these two companies

Scope of the study:

The present study is confined to the two leading units in FMCG industry namely HUL and P&G The study covers a period of five years from 2010-11 to 2013-14.

Research Methodology:

Research design: Descriptive Research Design

Type of data: secondary data

The data from company annual reports, journals and website will be used to collect information for the undergoing study.

Sampling: The balance sheets and P &L a/c statements of 2009-2010, 2010-2011, 2011-2012, and 2012-2013 will be taken for the analysis of the companies in the undergoing study.

Tools for analysis: Various Financial tools like ratios to evaluate the performance of the companies will be used for the analysis and interpretation.

The secondary data was collected from various sources like annual reports. Besides for framing conceptual framework, various books and published material in standard books and newspapers, Journals and websites has been made use of.

DATA ANALYSIS

Current Ratio:

One of important function of the financial manager is to maintain sufficient liquidity. Current ratio is an important criterion to test the liquidity and also the short term solvency. The ratio of 2:1 is ered as standard of current ratio.

Table & Graph No.1: Current Ratio

Year/Company	HUL	P&G
2009-10	0.56	0.51
2010-11	0.93	0.53
2011-12	0.91	0.61
2012-13	0.80	0.57
2013-14	0.83	0.73

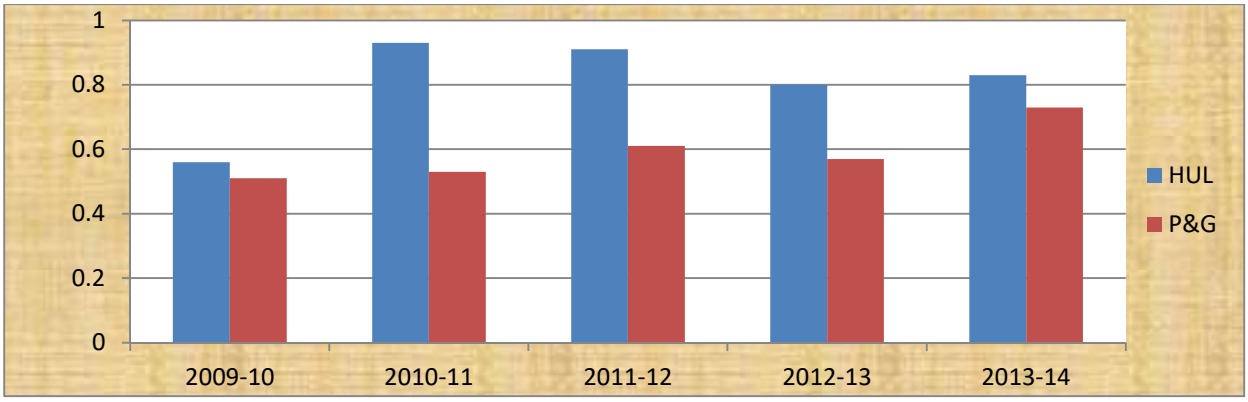

Interpretation: From the above table and graph it is clear that HUL have 0.65 times current ratio in the year 2009-10. It became 0.91 times in the year 2011-12 but in the last year of the study i.e. in the 2013-14 the current ratio of HUL is 0.83 times. On the other hand current ratio of P&G. Is0.51 times in 2009-10 and 0.73times in 2013-14 .From the above it can be concluded that the financial position of HUL is better than the P&G. in terms of current ratio because HUL have more variations in current ratio as compare to P&G

Quick Ratio: This ratio also tests liquidity. But it is a more refined test of liquidity and solvency. This Ratio takes into consideration the liquid assets only which are directly convertible into Cash. The current assets like inventories which are two steps away from the cash are excluded. The quick ratio is computed by dividing liquid assets by current liabilities. AQuick ratio of 1:1 is considered adequate.

Table & Graph No.2

Year/Company	HUL	P&G
2009-10	0.52	0.21
2010-11	0.47	0.17
2011-12	0.44	0.17
2012-13	0.47	0.74
2013-14	0.47	0.84

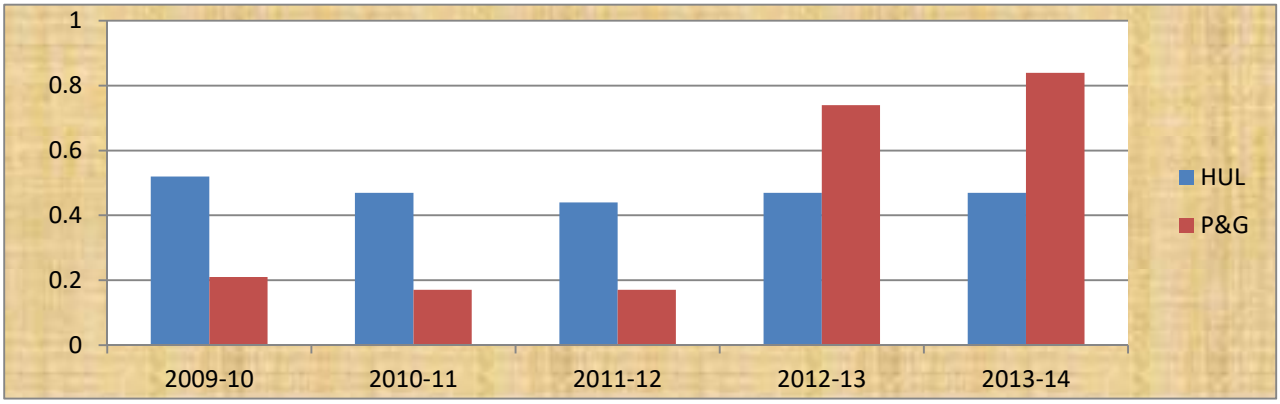

Interpretation: From the above table and graph it is clear that HUL have 0.52 times Quick ratio in the year 2009-10. It became 0.44 times in the year 2011-12 but in the last year of the study i.e. in the 2013-14 the Quick ratio of HUL is 0.47 times. On the other hand Quick ratio of P&G is 0.21 times in 2009-10 and 0.84 times in 2013-14. From the above it can be concluded that the financial position of HUL is better than the P&G. in terms of Quick ratio because HUL have more variations in Quick ratio as compare to P&G.

Gross Profit Ratio:

This ratio measures the gross margin of profit from sales. The higher the gross profit Ratio the better it is.

Table & Graph No.3

Year/Company	HUL	P&G
2009-10	0.14	0.56
2010-11	0.13	0.59
2011-12	0.15	0.59
2012-13	0.10	0.53
2013-14	0.11	0.47

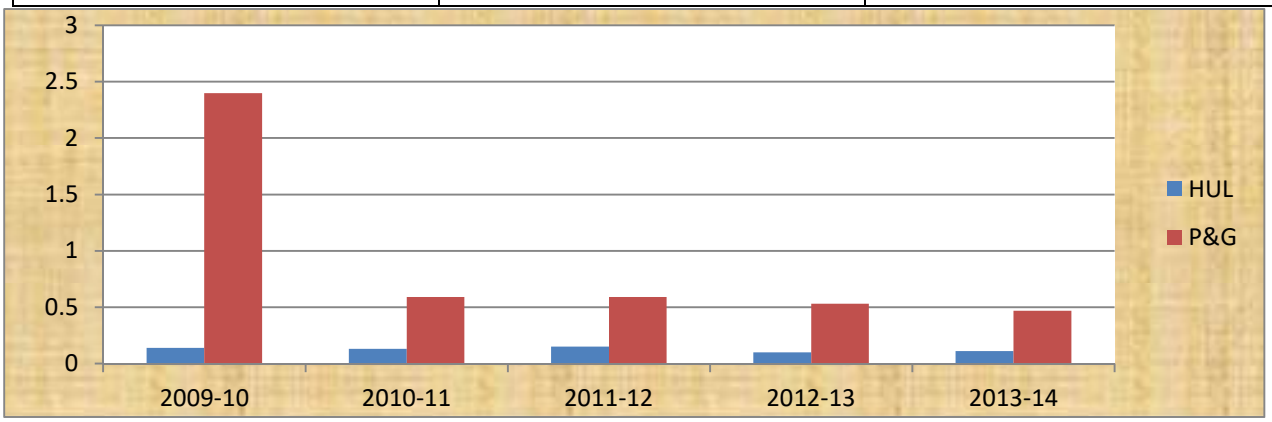

Interpretation: From the above table and graph it is clear that HUL have 0.14 times Gross Profit ratio in the Year 2009-10. It became 0.15 times in the year 2011-12 but in the last year of the study i.e. in the 2013-14 the Gross Profit ratio of HUL is 0.11 times. On the other hand Gross Profit ratio of P&G. is 0.56 times in 2009-10 and 0.47 times in 2013-14. From the above it can be concluded that the financial position of P & G is better than the HUL. In terms of Gross Profit ratio because P & G have more variations in Gross Profit ratio as compare to HUL

Inventory Turnover Ratio:

This ratio indicates whether stock has been efficiently used or not. A high ratio is considered better.

Table & Graph No.4: Inventory Turnover Ratio (In Times)

Year/Company	HUL	P&G
2009-10	9.27	6.50
2010-11	8.97	9.90
2011-12	6.92	15.88
2012-13	8.74	23.84
2013-14	9.93	31.24

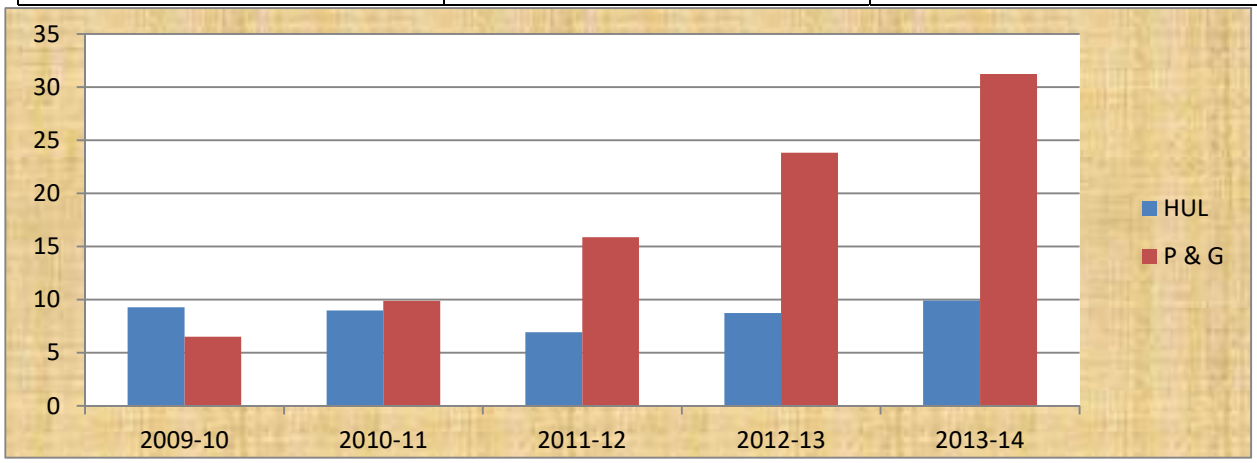

Interpretation: From the above table and graph it is clear that HUL have 9.27 times Inventory Turnover ratio in the Year 2009-10. It became 6.92 times in the year 2011-12 but in the last year of the study i.e. in the 2013-14 the Inventory Turnover ratio of HUL is 9.93 times. On the other hand Inventory Turnover ratio of P&G. is 6.50 times in 2009-10 and 31.24 times in 2013-14. From the above it can be concluded that the financial position of P & G is better than the HUL. In terms of Inventory Turnover ratio because P & G have more variations in Inventory Turnover ratio as compare to HUL.

Return on long term fund:

Table & Graph No: 5 Return on long term fund

Year/Company	HUL	P&G
2009-10	141.14	73.45
2010-11	101.77	41.50
2011-12	101.26	51.68
2012-13	92.65	48.67
2013-14	150.59	59.29

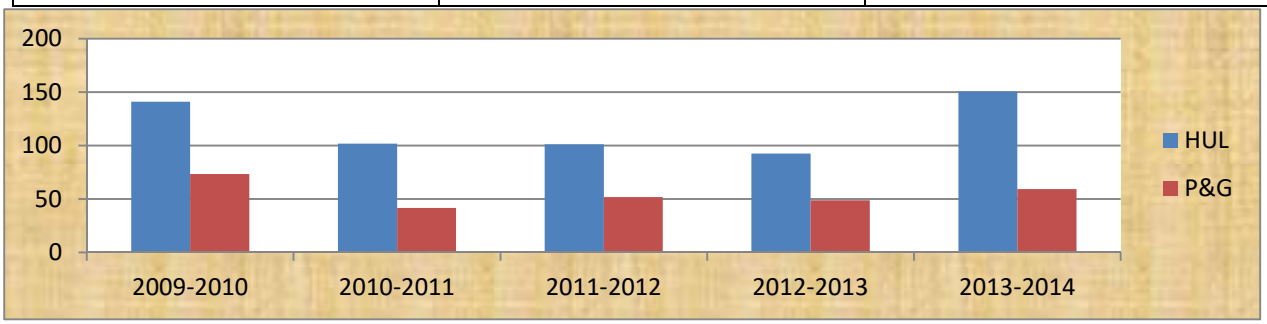

Interpretation: From the above table and graph it is clear that HUL have 141.14 times Return on long term investment fund in the year 2009-10. It became 101.26 times in the year 2011-12 but in the last year of the study i.e. in the 2013-14 return on investment fund of HUL is 150.59 times. On the other hand return on investment fund P&G. Is 73.45 times in 2009-10 and 59.29 times in 2013-14. From the above it can be concluded that the financial position of P & G is better than the HUL. In terms of return on investment fund because P & G have more variations in return on investment fund as compare to HUL

Operating Ratio:

Table & Graph No: 6 operating ratio

Year/Company	HUL	P&G
2009-10	13.73	0
2010-11	12.61	0
2011-12	11.04	0
2012-13	15.60	25.07
2013-14	19.45	21.45

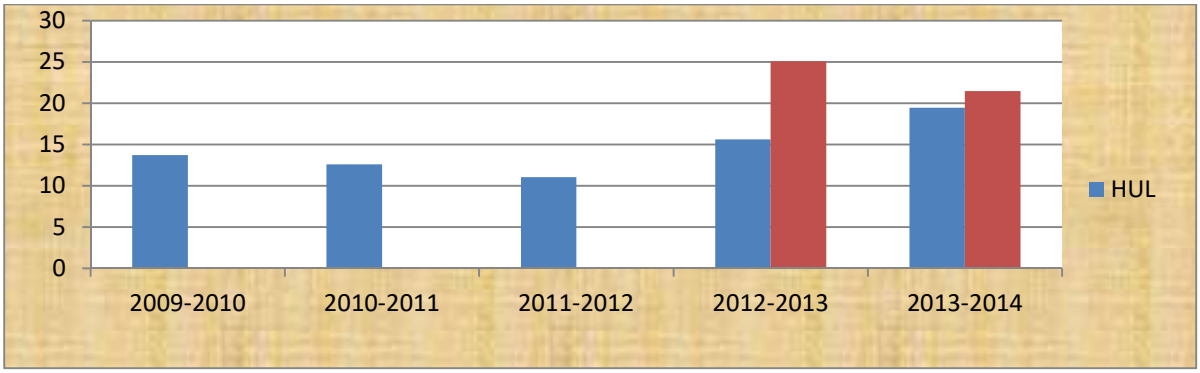

Interpretation: From the above table and graph it is clear that HUL have 13.73 times operating ratio in the year 2009-10. It became 11.04 times in the year 2011-12 but in the last year of the study i.e. in the 2013-14 return on operating ratio of HUL is 19.45 times. On the other hand operating ratio P&G. is 0 times in 2009-10 and 21.45 times in 2013-14. From the above it can be concluded that the financial position of P & G is better than the HUL. In terms of operating ratio because P & G have more variations in operating ratio as compare to HUL.

Dividend Payout Ratio:

Table & Graph No: 7 Dividend payout ratios

Year/Company	HUL	P&G
2009-10	76.39	0
2010-11	76.80	0
2011-12	71.51	0
2012-13	67.50	0
2013-14	121.84	0

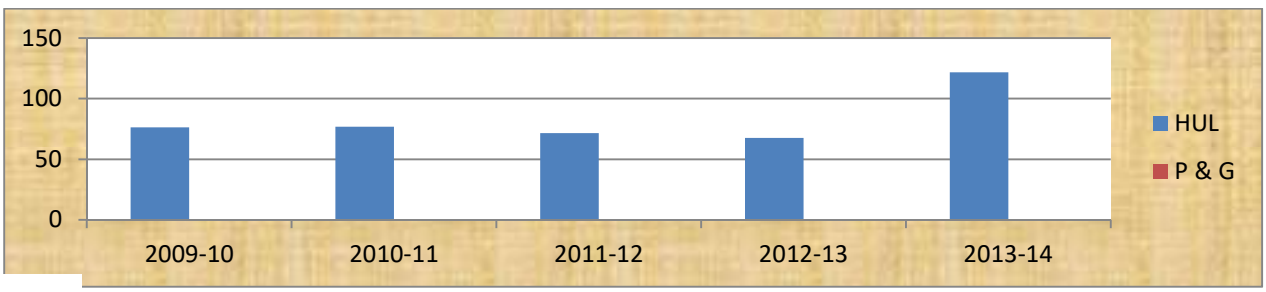

Interpretation: From the above table and graph it is clear that HUL have 76.39 times dividend payout ratio in the year 2009-10. It became 71.51 times in the year 2011-12 but in the last year of the study i.e. in the 2013-14 dividend payout ratio of HUL is 121.84 times. On the other hand dividend payout ratio P&G. is 0 times in 2009-10 and 0 times in 2013-14. From the above it can be concluded that the financial position of P & G is better than the HUL. In terms of dividend payout ratio because P & G have more variations in dividend payout ratio as compare to HUL.

Limitations of the study:

To know the extent to which the study is reliable it is necessary to note the limitations under which the study has been completed. The following important limitations have been noted while conducting the present study

1) The main source of information is annual reports. They represent financial information/position on particular date. What happened between such two dates cannot easily be presumed or predicated.

2) The annual reports mostly contain quantitative and financial information and as regards to qualitative aspect of financial performance, my source was limited due to far away location of head offices of the selected units.

3) The financial performance covering a large period say 25 years or 35 years can give a much clear picture of management practices of financial performance. Our study covering a period of 5 years can touch only a part of the problem.

Conclusion:

Competent management of finance is very important for the success of an enterprise.Term monetary performance is very dynamic term. The subject matter of financial Performance has been changing very rapidly. In present time greater importance is given to financial presentation. So, here an attempt is made by me to compare the financial presentation of the selected units i.e. HUL and P & G While analyzing the financial performance of the selected units, we include the analysis of working capital, analysis of fixed assets and analysis of profitability. Financial performance is an important yardstick to measure a company operational and financial efficiency. This aspect must form part of the company's strategic and operational thinking. Efforts should constantly be made to improve the financial position. This will yield greater effectiveness and get better investor's satisfaction.

HUL and P & G both the companies are major players in FMCG sector in India. After making the comparative analysis of both the firms it is found that performance of P & G is better than the HUL. It is so because the Net profit of P & G is greater than the HUL Similarly the inventory Management of the P & G is better than the HUL.

Reference:

1. Khandelwal., N. (2013). Working Capital Management in Small Scale Industries. In International Manuscript (1st ed., Vol. 2, p. 8). New Delhi: Ashish Publishing House.
2. Mathur, S. (2002). Working Capital Management and Control--Principles and Practice. In New Age International
3. Bhattacharya, H. (2007). Working Capital Management. In Prentice Hall of India Pvt. Ltd (8th ed., Vol. 9, p. 10). Delhi: Prentice Hall of India Pvt..
4. Bhalla, V. (2008). Working Capital Management. In Anmol Publications Pvt. Ltd., (2nd ed., Vol. 9, p. 8). New Delhi: Anmol Publications Pvt.
5. C. Jeevanandam (1st Ed.), "Management Accounting and Financial Management", Sultan Chand & Sons, ISBN-81-8054-013-8.
6. Prasanna Chandra (6th ED.),"Financial Management", Tata Mc Graw-Hill Publishing Company Ltd., New Delhi. ISBN-0-07-058548-2.
7. Deloof, M. (2003). "Does Working Capital Management affects Profitability of Belgian Firms?" Journal of Business Finance & Accounting, 30(3 & 4), 573-587.7. Gupta Shashi K. and Sharma R.K.(11th Ed.-2008), " Management Accounting", Kalyani Publishers, New Delhi, ISBN-978-81-272-4790-4.
8. Hampton, J. (1983). Financial Decision Making --Concepts, Problems and Cases (4th ed.). New Delhi: Prentice Hall.
9. Khan M Y and Jain P K (Fifth Ed.), "Financial Management", Tata Mc Graw- Hill Publishing Company Limited, New Delhi, ISBN-0-07-463225-6.
10. P. Periasamy (1st ED.-2009),"Working Capital Management", Himalaya Publishing House, Delhi, ISBN-978-81-8488-171-4.